

Response to Reviewer 1

The authors thank the reviewer 1 for a thoughtful review of the manuscript. The responses for the
5 reviewer's specific comments are as follows.

General Comment:

*This paper describes an evaluation of different observing locations in Asia to infer Asian surface CO₂
fluxes. The authors use the Carbontracker inversion system, with model generated pseudo-data, to assess
10 different observing networks. They compare fluxes estimated with the existing network, with alternative
networks based on random addition or relocation of sites, and the choice of sites using sensitivities from
the inversion system. This contrasts with previous network design studies that use optimisation to locate
the best observing sites, with higher computational cost.*

*Some aspects of the methodology need improved description, as described below. I have some concerns
15 with the methodology, also described below, however it is possible that I have misunderstood what was
done and improved description would give me a better understanding of the methodology and address
some of my concerns. There is a need for minor improvements to the English throughout, but this would
be addressed with copy-editing and I don't believe it has contributed to any difficulty in my understanding
of the methodology or results.*

20 **Author's response:** Following the reviewer's suggestions, we have tried to improve descriptions.
We also have addressed more explanations for the concerns with the methodology. Specific responses
to the reviewer's comments and revisions are shown below.

Specific Comments:

1. *Self-sensitivity (page 4, line 6 and section 2.2) - it is not completely clear to me what sensitivity is used in this paper. On page 4, line 8 'the relative impact of each CO₂ observation for the optimized surface carbon flux can be calculated ... and used as a strategy for selecting potential sites of CO₂ mole fraction observations', however on page 8, line 8 'contribution of the observation vector (y^0) to the analysis at the observation space (y^a)'. From the description in the paper, I understand y^a to be the model equivalent of the CO₂ mole fraction in air, also described as the predicted observation in Liu et al (2009) that the authors refer to. These are two different quantities (i.e. sensitivity of fluxes or sensitivity of surface mole fraction). Which was used in this study? I can see value in considering the sensitivity of the optimised flux (or perhaps the scale factor in this study) to each observation, but I am not as clear on the value of the sensitivity of the predicted observation. Of course they are related, but not the same. I am also not clear about how time affects the sensitivities. For example, some information comes from distant sites but with a lag. When is the analysis sensitivity calculated -before lagged information has had a chance to improve an analysis estimate? If so, that would downweight information from other gridcells that arrive after a lag. Thus I have concerns about the methodology, but I admit that it is not clear to me exactly what was done.*

Author's response: The self-sensitivity is calculated in the observation sites. As denoted in Eq. (11), the self-sensitivity is the gradient of the analysis at the observation space (\mathbf{y}^a) to the observation vector (\mathbf{y}^0). Here, \mathbf{y}^a represents the projection of analysis state vector \mathbf{x}^a on the observation space or model analysis equivalent to observations at observation locations. The model analysis \mathbf{x}^a (i.e., optimized surface CO₂ flux) is on the model grid point, whereas the model analysis equivalent to observations \mathbf{y}^a (i.e., model analysis equivalent CO₂ mole fraction) is on the observation locations (i.e., observation space). As the reviewer denoted, they are not the exactly same although they are closely related as in Eqs. (11), (12), and (13). The self-sensitivity represents the contribution of observations to the model analysis in grid point as well as that in observation locations. Liu et al. (2009) deals with the sensitivity in numerical weather prediction (NWP) problem, thus it considers predicted observation. However, in this study, the analysis equivalent observation is used because the

prediction is not much considered in CO₂ data assimilation. Although the self-sensitivity is qualitatively related with both the model analysis in grid point as well as that in observation locations, the quantity used in this study is the sensitivity of “model analysis equivalent CO₂ mole fraction at observation space” to “observed CO₂ mole fractions”. Thus, we have revised the text on page 4, line
5 8 as follows.

“Similar to the numerical weather prediction (NWP), the relative impact of each CO₂ mole fraction observation for the model analysis equivalent CO₂ mole fraction induced by the optimized surface CO₂ flux can be calculated (Kim et al., 2014a, 2017) and used as a strategy for selecting potential sites of CO₂ mole fraction observations.”

10 Since the analysis (i.e., optimized surface CO₂ flux) in this study is calculated considering the time lag, the effect of time lag is already included in the sensitivity calculation. As mentioned in Kim et al. (2014a), CarbonTracker adopts a smoother window to reflect the transport speed of CO₂, which is based on the temporal relationship between the surface CO₂ flux and atmospheric CO₂ observations, as found in Bruhwiler et al. (2005) (Peters et al., 2005). For this reason, the scaling factor is optimized
15 for 5 weeks of lag, which implies that the observations made in the most recent week affect the optimized surface CO₂ flux in the preceding 4 weeks. The optimization of the scaling factor during the data assimilation process is presented in Fig. 1 in Kim et al. (2014a) as shown below. In each assimilation cycle, 5 weeks of analysis scaling factors are estimated by observations from the most recent week. After the fifth cycle, the scaling factor estimated by these 5 weeks of observations is
20 saved as the optimized scaling factor and used to calculate the optimized (i.e., analysis) surface CO₂ flux.

The self-sensitivity is calculated using the analysis produced by the process above. Thus, the analysis surface CO₂ flux already considers the time lag associated with the distant information. Whether the 5 weeks of lag is enough to consider the distant information is fully studied in Peters et al. (2007) and
25 Kim et al. (2018b).

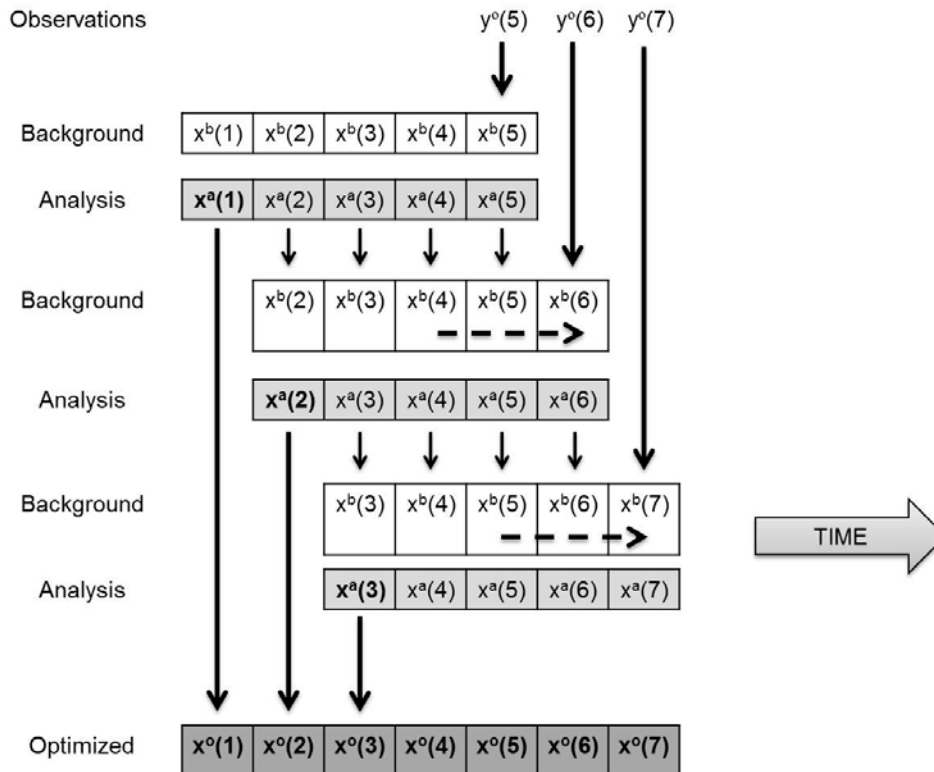


Figure 1. Schematic diagram of the assimilation process employed in CarbonTracker. In each analysis cycle, observations made within one week are used to update the state vectors with a five-week lag. The dashed line indicates how the simple dynamic model uses analysis state vectors from the previous one and two weeks to produce a new background state vector for the current analysis time. The TM5 model is used as the observation operator to calculate the model CO₂ concentration for each corresponding observation location and time. (Kim et al. 2014a, ACP)

2. Simulated hypothetical observations (section 2.3) - there are no details or references given about the
 10 EXTASI experiment - are the EXTASI fluxes based on the same flux modules as used in this study but with
 different scale factors? Therefore, are there differences in the spatial distribution of fluxes within the
 ecoregions that are used to generate the simulated hypothetical observations compared to the flux
 modules, as there would be between modelled fluxes and real world fluxes in an inversion of real

observations? This is perhaps most relevant for the two regions that each account for close to 20% of the domain. If the distribution is the same, that's probably ok, but it should be mentioned, as model error in the spatial distribution within each region is not considered.

Author's response: In EXTASI experiment, the surface CO₂ fluxes are optimized by the inverse modeling using the real observation data (i.e., observed CO₂ mole fractions). Thus, EXTASI produced optimized surface CO₂ flux (from the inverse modeling using real CO₂ mole fraction observations). In contrast, SF1 experiment produced another estimated surface CO₂ flux (by setting scaling factor as 1). Thus, as the reviewer mentioned, EXTASI and SF1 are based on the same prior flux modules with different scale factors. The EXTASI produces fluxes that is closer to real fluxes (although the real fluxes are not exactly known), compared to SF1.

Using the above two CO₂ fluxes, two model CO₂ mole fractions were generated and averaged to have the hypothetical true CO₂ mole fraction observations. We made hypothetical true CO₂ mole fractions this way because we liked to produce hypothetical “true data” close to real data but not the same. If the model CO₂ mole fractions produced by EXTASI are used as “true data”, then they may be similar to the real observed CO₂ mole fractions, but they are constrained much by the real observation network. This configuration causes that, when we choose observation sites using several strategies, the experiment using the current observation network (i.e., CNTL in this study) has more benefits compared to other network designs. To be fairly compared the results from several network configurations, we have made hypothetical true CO₂ fractions that are somewhat similar to the real feature but still hypothetical.

Following the reviewer's suggestion, we have clarified and added details of the EXTASI experiment as follows. The revised parts are underlined.

“In this paper, simulated hypothetical observations were created and used to design the observation network. Simulated hypothetical observations with similar values and seasonal variations compared to real CO₂ observations were generated by averaging model CO₂ mole fractions from the experiment conducted with real NOAA observation data (EXTASI) and model CO₂ mole fractions from the

experiment with a fixed scaling factor of 1 (SF1). Both EXTASI and SF1 experiments were done for the year of 2008. In EXTASI experiment, the real CO₂ mole fraction data were used to update the scaling factors in Eq. (1) to estimate the surface CO₂ fluxes. In contrast, in SF1 experiment, the scaling factors were fixed as 1.

5 Figure 2 shows the station-averaged time series of CO₂ mole fractions from real observations (OBS), EXTASI, SF1, and an average (i.e., simulated hypothetical observations: TRUE, hereafter) of EXTASI and SF1.”

3. *Average of random redistribution (page 11, line 1) - My understanding from the text is that REDIST is*
10 *created by averaging the fluxes from three random redistribution experiments of 7 sites. Firstly, is this correct? And if it is, I am concerned that this may lead to a better solution than you would expect from just 7 sites, as $7 \times 3 = 21$ sites were actually used to generate the average. Errors in the individual results may cancel in the average. The statistics of the average may not reflect the statistics of individual experiments, and therefore it would be an unfair comparison. The ADD case is also an average of three*
15 *experiments, so would potentially have the same issue. Perhaps it would be a fairer comparison to instead calculate the PC, BIAS, RMSD and UR statistics for the individual experiments then average these statistics?*

Author’s response: As the reviewer mentioned, we did three random redistribution experiments and averaged the results. In each experiment, 7 sites were used and statistics (i.e., PC, BIAS, and RMSD)
20 were calculated. This experiment was done three times independently. In each experiment, 7 sites were selected randomly. We calculated average statistics for three experiments rather than statistics for individual experiment since the statistics of individual experiment can be easily skewed by specific configuration or selection of sites by only one experiment. To avoid the sampling error that can possibly be caused by only one sampling, we did three experiments with different configurations
25 to get more general results. This experimental configuration is used in previous observation network studies as Yang et al. (2014). Thus, we have revised the text as follows. The added parts are underlined.

“Figures 3b, c, and d show the distribution of three observation networks, in which the seven observation sites in Asia are randomly redistributed. To obtain general results without sampling error, each random redistribution experiment was performed three times with different sets of randomly distributed observation sites, as denoted in previous observation network studies (e.g., Yang et al. 2014). The average of three random redistribution experiments was denoted as REDIST, to check the impact of the reallocation of the existing observation network.”

4. *What affects the self-sensitivity of an individual gridcell in the ALL case? In Fig 6, most of the gridcells with high self-sensitivity are near the boundaries of the regions used for this calculation. Presumably this is because they contain some information not available from neighboring gridcells in the ALL case. But for gridcells with many neighbors that contain similar information to each other, the information from any one of those gridcells may not be needed when all of the others are available, as in the ALL case. But that does not mean that at least some of these gridcells that rank low in the ALL case are unimportant in a case with a much lower number of observing sites. The authors point out on page 17, line 18 that self-sensitivity is generally inversely proportional to the number of assimilated observations in an ecoregion, and that makes sense, but within a region, does the self-sensitivity pick out some sites that will give most value in a network with few sites, or just those with most sensitivity in a case with many sites (ALL)? In network design studies that use optimisation, the value of observation sites is determined for a network that is closer to the expected size of the potential network. I am not yet convinced of the value of determining the worth of any single site from the self-sensitivity in the ALL case when many more sites than would be practical are included. This is my greatest concern about the methodology, and I believe this would need to be addressed for the paper to be published. Of course, exactly what the self-sensitivity is (sensitivity of fluxes or surface mole fraction) is also important here (see above comment).*

Author’s response: As mentioned in page 17, four influential regions with high sensitivities are located in western Siberia, the southern part of the Tibetan Plateau, and southeastern and northeastern Asia. Except the western Siberia, the other regions do not coincide much with the boundaries of the model domain. As defined, the self-sensitivity represents how CO₂ mole fraction observations affect

the model analysis equivalent CO₂ mole fraction observations at observation sites. Since the model grid points at 2° intervals are the observation sites in ALL experiment, if the self-sensitivity value at some grid point is large, then the observation at that grid point will affect highly the model analysis equivalent of CO₂ mole fraction observations. All grid points in ALL experiment are in same condition: 1) the observation sites at every 2° intervals on the land are used, 2) at every sites, only one simulated CO₂ mole fraction values around afternoon (i.e., 13 local standard time (LST)) are assimilated per day for one year), and 3) the self-sensitivities at every sites are calculated and averaged as shown in Fig. 6. Thus, the self-sensitivity based on these same conditions can be a measure to determine which observation sites should be used for assimilation to have a large effect on the model analysis equivalent at observation sites.

In Page 17 line 18, we mention that the self-sensitivity is generally inversely proportional to the number of assimilated observations, as shown in Kim et al. (2014a, 2017). This inversely proportional relationship is for observation numbers and self-sensitivity at one site, not for many observation sites case vs few or no observation sites case.

The genetic algorithm (GA) method which considers many sets of observation networks and finds out the network with minimum error with much computations, can be considered as the forward approach. In contrast, the method in this study uses the backward approach that can calculate the contribution of observations to the analysis equivalent mole fractions with much smaller computation. Using the self-sensitivity, we can select the potential observation site one by one. Practically, redistributing all observation sites at once is not easy or is even impossible. Adding or redistributing some sites given existing observation sites may be a more practical way to design the observation network. Once we have self-sensitivity value, we can use the value to determine the observation sites that would affect much on the analysis results. Using the self-sensitivity to determine the potential sites, we did forward calculation to verify whether the sites by the strategy are good or not.

The definition of the self-sensitivity is already explained in detail in the response to the specific comment 1 above.

Minor points:

5. Page 1, line 10 - *"Inverse modeling derives estimated CO₂ mole fractions in the air from calculated surface carbon fluxes using model and observed CO₂ mole fraction data"* - No, forward modelling derives CO₂ mole fractions in the air from surface fluxes. Inverse modeling derives surface fluxes from CO₂ mole fractions in the air.

Author's response: We have revised the confusing description of the inverse modeling as follows. The revised parts are underlined.

10 “Continuous efforts have been made to monitor atmospheric CO₂ mole fractions as it is one of the most influential greenhouse gases in Earth's atmosphere. The atmospheric CO₂ mole fractions are mostly determined by CO₂ exchanges at the Earth's surface (i.e., surface CO₂ flux). Inverse modeling, which is a method to estimate the CO₂ exchanges at the Earth's surface, derives surface CO₂ fluxes using model and observed atmospheric CO₂ mole fraction data.”

15 6. Page 2, line 7 - *"Inverse modeling uses observation data and transport models to estimate the sources and sinks of surface carbon flux and associated atmospheric CO₂ mole fractions"* - better than the previous description, but doesn't specify what observation data are used (should be CO₂ mole fractions in air). The associated modelled atmospheric CO₂ mole fractions can be estimated from the inferred fluxes (or perhaps during the inversion), but I don't consider that part of the inverse calculation.

Author's response: We have revised the text as follows. The revised parts are underlined.

20 “Inverse modeling, one of the methods to complete this mission, uses observed atmospheric CO₂ mole fraction data and transport models to estimate the sources and sinks of surface CO₂ flux (Enting, 2002; Gurney et al., 2002).”

7. Page 3, line 14 - Add 'alone' after 'data' i.e. Assimilating XCO₂ data alone ...

Author's response: We have added the text following the reviewer's suggestion.

8. *Page 3, line 22 and many other locations - OSSEs (with an 's' at the end) is often used for the plural of OSSE. I.e. We conducted one OSSE, and they conducted many OSSEs.*

5 **Author's response:** As many other references (e.g., Wang et al. 2018), we have used "OSSEs" for the plural of "OSSE". Considering the reviewer's suggestion, in the last paragraph of Section 1, we have replaced "OSSEs" by "many OSSEs" as follows.

"In this study, many OSSEs were conducted using CarbonTracker (CT) to~"

10 9. *Page 4, line 12 - "which does not seem feasible in the near future" - what is meant here? Is the 43 site network not feasible? Or the 233 site network (is this not like the ALL case considered here, to see what would be possible with observations everywhere)? Or are the authors referring to the computation of the network design calculation for many sites?*

Author's response: We meant that many $^{14}\text{CO}_2$ sites may not be feasible in the near future in Asia. But we found that the original meaning does not fit in the paragraph well. Thus, we have revised the text as follows.

"Although Wang et al. (2018) showed the potential impact of adding observation sites on the existing $^{14}\text{CO}_2$ sites in Europe using OSSEs, the potential $^{14}\text{CO}_2$ observation sites were not chosen based on specific selection strategies."

20

10. *Page 4, line 24 - I would add at the end of the sentence ', as an alternative to optimisation that has been used in previous studies' to make it clear that optimisation is not used in this study. Alternatively (or perhaps in addition), point out clearly elsewhere in the introduction that optimisation of the network*

is not part of this study, as that point was initially not clear to me. (At page 4, line 3, problems with IO and GA are discussed, but that doesn't mean another optimisation method wasn't going to be used).

Author's response: In my knowledge, the IO and GA are methods to select observation sites for observation network design until now. We could not find other methods used for determining surface
5 CO₂ observation network. The IO and GA are strategies selecting observation sites to minimize the error in their own framework. The IO and GA are called as the optimization method, but one of them has lower error than another in specific cases (Nickless et al. 2015).

Instead of using the term “optimization”, we proposed a selection strategy based on influence matrix. If the observation network is designed in the region without observation sites, then the IO and GA
10 methods would be useful. When adding observation sites over the region with existing observation sites, redistributing all observation sites at once may not be easy or may be even impossible. Adding or redistributing some sites given existing observation sites may be a more practical way to design the observation network.

Considering the reviewer's suggestion, we have revised the text as follows. The added parts are
15 underlined.

“In the case of addition experiments, random addition and addition based on influence matrix (self-sensitivity) as well as ecoregion information of the model were considered as strategies, as alternatives to IO and GA that have been used in previous studies.”

“Due to time and computing restraints, the IO and GA methods seem ineffective or unfeasible for
20 designing the observation network on continental scales like Asia. In addition, determining and redistributing all observation sites at once using the IO and GA methods may not be practical for most regions with existing observation sites. Adding or redistributing some sites given existing observation sites may be a more practical way to design the observation network.”

We have already mentioned that our purpose is to identify "a better" in situ observation network for
25 optimizing surface CO₂ flux estimation in Asia. The text is shown in page 4, line 20, as follows.

“In this study, many OSSEs were conducted using CarbonTracker (CT) to identify a better in-situ observation network for the purpose of optimizing surface CO₂ flux estimation in Asia.”

11. Page 5, section 2.1 - *There are many details of the inversion that are not clear: Does the inversion run globally with a focus on Asia, or just run over Asia as a regional inversion (i.e. are fluxes outside the Asian domain estimated)? How many ecoregions are used in this study? (Is 156 regions a global number or for Asia? What are the 240 ecoregions? There are 40 lines in Table 3, is that the number for Asia? Could say ‘We estimate x scale factors for y times’.) Is it possible to include a map of the ecoregions for Asia? How contiguous are the ecoregions?*

10 **Author’s response:** The inversion run is done globally with a focus on Asia using a nesting domain over Asia. The ecoregions used is 156 regions globally, 40 in the verification region (black dashed box in Fig. 1). As mentioned in the manuscript, 240 is the number of total ecoregions of the earth including ocean and unused vegetation types. The number of effective ecoregions globally is 156, and the 40 is the number of ecoregions in the verification region. The 40 ecoregions include mostly ecoregions of Asia and a very small portion of ecoregions of Europe. Since the portion of ecoregions (i.e., ecoregion indices of 191, 193, 194, 197, 201 in Table 3) of Europe is approximately 0.5% of the verification region, including ecoregions of Europe does not affect much on the verification results. To clarify, we have included Transcom region as well as Land ecosystem type in Table 3. In addition, we have revised the text as follows. The added parts are underlined. We also have included the map of ecoregions for Asia in Fig. 1b.

15 “This means that the optimization of the scaling factors that were assigned to the ecoregions of the earth is crucial for the estimation of simulated surface CO₂ fluxes. The ecoregions are defined as the mix of the modified 19 vegetation types from Olson et al. (1992) and 11 Transcom regions (Gurney et al., 2002) on land, with 30 ocean regions. As all 19 vegetation types are not used for the 11 Transcom regions, the number of effective ecoregions of the earth is 156 (Peters et al., 2010).”

5 “The horizontal resolution of TM5 is 3° x 2° globally and the nested horizontal grid is 1° x 1° over Asia, with verification region inside of the nested domain over Asia (Fig. 1). The number of ecoregions of the verification region is 40, in which 36 are the Asian ecoregions and 4 are the ecoregions of Europe. Since the proportion of the 4 European ecoregions is approximately 0.5% of the verification region (Table 3), the verification region was considered to be located over Asia. A two-way nested grid was used to optimize surface CO₂ fluxes in Asia. The model run including both forward and inversion runs was done globally with nesting over Asia and verification was done over the verification region located in Asia.”

10 *12. Page 5, line 9 - I would mention up front that the fluxes from the flux modules are scaled, and not wait until line 19. e.g. at line 9 ‘The estimated surface CO₂ fluxes are mainly calculated by scaling fluxes from the flux modules composed ...’*

Author’s response: We have revised the text as the reviewer suggested.

15 *13. Page 5, line 28 - the sentence that begins ‘In addition, also ...’ is not clear. It does not say what the model counterparts are. I would replace that sentence with something like ‘From this spatiotemporal CO₂ distribution, the model equivalents of atmospheric CO₂ at the times and locations of the observation data can be calculated, and these are used in the data assimilation process.’*

Author’s response: To clarify, we have revised the text considering the reviewer’s suggestion.

20 “In addition, from this spatiotemporal CO₂ distribution, the model atmospheric CO₂ concentrations at the times and locations of the observation data are calculated, and these are used for the data assimilation process.”

14. Page 7, line 17 - I would say ‘A statistical method’ rather than ‘The statistical method’, otherwise a reader would wonder which method is ‘the’ method. I would replace ‘feasible’ with ‘meaningful’.

Author’s response: We have revised the paragraph including the text as follows. We kept “feasible” since what we meant is “possible”. The revised parts are underlined.

5 “In the EnSRF, the covariance localization method is necessary to reduce the impact of the sampling error due to the limited size of the ensemble and to avoid filter divergence due to the underestimation of the background error covariance (Houtekamer and Mitchell, 2001). Because calculating the physical distance between scaling factors is not feasible, instead of the covariance localization method, a statistical method is applied in this study.”

10

15. Page 8, line 8 - define y_a (e.g. = Hx_a) and give some information about what it is (e.g. model equivalent of observations, or predicted observation).

Author’s response: We have revised the text as follows. The added parts are underlined.

15 “The analysis of the state vector and the influence matrix (\mathbf{S}^0) that shows the contribution of the observation vector (\mathbf{y}^0) to the analysis at the observation space (\mathbf{y}^a) (i.e., the projection of analysis state vector \mathbf{x}^a on the observation space or model analysis equivalent to observations at observation locations) can be defined as:”

20 16. Page 8, line 12 - replace ‘size of observation’ with either ‘size of the observation vector, n ’ or ‘number of observations, n ’. Is that the number of observations at only one time or all times?

Author’s response: The original text was wrong. The dimension of \mathbf{I}_n corresponds to the dimension of the analysis state vector \mathbf{x}^a . Thus, we have revised the text as follows. The revised parts are underlined.

“where, \mathbf{I}_n is the identity matrix with the size of n -dimensional analysis state vector.”

17. Page 8, line 25 - do you (and should you) assume no correlations between observation errors? It seems to me that the errors in your simulated data would be correlated, and also likely in the real world.

5 **Author’s response:** The observation errors in data assimilation are usually assumed to have no correlations. Although the observation errors in real world would be correlated, this no correlation assumption is very common and may be only way in this ensemble sensitivity study and data assimilation. Using this assumption, \mathbf{R}^{-1} in Eq. (12) can be simplified as $\frac{1}{\sigma_j^2}$ in Eq. (14). Please note Liu et al. (2009).

10

18. Page 9, line 6 - please give more explanation of what S^o is, e.g. ‘In our case, this would be the contribution of a CO₂ observation to the inferred CO₂ at that model gridcell/time’ - is that the correct explanation?

15 **Author’s response:** We have revised the paragraph including the line as follows. The revised parts are underlined.

20 “According to Liu et al. (2009) and Kim et al. (2014a), \mathbf{S}^o represents the sensitivity of the analysis state vector \mathbf{y}^a to the observation state vector \mathbf{y}^o in the observation space (i.e., location). \mathbf{S}^o has a value between 0 and 1, which shows the contribution of a CO₂ observation to the analyzed CO₂ at the observation site. If \mathbf{S}^o is close to 0, the analysis is mainly derived from the background. In contrast, the influence of observation data to the analysis increases as \mathbf{S}^o goes to 1. The self-sensitivity was used as a criterion for selecting the observation locations in designing the observation network.”

19. Page 10, line 2 - please explain ‘On the basis of the nautical time zone’. Also explain ‘13 LST’.

Author’s response: The text means the 13 local standard time (LST) (i.e., afternoon in local standard time) at each time zone. To clarify, we have revised the text as follows. The revised parts are underlined.

5 “The simulated values around afternoon (i.e., 13 local standard time (LST)) in the mid-latitudes in the northern hemisphere are averaged and utilized as TRUE data.”

20. Page 10, line 9 - ‘Model-data mismatch (MDM) was set to 3’ - what does the setting of 3 mean? Is it a setting within Carbontracker, in which case it should be explained.

10 **Author’s response:** MDM corresponds to the observation error covariance in data assimilation. The observation error for CO₂ mole fraction observations at continuous surface observation sites is set to 3 ppm in CarbonTracker. The number 3 ppm for continuous surface observation sites is usually used in other inversion modeling system, either. To clarify, we have added text (underlined) as follows.

15 “Model-data-mismatch (MDM) (i.e., observation error) for CO₂ observation was set to 3 ppm, consistent with the previous setting of 3 ppm for continuous observation site types (Peters et al., 2007; Kim et al., 2014b, 2017).”

21. Page 11, line 25 - add ‘for observation j’ to ‘The normalized self-sensitivity for observation j is defined...’

Author’s response: For consistency, we have revised the text as follows.

20 “The normalized self-sensitivity for *j*th observation \sim ”

22. Page 12, section 2.4 - define *n* for equations 16-18.

Author's response: “ n ” is the total number of model grid-point in the verification domain shown in Fig. 1. Thus, we have revised the text as follows. The added parts are underlined.

5 “where EXP_i and $TRUE_i$ are the surface CO₂ fluxes at the i th model grid-point of an experiment and TRUE, respectively, and n is the total number of model grid-point in the verification domain shown in Fig. 1.”

23. Page 15, line 10 - ‘the three experiments show increasing trends’ - be careful that this in not misinterpreted as a trend with time. I assume you mean that for RMSD in the summer, CTRL>ADD>ALL? Please clarify what is meant here.

10 **Author's response:** We have revised the text as follows. The revised parts are underlined.

“In terms of the RMSD, the three experiments show larger values in the summer compared to other seasons (Fig. 5c)”

15 24. Page 16, line 9 - what does ‘enabled in the CT2013B framework’ mean? There may be a better way to express this.

Author's response: We have revised the text as follows. The revised parts are underlined.

“In particular, the ALL experiment, which added many observation sites under the given modeling framework, shows a high level of reproducibility of TRUE.”

20 25. Page 16, line 16 - ‘showing the impact of each observation site for the model simulation results’ - could you be more specific here about what quantity the impact of the observation sites is calculated for.

Author's response: As denoted in Section 2.2, the self-sensitivity is the sensitivity of inverse model results with respect to the observations assimilated in EnKF data assimilation system in CarbonTracker. For each observation at each observation site, the self-sensitivity is calculated. For each observation site, all self-sensitivities are added up to have self-sensitivity at that site. To clarify,
5 we have revised the text as follows. The revised parts are underlined.

“Since the self-sensitivity is the metric showing the impact of observations at each observation site for the model simulation results, as stated in Sect. 2.2, ~”

26. *Page 17, line 13 and Table 3 - could the ecoregions be described in terms of vegetation types rather
10 than just as a number which may not mean anything to the reader?*

Author's response: We have included ecosystem types in text and tables (Tables 3, 4, and 5). We also have added Transcom region information in Tables 3, 4, and 5.

27. *Page 18, line 8-9 - These sentences are difficult to follow, consider rephrasing without the ‘this is in
15 contrast’ beginning to each new sentence.*

Author's response: We have revised the text as follows. The revised parts are underlined.

“Nevertheless, the ECOSS experiment that considered both self-sensitivity and ecoregion information maintains lower RMSD than the ADD experiment over the experimental period. Additionally, except in the period from April to late-August, the RMSD of SS is lower than that of
20 ADD, which differs from ADD that is mainly better than CNTL in summer, as shown in Fig. 5. Thus, compared to ADD and CNTL, the SS (ECOSS) experiment demonstrates improvement in the other seasons except summer (over the experimental period).”

28. Page 19, line 5 - *'because they were derived from an uneven distribution of observation sites' - do you mean an uneven number of sites for each ecoregion?*

Author's response: We have revised the text as the reviewer indicated.

5 29. Page 19, line 13 - *add 'each' after 'one observation site'*

Author's response: We have added the word following the reviewer's suggestion.

30. Page 20, line 5 - *I don't think 'and this is in contrast' is the appropriate wording here.*

Author's response: We have revised the text as follows. The revised parts are underlined.

10 “The NSS, NECOSS1, and NECOSS2 experiments show lower RMSDs compared to the ADD experiment (Fig. 8c). The RMSD of NSS is lower than that of ADD for most of the time, which is different from SS that showed a degradation in summer and little improvement in other seasons compared to ADD in Fig. 7c.”

15 31. Page 21, line 18 - *replace 'below 50oN' with 'north of 50oN'*

Author's response: We have changed “below 50° N” with “south of 50° N” since “south” is what we meant.

32. Page 21, line 20 - *replace 'slight increases in UR' with 'slightly more UR'*

20 **Author's response:** We have revised the text following the reviewer's suggestion.

33. Page 21, line 21 - add 'than REDIST' after 'including China and India'.

Author's response: We have added the text following the reviewer's suggestion.

34. Table 6 - Bias in Fig 7 looks like it is lower for ADD than SS and ECOSS – is this consistent with the
5 numbers in Table 6? Is the signed biased averaged, or the magnitude?

Author's response: As shown in Eq. (17), the BIAS is calculated as the average of summed differences between experiment results and truth. Thus, the differences have signs, and those signed values at model grid points are summed and averaged.

The BIAS values of ADD show many positive and negative values and they are cancelled out when
10 summed over model grid points. In contrast, the BIAS values of SS and ECOSS experiments show dominant specific signs. In this case, the BIAS values are not cancelled out and show large values with a certain sign (positive or negative). In Fig. 7, the SS shows large positive BIAS on June 7. In this case, the SS shows positive BIAS on most of the grid points, thus they are added up to have large positive BIAS. In contrast, the ADD shows relatively small BIAS, but the BIAS values of ADD on
15 that day on the grid points are not small in magnitude with different signs, thus they are cancelled out when summed.

In contrast, the RMSD considers the magnitude of BIAS as in Eq. (18). Thus, in terms of the magnitude of the error, we have to look at the RMSD instead of the BIAS. Although some BIAS values of SS and ECOSS show large magnitude on specific days, the average values of BIAS and
20 RMSD of SS and ECOSS are smaller than that of ADD.

Therefore, the BIAS in Fig. 7 and Table 6 are consistent.

35. Figs 3m and 6 - the gap in observing sites in Figs 3m and 6 over the Himalayas is presumably due to elevation and therefore practicality of an observing site? Is this worth mentioning?

Author's response: We have omitted locations that are 2000 m above the mean sea level considering the maintenance of the observing sites. We have added the reason for the gap in observing sites over the Tibetan Plateau as follows. The added parts are underlined.

5 “In addition, the observation networks that have observation sites at every 2° intervals on the land (Fig. 3m, ALL experiment) are suggested as the reference to examine the maximum possible impact of additional observation sites. In ALL experiment, the observation locations that are located 2000 m above the mean sea level over the Tibetan Plateau are not included due to difficult accessibility and maintenance as practical observing sites.”

10 References

- Kim, H., Kim, H. M., Kim, J. and Cho, C.-H.: Effect of data assimilation parameters on the optimized surface CO₂ flux in Asia, *Asia-Pacific J. Atmos. Sci.*, 54(1), 1–17, doi:10.1007/s13143-017-0049-9, 2018b.
- 15 Kim, J., Kim, H. M. and Cho, C. H.: Influence of CO₂ observations on the optimized CO₂ flux in an ensemble Kalman filter, *Atmos. Chem. Phys.*, 14(24), 13515–13530, doi:10.5194/acp-14-13515-2014, 2014a.
- Kim, J., Kim, H. M., Cho, C. H., Boo, K. O., Jacobson, A. R., Sasakawa, M., Machida, T., Arshinov, M. and Fedoseev, N.: Impact of Siberian observations on the optimization of surface CO₂ flux, *Atmos. Chem. Phys.*, 17(4), 2881–2899, doi:10.5194/acp-17-2881-2017, 2017.
- 20 Nickless, A., Ziehn, T., Rayner, P. J., Scholes, R. J. and Engelbrecht, F.: Greenhouse gas network design using backward Lagrangian particle dispersion modelling - Part 2: Sensitivity analyses and South African test case, *Atmos. Chem. Phys.*, 15(4), 2051–2069, doi:10.5194/acp-15-2051-2015, 2015.

- Peters, W., Miller, J. B., Whitaker, J., Denning, A. S., Hirsch, A., Krol, M. C., Zupanski, D., Bruhwiler, L. and Tans, P. P.: An ensemble data assimilation system to estimate CO₂ surface fluxes from atmospheric trace gas observations, *J. Geophys. Res. Atmos.*, 110(D24), D24304, doi:10.1029/2005JD006157, 2005.
- 5 Peters, W., Jacobson, A. R., Sweeney, C., Andrews, A. E., Conway, T. J., Masarie, K., Miller, J. B., Bruhwiler, L. M. P., Petron, G., Hirsch, A. I., Worthy, D. E. J., van der Werf, G. R., Randerson, J. T., Wennberg, P. O., Krol, M. C. and Tans, P. P.: An atmospheric perspective on North American carbon dioxide exchange: CarbonTracker, *Proc. Natl. Acad. Sci.*, 104(48), 18925–18930, doi:10.1073/pnas.0708986104, 2007.
- 10 Peters, W., Krol, M. C., van der Werf, G. R., Houweling, S., Jones, C. D., Hughes, J., Schaefer, K., Masarie, K. A., Jacobson, A. R., Miller, J. B., Cho, C. H., Ramonet, M., Schmidt, M., Ciattaglia, L., Apadula, F., Heltai, D., Meinhardt, F., di Sarra, A. G., Piacentino, S., Sferlazzo, D., Aalto, T., Hatakka, J., Ström, J., Haszpra, L., Meijer, H. A. J., van Der Laan, S., Neubert, R. E. M., Jordan, A., Rodó, X., Morguá, J. A., Vermeulen, A. T., Popa, E., Rozanski, K., Zimnoch, M., Manning, A. C., Leuenberger, M., Uglietti, C., Dolman, A. J., Ciais, P., Heimann, M. and Tans, P.: Seven years of recent European net terrestrial carbon dioxide exchange constrained by atmospheric observations, *Glob. Chang. Biol.*, 16(4), 1317–1337, doi:10.1111/j.1365-2486.2009.02078.x, 2010.
- 15 Wang, Y., Broquet, G., Ciais, P., Chevallier, F., Vogel, F., Wu, L., Yin, Y., Wang, R. and Tao, S.: Potential of European ¹⁴CO₂ observation network to estimate the fossil fuel CO₂ emissions via atmospheric inversions, *Atmos. Chem. Phys.*, 185194(July), 4229–4250, doi:10.5194/acp-18-4229-2018, 2018.
- 20 Yang, E.-G., H. M. Kim, J. Kim, and Kay J. K.: Effect of observation network design on meteorological forecasts of Asian dust events, *Monthly Weather Review*, 142, 4679-4695, doi:10.1175/MWR-D-14-00080.1, 2014.

Response to Reviewer 2

The authors thank the reviewer 2 for a thoughtful review of the manuscript. The responses for the
5 reviewer's specific comments are as follows.

General Comment:

*This paper describes an impact of observation network against carbon cycle estimation by using CarbonTracker (CT). An important aspect is that the authors showed realistic solution this means that
10 we have the potential to realize this observation network in the future. This viewpoint is very important, and I think it is necessary to advance research in this field in the future. I'd like to comment from a different perspective than Reviewer 1. I think authors need to do some additional experiments to take advantage of the excellent features of this paper. One important issue is that the authors show that root mean square error increases in many experiments in summer, but the reason is not well specified. Authors
15 should consider this reason and suggest ways to reduce large summer uncertainty, if possible, without using ALL observations. The other issue is that authors should use observation sites registered in NOAA ObsPack but not assimilated in CT. This is because these stations are in operation and can be a precondition to be considered when considering future network expansion. The last issue is that this paper focuses on only ground observation network. Although it is considered unrealistic to use all observation
20 points (ALL), the OSSE should be implemented in consideration of the observable area of satellite which can supply much more observation area than ground observation network even if the observation accuracy is inferior, if the authors want to evaluate the construction of a more realistic carbon cycle observation network.*

Author's response: We have added discussions for large summer uncertainties. The specific
25 discussions can be found in the responses to the specific comments 3 and 5 below.

We have added the Section 3.6 that considers many observation sites registered in NOAA ObsPack. The results based on the observation sites registered in NOAA ObsPack are very similar to those based on 7 observation sites used for CT2013B.

5 The purpose of this study is introducing the selection strategy (i.e., self-sensitivity and ecoregion information) for potential observation sites. Thus, we have examined these strategies using the ground observation sites. For the satellite observations, the self-sensitivity for the satellite observations are not well known yet. We have to know characteristics, spatial, and temporal distributions of self-sensitivities for satellite observations and how the self-sensitivities of satellite observations are different from those of the ground observations. Thus, the observation network design using both the
10 ground observations and satellite observations will be studied in the future after the self-sensitivities for satellite observations are fully studied. In Section 4, we have added texts (underlined) considering this issue as follows.

“Although the simulation results showed an improvement in performance, the results also suggested that adding 10 extra observation sites in Asia may not be sufficient to fully optimize surface CO₂
15 fluxes, and more observation sites are required. Reliable observation data from some satellite sensors could supplement the model simulations on the basis of continuous surface observation sites. As the quality of satellite observation data increases, the observation network design for both surface and satellite observation data using the strategies (i.e., normalized self-sensitivity and ecoregion information) of this study will be investigated in the future.”

20

Specific Comments:

1. Page 3, line 20: As we can expect an increase in satellite observation data and quality improvement in the future, so it is necessary to consider the mixed use of ground observation data and satellite observation data.

Author's response: The purpose of this study is showing the validity of the selection strategy (i.e., self-sensitivity and ecoregion information) for potential observation sites. Thus, we have examined these strategies using the ground observation sites. For the satellite observations, the self-sensitivity for the satellite observations are not well known yet. We have to know characteristics, spatial, and temporal distributions of self-sensitivities for satellite observations and how the self-sensitivities of satellite observations are different from those of the ground observations. Thus, the observation network design using both the ground observations and satellite observations will be studied in the future after the self-sensitivities for satellite observations are fully studied. In Section 4, we have added texts (underlined) considering this issue as follows.

10 “Although the simulation results showed an improvement in performance, the results also suggested that adding 10 extra observation sites in Asia may not be sufficient to fully optimize surface CO₂ fluxes, and more observation sites are required. Reliable observation data from some satellite sensors could supplement the model simulations on the basis of continuous surface observation sites. As the quality of satellite observation data increases, the observation network design for both surface and satellite observation data using the strategies (i.e., normalized self-sensitivity and ecoregion information) of this study will be investigated in the future.”

2. Page 3, line 25: *The authors should refer Patra et al., 2003 as this paper showed global CO₂ observation network design.*

20 **Author's response:** We have referred Patra et al. 2003 as follows. The added text is underlined.

“Observation system simulation experiments (OSSEs), using simulated observation data, provide an opportunity to evaluate the impact of observation data from the current and potential observation sites on the performance of the modeling system (Patra et al., 2003; Yang et al., 2014; Byrne et al., 2017; Wang et al., 2018).”

25

3. Page 9, Line 14 -15: *The difference between hypothetical observations (TRUE) and real observation (OBS) is large in the summer, and this seems to be a cause of the increase in summer RMSD in each subsequent experiment. In order to analyze the cause of the increase in summer RMSD, another observation data that is close to actual observation should be used additionally.*

5 **Author's response:** As the reviewer mentioned, the difference between hypothetical observations (TRUE) and real observations (OBS) is large in the summer, which causes the increase in summer RMSD in OSSE experiments.

We made hypothetical TRUE CO₂ mole fraction data different from OBS because we liked to produce hypothetical true data close to real data but not the same. The estimated model CO₂ mole fractions may represent or similar to the real observed CO₂ mole fractions, but they are constrained much by the real observation network. Thus, when we choose observation sites using several strategies, the experiment using the current observation network (i.e., CNTL in this study) has more benefits compared to other network designs. To be fairly compared the results from several network configurations, we have made hypothetical true CO₂ fraction data that is somewhat similar to the real feature but still hypothetical.

The large RMSD in summer is caused by the sensitivity of CO₂ flux estimated by inversions using different set of observations. In Fig. 6 of Kim et al. (2017) below, it is shown that the largest difference in surface CO₂ flux between the two experiments (i.e., inversion experiments with and without Siberian JR station observations) occurs in June and July, which represent the active season of the terrestrial ecosystem with a large surface CO₂ flux uncertainty. This feature is also shown in Fig. 6 of Kim et al. (2018b) below. The optimized biosphere fluxes that are weekly cumulated for EB (Eurasian Boreal), ET (Eurasian Temperate), and TA (Tropical Asia) averaged over 2007-2009 show that the differences between experiments become greater from the summer, which implies that the absorption of vegetation in summer has a large impact on the results of each experiment.

25 Thus, we have revised 2nd paragraph of Section 2.3 and associated texts of Section 3.1 as follows. The added parts are underlined.

“Figure 2 shows the station-averaged time series of CO₂ mole fractions from real observations (OBS), EXTASI, SF1, and an average (i.e., simulated hypothetical observations: TRUE, hereafter) of EXTASI and SF1. The time series of EXTASI is the closest to that of OBS, whereas that of SF1 with a static scaling factor (i.e., 1) differs from OBS, particularly in summer. Kim et al. (2017, 2018b) have shown that the largest difference in surface CO₂ flux estimation between experiments with different settings appears in summer, which is associated with more sensitive response of inversion results to the inversion model configurations for the active season of the terrestrial ecosystem.”

“Regarding the BIAS, the three experiments have common variations that increase and decrease around zero, and have high amplitudes in summer compared to other seasons (Fig. 4b), which is associated with large uncertainties in the CO₂ mole fraction observations in summer shown in Fig. 2. In particular, CNTL_MOD (CNTL) shows the maximum positive BIAS of 23.74 (16.43) in early June. In contrast, the BIAS of REDIST is approximately 10.28 at the same time and maintains its value closest to zero among the three experiments. Considering the impact of BIAS on steady simulations of the model, the time series of BIAS also supports that the observation network of REDIST can perform more reliably in optimizing surface CO₂ fluxes in Asia compared to that of CNTL.

The RMSDs of all three experiments increase much in summer (Fig. 4c), which may be caused by large uncertainties in the CO₂ mole fraction observations in summer shown in Fig. 2.”

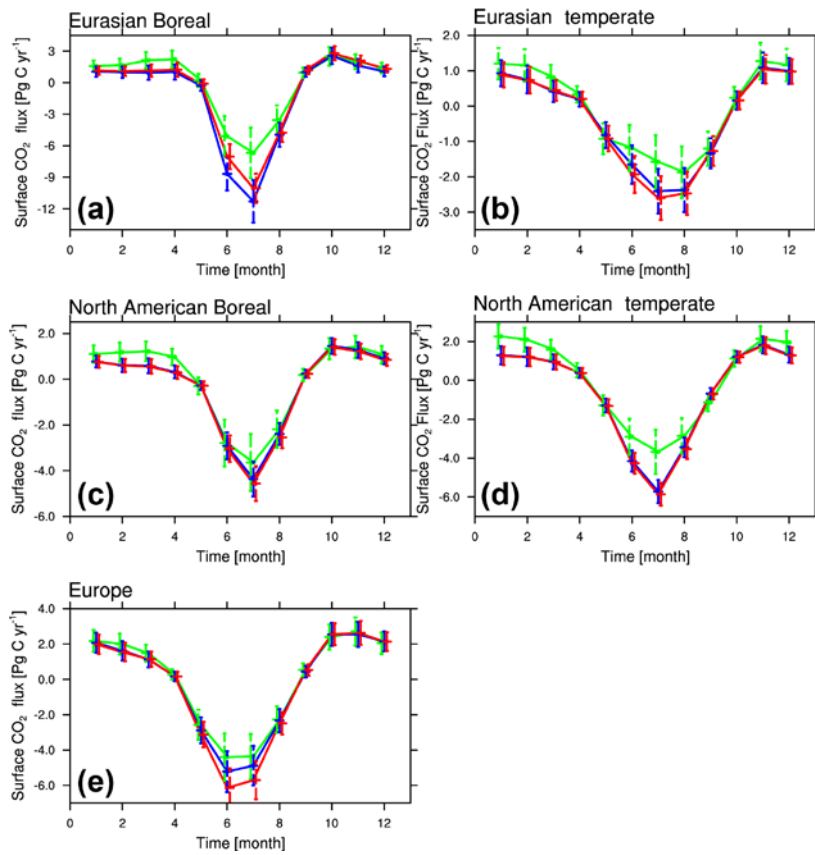


Figure 6. The monthly prior (green) and optimized biosphere fluxes averaged from 2002 to 2009 of the CNTL (blue) and JR (red) experiments with their uncertainties over the (a) Eurasian boreal, (b) Eurasian temperate, (c) North American boreal, (d) North American temperate, and (e) Europe. (Kim et al. 2017, ACP)

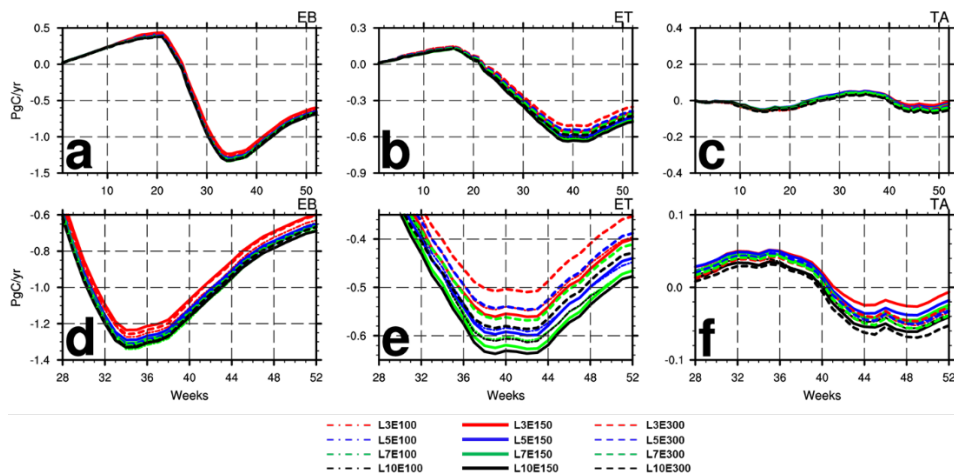


Figure 6. Weekly cumulative flux in: (a) EB, (b) ET, (c) TA region averaged over 2007-2009. (d), (e), and (f) are the magnifications of (a), (b), and (c) in the latter part of year, respectively. Note that EB, ET, and TA region use different scales in y-axis. (Kim et al. 2018b, APJAS)

5

4. Page 11, Line 24: *In addition to the ALL observation network, XCO2 observations of already operated satellites (ex. GOSAT, OCO-2) should be discussed as well as the expansion of the ground observation network.*

Author's response: The purpose of this study is showing the validity of the selection strategy (i.e., self-sensitivity and ecoregion information) for potential observation sites. Thus, we have examined these strategies using the ground observation sites. For the satellite observations, the self-sensitivity for the satellite observations are not well known yet. We have to know characteristics, spatial, and temporal distributions of self-sensitivities for satellite observations and how the self-sensitivities of satellite observations are different from those of the ground observations. Thus, the observation network design using both the ground observations and satellite observations will be studied in the future after the self-sensitivities for satellite observations are fully studied. In Section 4, we have added texts (underlined) considering this issue as follows.

“Although the simulation results showed an improvement in performance, the results also suggested that adding 10 extra observation sites in Asia may not be sufficient to fully optimize surface CO₂ fluxes, and more observation sites are required. Reliable observation data from some satellite sensors could supplement the model simulations on the basis of continuous surface observation sites. As the quality of satellite observation data increases, the observation network design for both surface and satellite observation data using the strategies (i.e., normalized self-sensitivity and ecoregion information) of this study will be investigated in the future.”

5. Page 13, Line 16-17: *Authors should clarify why RMSD grows in summer. Additional experiments using another hypothetical observation data closer to actual observation data may help. Other possible factors are meteorological conditions and rectifier effects.*

Author’s response: As the reviewer mentioned, the difference between hypothetical observations (TRUE) and real observations (OBS) is large in the summer, which causes the increase in summer RMSD in OSSE experiments.

15 We made hypothetical TRUE CO₂ mole fraction data different from OBS because we liked to produce hypothetical true data close to real data but not the same. The estimated model CO₂ mole fractions may represent or similar to the real observed CO₂ mole fractions, but they are constrained much by the real observation network. Thus, when we choose observation sites using several strategies, the experiment using the current observation network (i.e., CNTL in this study) has more benefits compared to other network designs. To be fairly compared the results from several network configurations, we have made hypothetical true CO₂ fraction data that is somewhat similar to the real feature but still hypothetical.

25 The large RMSD in summer is caused by the sensitivity of CO₂ flux estimated by inversions using different set of observations. In Fig. 6 of Kim et al. (2017) below, it is shown that the largest difference in surface CO₂ flux between the two experiments (i.e., inversion experiments with and without Siberian JR station observations) occurs in June and July, which represent the active season of the

terrestrial ecosystem with a large surface CO₂ flux uncertainty. This feature is also shown in Fig. 6 of Kim et al. (2018b) below. The optimized biosphere fluxes that are weekly cumulated for EB (Eurasian Boreal), ET (Eurasian Temperate), and TA (Tropical Asia) averaged over 2007-2009 show that the differences between experiments become greater from the summer, which implies that the absorption of vegetation in summer has a large impact on the results of each experiment.

Thus, we have revised 2nd paragraph of Section 2.3 and associated texts of Section 3.1 as follows. The added parts are underlined.

“Figure 2 shows the station-averaged time series of CO₂ mole fractions from real observations (OBS), EXTASI, SF1, and an average (i.e., simulated hypothetical observations: TRUE, hereafter) of EXTASI and SF1. The time series of EXTASI is the closest to that of OBS, whereas that of SF1 with a static scaling factor (i.e., 1) differs from OBS, particularly in summer. Kim et al. (2017, 2018b) have shown that the largest difference in surface CO₂ flux estimation between experiments with different settings appears in summer, which is associated with more sensitive response of inversion results to the inversion model configurations for the active season of the terrestrial ecosystem.”

“Regarding the BIAS, the three experiments have common variations that increase and decrease around zero, and have high amplitudes in summer compared to other seasons (Fig. 4b), which is associated with large uncertainties in the CO₂ mole fraction observations in summer shown in Fig. 2. In particular, CNTL_MOD (CNTL) shows the maximum positive BIAS of 23.74 (16.43) in early June. In contrast, the BIAS of REDIST is approximately 10.28 at the same time and maintains its value closest to zero among the three experiments. Considering the impact of BIAS on steady simulations of the model, the time series of BIAS also supports that the observation network of REDIST can perform more reliably in optimizing surface CO₂ fluxes in Asia compared to that of CNTL.

The RMSDs of all three experiments increase much in summer (Fig. 4c), which may be caused by large uncertainties in the CO₂ mole fraction observations in summer shown in Fig. 2.”

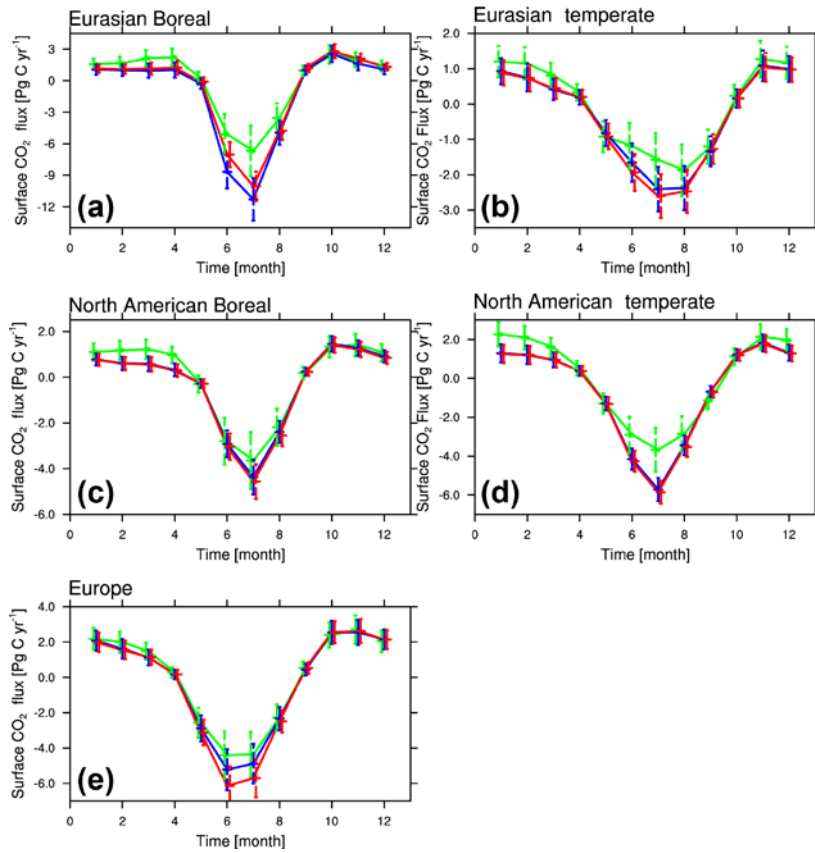


Figure 6. The monthly prior (green) and optimized biosphere fluxes averaged from 2002 to 2009 of the CNTL (blue) and JR (red) experiments with their uncertainties over the (a) Eurasian boreal, (b) Eurasian temperate, (c) North American boreal, (d) North American temperate, and (e) Europe. (Kim et al. 2017, ACP)

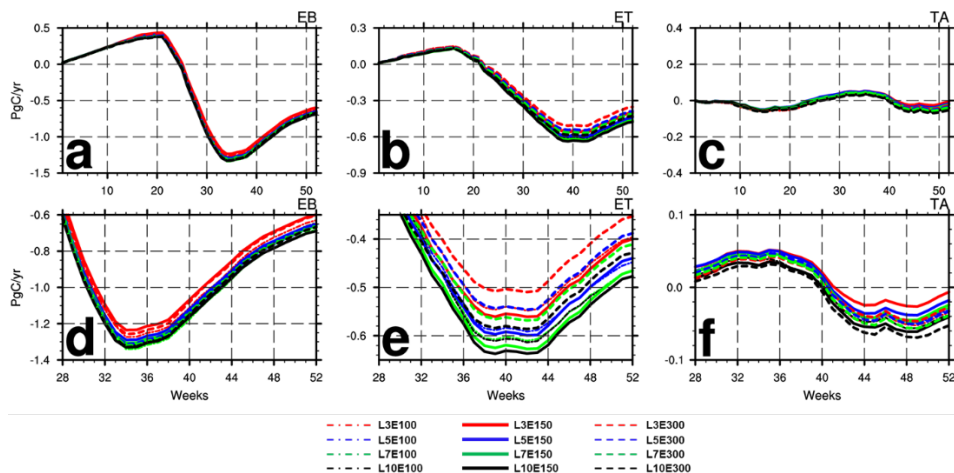


Figure 6. Weekly cumulative flux in: (a) EB, (b) ET, (c) TA region averaged over 2007-2009. (d), (e), and (f) are the magnifications of (a), (b), and (c) in the latter part of year, respectively. Note that EB, ET, and TA region use different scales in y-axis. (Kim et al. 2018b, APJAS)

5

6. Page 15, Section 3.2: *As already mentioned, the authors should evaluate the observation sites that are included in ObsPack and not assimilated in CT, in the sense that they are most feasible.*

Author's response: We have added the Section 3.6 that considers many observation sites registered in NOAA ObsPack. We also have added Figs. 11 and 12 in the Section 3.6. The results based on the observation sites registered in NOAA ObsPack are similar to those based on 7 observation sites used for CT2013B.

7. Page 16, Section 3.3: *As shown in general comments, authors should implement OSSE that assumes satellites in actual operation (data coverage, accuracy, etc.).*

15 **Author's response:** The purpose of this study is showing the validity of the selection strategy (i.e., self-sensitivity and ecoregion information) for potential observation sites. Thus, we have examined these strategies using the ground observation sites. For the satellite observations, the self-sensitivity

for the satellite observations are not well known yet. We have to know characteristics, spatial, and temporal distributions of self-sensitivities for satellite observations and how the self-sensitivities of satellite observations are different from those of the ground observations. Thus, the observation network design using both the ground observations and satellite observations will be studied in the future after the self-sensitivities for satellite observations are fully studied. In Section 4, we have added texts (underlined) considering this issue as follows.

“Although the simulation results showed an improvement in performance, the results also suggested that adding 10 extra observation sites in Asia may not be sufficient to fully optimize surface CO₂ fluxes, and more observation sites are required. Reliable observation data from some satellite sensors could supplement the model simulations on the basis of continuous surface observation sites. As the quality of satellite observation data increases, the observation network design for both surface and satellite observation data using the strategies (i.e., normalized self-sensitivity and ecoregion information) of this study will be investigated in the future.”

8. Page 18, Line 1-2: Authors should consider and show the reason (There are other similar examples).

Author’s response: The SS strategy determines the potential observation sites based on SS values. The SS values can be concentrated in relatively small area, or in certain ecoregions. This concentration of large SS values can cause few observation sites in other ecoregions since we have a limited number of observation sites as an addition constraint. Thus, the SS strategy can cause a larger bias in certain period. To clarify, we have revised the text as follows. The added and revised parts are underlined.

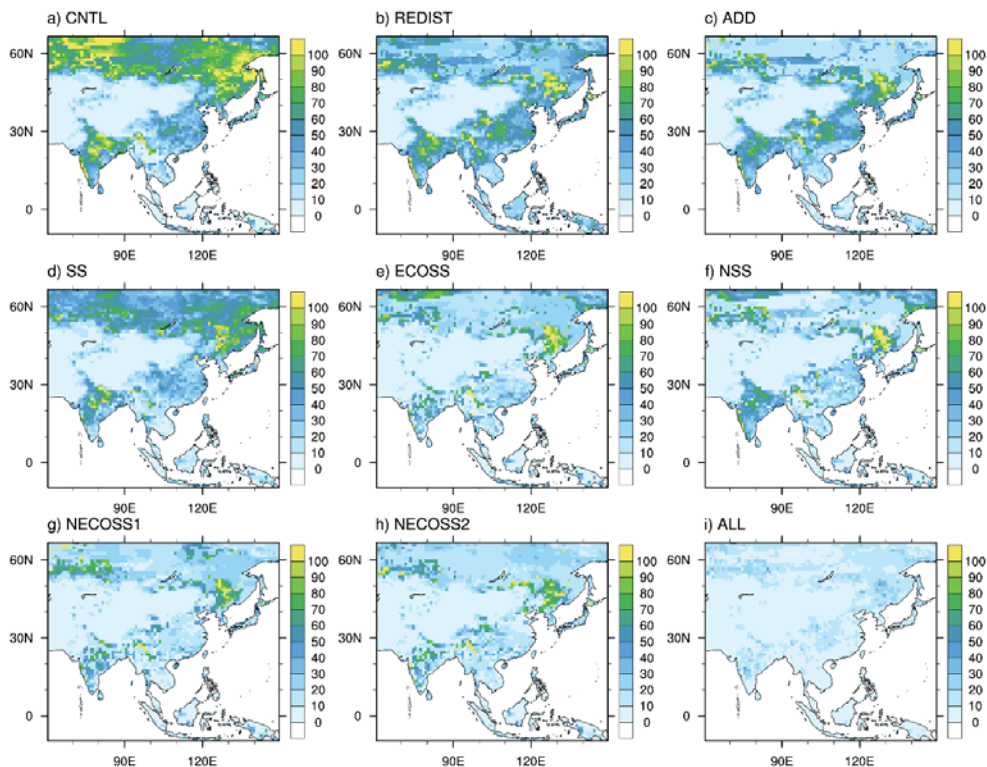
“However, the BIAS of SS shows a sudden increase in early June, with a maximum positive BIAS of 21.79 (Fig. 7b), which is associated with concentrated sites by large SS values in certain ecoregions that cause not enough DA in other ecoregions. Although the BIAS of ECOSS is generally closer to 0 than that of ADD, except in July, ECOSS shows the maximum negative BIAS of -15.78 in late July. These tendencies suggest that the DA method that optimizes parameters such as the scaling factor

used in CT2013B may occasionally have trouble in optimizing surface CO₂ fluxes when using limited observation sites for a larger area.”

9. Page 20, Section 3.5: *Authors should show summer RMSD of surface CO₂ fluxes and discuss their features.*

Author’s response: Following the reviewer’s suggestion, we investigated the summer (from June to August) RMSD of surface CO₂ fluxes (Fig_rev2). Although the magnitude of the summer RMSD is stronger than that of all year (Fig. 9 in the manuscript), the characteristics of the spatial distributions for all year and for three months in summer are very similar. Since the summer RMSD governs the RMSD of all year, they are similar. Thus, we have not included the Figure for summer RMSD in the revised manuscript. Instead, we have included the text below at the end of the first paragraph of Section 3.5.

“The spatial RMSD distribution during the summer from June to August (not shown) is also similar to that for whole year shown in Fig. 9.”



Figure_rev2. The spatial distribution of the average of weekly RMSD of surface CO₂ fluxes (gC m⁻² yr⁻¹) from June to August for a) the CNTL, b) the REDIST, c) the ADD, d) the SS, e) the ECOSS, f) the NSS, g) the NECOSS1, h) the NECOSS2, and i) the ALL experiments.

5

10. Table 3-6: Since Ecoregion Index is difficult to understand intuitively, authors should include the region number and vegetation type.

Author's response: Following the reviewer's suggestion, we have added Transcom region and ecosystem type information in Tables 3, 4, and 5.

10

11. Figure 1: The authors should specify Transcom region boundaries in Asia. If the vegetation type can be illustrated, it is still preferable.

Author's response: Following the reviewer's suggestion, we have included the map of Transcom regions and ecoregions for Asia in Fig. 1b. We also have added Transcom region information in Tables 3, 4, and 5.

5 References

- Byrne, B., Jones, D. B. A., Strong, K., Zeng, Z. C., Deng, F. and Liu, J.: Sensitivity of CO₂ surface flux constraints to observational coverage, *J. Geophys. Res. Atmos.*, 122(12), 6672–6694, doi:10.1002/2016JD026164, 2017.
- Kim, H., Kim, H. M., Kim, J. and Cho, C.-H.: Effect of data assimilation parameters on the optimized surface CO₂ flux in Asia, *Asia-Pacific J. Atmos. Sci.*, 54(1), 1–17, doi:10.1007/s13143-017-0049-9, 2018b.
- Kim, J., Kim, H. M., Cho, C. H., Boo, K. O., Jacobson, A. R., Sasakawa, M., Machida, T., Arshinov, M. and Fedoseev, N.: Impact of Siberian observations on the optimization of surface CO₂ flux, *Atmos. Chem. Phys.*, 17(4), 2881–2899, doi:10.5194/acp-17-2881-2017, 2017.
- Patra, P. K., Maksyutov, S. and TransCom-3 modelers: Sensitivity of optimal extension of observation networks to the model transport, *Tellus B*, 55, 498– 511, 2003.
- Wang, Y., Broquet, G., Ciais, P., Chevallier, F., Vogel, F., Wu, L., Yin, Y., Wang, R. and Tao, S.: Potential of European 14 CO₂ observation network to estimate the fossil fuel CO₂ emissions via atmospheric inversions, *Atmos. Chem. Phys.*, 185194(July), 4229–4250, doi:10.5194/acp-18-4229-2018, 2018.
- Yang, E.-G., H. M. Kim, J. Kim, and Kay J. K.: Effect of observation network design on meteorological forecasts of Asian dust events, *Monthly Weather Review*, 142, 4679-4695, doi:10.1175/MWR-D-14-00080.1, 2014.

Design and evaluation of CO₂ observation network to optimize surface CO₂ fluxes in Asia using observation system simulation experiments

Jun Park¹ and Hyun Mee Kim¹

¹Atmospheric Predictability and Data Assimilation Laboratory, Department of Atmospheric Sciences,
5 Yonsei University, Seoul, Republic of Korea

Correspondence to: Hyun Mee Kim (khm@yonsei.ac.kr)

Abstract. Continuous efforts have been made to monitor atmospheric CO₂ mole fractions as it is one of
10 the most influential greenhouse gases in Earth's atmosphere. The atmospheric CO₂ mole fractions are
mostly determined by CO₂ exchanges at the Earth's surface (i.e., surface CO₂ flux). Inverse modeling,
which is ~~a one-of-the~~ methods to estimate the CO₂ exchanges at the Earth's surface~~carry out such
monitoring~~, derives ~~estimated CO₂ mole fractions in the air from calculated~~ surface CO₂ carbon fluxes
using model and observed atmospheric CO₂ mole fraction data. Although observation data is crucial for
15 successful modeling, comparatively fewer in-situ observation sites are located in Asia compared to
Europe or North America. Based on the importance of the terrestrial ecosystem of Asia for global carbon
exchanges, more observation stations and an effective observation network design are required. In this
paper, several observation network experiments were conducted to optimize the surface CO₂ carbon flux
of Asia using CarbonTracker and observation system simulation experiments (OSSEs). The impacts of
20 the redistribution of and additions to the existing observation network of Asia were evaluated using
hypothetical in-situ observation sites. In the case of the addition experiments, 10 observation stations,
which is a practical number for real implementation, were added through three strategies: random addition,
the influence matrix (i.e., self-sensitivity), and ecoregion information within the model. The simulated
surface CO₂ carbon flux in Asia in summer can be improved by redistributing the existing observation
25 network. The addition experiments revealed that considering both the distribution of normalized self-
sensitivity and ecoregion information can yield better simulated surface CO₂ carbon fluxes compared to
random addition, regardless of the season. This study provides a diagnosis of the existing observation
network and useful information for future observation network design in Asia to estimate the surface

CO₂carbon flux, and also suggests the use of an influence matrix for designing CO₂carbon observation networks. Unlike other previous observation network studies with many numerical experiments for optimization, comparatively fewer experiments were required in this study. Thus, the methodology used in this study may be used for designing observation networks for monitoring greenhouse gases at both
5 continental and global scales.

1. Introduction

CO₂ is one of the most influential greenhouse gases in Earth's atmosphere (Lacis et al., 2010). Thus, monitoring CO₂ is very important to understand and constrain CO₂ in the atmosphere. To monitor atmospheric CO₂ precisely, continuous efforts are necessary. Inverse modeling, one of the methods to
10 complete this mission, uses observed atmospheric CO₂ mole fraction ~~observation~~-data and transport models to estimate the sources and sinks of surface CO₂carbon flux ~~and associated atmospheric CO₂ mole fractions~~ (Enting, 2002; Gurney et al., 2002). Bayesian synthesis (Enting, 2002), four dimensional variational data assimilation methods (4DVar; Chevallier et al., 2009a, 2009b, 2010; Kou et al., 2017), and Ensemble Kalman Filter (EnKF; Peters et al., 2005, 2007, 2010; Feng et al., 2009, 2016; Kang et al.,
15 2011, 2012; Peylin et al., 2013; Kim et al., 2014a, 2014b, 2017, 2018a, 2018b) have been implemented and utilized to conduct inverse modeling. By comparing 13 inverse modeling systems, Peylin et al. (2013) showed that simulation results were similar to each other for regions with many observations, but dissimilar for regions with sparse observation coverage (e.g. the tropics and southern hemisphere).

The terrestrial system in the northern hemisphere is crucial for global carbon exchanges, and Asia
20 covers the largest area in the northern hemisphere (Hayes et al., 2011; Le Quéré et al., 2018). Asia also includes the Siberian region, which represents one of the significant areas for sources and sinks of atmospheric CO₂ (Schulze et al., 1999; Houghton et al., 2007; Tamocai et al., 2009; Kurganova et al., 2010; Schepaschenko et al., 2011; Siewert et al., 2015). Thus, the precise estimation of the surface CO₂carbon flux in Asia is highly necessary and required to fully understand global carbon exchanges.
25 However, comparatively fewer in-situ observation sites are located in Asia compared to Europe and North America. Although the Center for Global Environmental Research (CGER) of the National Institute for Environmental Studies (NIES) in Japan, collaborating with the Russian Academy of Science (RAS), has

built nine tower observation sites (Japan-Russia Siberian Tall Tower Inland Observation Network, JR-STATION) in Asia, and several studies have been conducted using continuously observed atmospheric CO₂ and CH₄ mole fractions since 2002 (Saeki et al., 2013; Sasakawa et al., 2010, 2013; Kim et al., 2017), the towers of the JR-STATION are mainly located in the Siberian region. In addition, eight stations
5 of the JR-STATION are located in western Siberian. These JR-STATION sites, therefore, do not seem to be well-suited for optimizing the surface ~~CO₂carbon~~ flux for the entire Asia region, and in-situ observation sites in Asia are still fewer compared to those in Europe or North America, even when the JR STATION sites are considered.

In the meantime, the satellite-retrieved dry-air column-average mole fraction of CO₂ (XCO₂) could
10 be used to supplement observations in the sparse observation regions, including Asia (Chevallier et al., 2009a, 2009b, 2010; Maksyutov et al., 2013; Reuter et al., 2014; Feng et al., 2016). However, by comparing CO₂ mole fractions observed in four World Meteorological Organization (WMO) Global Atmosphere Watch (GAW) stations in China to satellite-retrieved products from the Greenhouse Gases Observing Satellite (GOSAT), Cheng et al. (2018) reported that satellite-retrieved CO₂ mole fractions
15 showed similar seasonal variations to those of in-situ observations but the magnitudes retrieved from the satellite were comparatively lower than those of in-situ observations. Assimilating XCO₂ data alone is therefore generally less effective than assimilating in-situ observations (Chevallier et al., 2009a; ~~Fischer et al., 2017~~). In contrast, Maksyutov et al. (2013) noted that uncertainties in surface CO₂ flux estimations in sparse in-situ observation regions could be reduced when in-situ observations and GOSAT observation
20 data were used simultaneously. In particular, Fischer et al. (2017) showed that uncertainties in surface CO₂ flux estimation could be further decreased, even for the regions with in-situ observation sites, when in-situ observations and satellite-retrieved observations are used together. Thus, in-situ observation networks need to be well established to better utilize non in-situ observations like XCO₂.

Observation system simulation experiments (OSSEs), using simulated observation data, provide an
25 opportunity to evaluate the impact of observation data from the current and potential observation sites on the performance of the modeling system (~~Patra et al., 2003~~; Yang et al., 2014; Byrne et al., 2017; Wang et al., 2018; ~~Wu et al., 2018~~). Thus, OSSE can be used to evaluate the performance of current observation networks and to design future observation networks. Although several studies have been conducted to

achieve this aim, most observation network design studies were restricted to comparatively smaller national scales such as Australia, California in the USA, and South Africa (Ziehn et al. 2014, 2016; Lucas et al., 2015; Nickless et al., 2015). As potential observation sites are few in these studies due to the relatively small study area, these studies suggest an optimized network derived from a myriad of calculations using the incremental optimization (IO) and the genetic algorithm (GA). Due to time and computing restraints, the IO and GA methods seem ineffective or unfeasible for designing the observation network on continental scales like Asia. In addition, determining and redistributing all observation sites at once using the IO and GA methods may not be practical for most regions with existing observation sites. Adding or redistributing some sites given existing observation sites may be a more practical way to design the observation network.

The influence matrix (i.e., analysis sensitivity or self-sensitivity) denotes the sensitivity of the analysis to the observations (Cardinali et al., 2004; Liu et al., 2009; Kim et al. 2014a; Kim et al. 2017). Similar to the numerical weather prediction (NWP), the relative impact of each CO₂ mole fraction observation for the model analysis equivalent CO₂ mole fraction induced by the optimized surface CO₂carbon flux can be calculated (Kim et al., 2014a, 2017) and used as a strategy for selecting potential sites of CO₂ mole fraction observations. The influence matrix would be a very efficient and intelligent strategy to select observation sites because the calculated impact of observation on the CO₂ estimation is used to select observation sites. Although Wang et al. (2018) showed the potential impact of adding observation sites on the existing ¹⁴CO₂ sites in Europe using OSSEs, ~~they considered the potential ¹⁴CO₂ a considerable number of~~ observation sites were not chosen based on, which does not specific selection strategies. seem to be feasible in the near future. Moreover, studies on diagnosing the current CO₂ mole fraction observation network and evaluating the impact of adding and redistributing in-situ CO₂ mole fraction observation sites in Asia are few up to this time. Considering the importance of the Asia region for global carbon exchange, studies on the observation network design in Asia to accurately estimate the surface CO₂carbon flux are highly necessary. Such observation network studies could also provide helpful information for researchers and administrators who design the future observation network under practical conditions.

In this study, many OSSEs were conducted using CarbonTracker (CT) to identify a better in-situ observation network for the purpose of optimizing surface CO₂carbon flux estimation in Asia. Based on the hypothetical simulated observations, redistribution and addition experiments were performed to evaluate the performance of the existing observation network and the impact of additional observation sites, respectively. In the case of addition experiments, random addition and addition based on influence matrix (self-sensitivity) as well as ecoregion information of the model were considered as strategies, as alternatives to IO and GA that have been used in previous studies. Section 2 briefly introduces the CT, influence matrix, hypothetical observations, experimental framework, and verification methods. Section 3 presents the results of the observation network design experiments, and Sect. 4 provides a summary and the conclusions of this study.

2. Methodology

2.1 CarbonTracker and data assimilation methods

CT2013B, developed by the Earth System Research Laboratory (ESRL) at the National Oceanic and Atmospheric Administration (NOAA), was used for this study. CT2013B estimates the surface CO₂carbon flux using inverse modeling and has been widely used to calculate surface CO₂carbon fluxes in North America, Europe, and Asia (Peters et al., 2004, 2005, 2007, 2010; Kim et al., 2012, 2014a, 2014b, 2017; Cheng et al., 2013; Kim et al., 2016, 2018a, 2018b).

CT2013B consists of a priori flux modules, a transport model (TM5), observation data, and EnKF data assimilation. The estimated surface CO₂ fluxes are mainly calculated by scaling fluxes from the flux modules composed of biosphere, ocean, fossil fuel, and fire fluxes. The optimized grid-point surface CO₂ fluxes within TM5 were derived as follows:

$$F(x, y, t) = \lambda_r \cdot F_{\text{bio}}(x, y, t) + \lambda_r \cdot F_{\text{ocean}}(x, y, t) + F_{\text{ff}}(x, y, t) + F_{\text{fire}}(x, y, t) \quad (1)$$

where $F_{\text{bio}}(x, y, t)$, $F_{\text{ocean}}(x, y, t)$, $F_{\text{ff}}(x, y, t)$, and $F_{\text{fire}}(x, y, t)$ denote a priori emissions of the biosphere, ocean, fossil fuel, and fires, respectively; λ_r is the scaling factor with a 1-week resolution for

ecoregions; x , y , and t denote the zonal direction, the meridional direction, and time, respectively. λ_r is used for optimization of the surface CO₂ flux through interactions with a priori emissions of the biosphere and the ocean. Thus, EnKF data assimilation in CT2013B optimizes not surface CO₂ fluxes but the scaling factor. This means that the optimization of the scaling factors that were assigned to the 240-ecoregions of the earth is crucial for the estimation of simulated surface CO₂ fluxes. The ecoregions are defined as the mix of the modified 19 vegetation types from Olson et al. (1992) and 11 Transcom regions (Gurney et al., 2002) on land, with 30 ocean regions. As all 19 vegetation types are not used for the 11 Transcom regions, the number of effective ecoregions of the earth is 156 (Peters et al., 2010).

TM5 is an off-line transport model used to calculate the transport of CO₂ (Krol et al., 2005), which utilizes the atmospheric fields of the ERA-interim reanalysis data of the European Centre for Medium-Range Weather Forecasts (ECMWF). TM5 utilizes the estimated surface CO₂ fluxes at each grid-point suggested in Eq. (1) to calculate the spatiotemporal distribution of the model atmospheric CO₂ concentrations. ~~In addition, from this spatiotemporal CO₂ distribution, In addition, it also calculates~~ the model atmospheric CO₂ concentrations at the counterparts corresponding to the sometimes and locations and time of the observation data are calculated, and these are which are used for the data assimilation process. The horizontal resolution of TM5 is 3° x 2° globally and the nested horizontal grid is 1° x 1° over Asia, with verification region inside of the nested domain over Asia (Fig. 1). The number of ecoregions of the verification region is 40, in which 36 are the Asian ecoregions and 4 are the ecoregions of Europe. Since the proportion of the 4 European ecoregions is approximately 0.5% of the verification region (Table 3), the verification region was considered to be located over Asia. A two-way nested grid was used to optimize surface CO₂ fluxes in Asia. The model run including both forward and inversion runs was done globally with nesting over Asia and verification was done over the verification region located in Asia. A two-way nested grid was used in this study to optimize surface CO₂ fluxes in Asia (Fig. 1). Table 1 summarizes the priori flux emissions used for the flux module and describes the TM5 setup.

An Ensemble Square Root Kalman Filter (EnSRF), one of the EnKF data assimilation methods (Evensen, 1994; Whitaker and Hamill, 2002), was employed in this study to optimize the scaling factor.

EnSRF assimilates observation data one by one, and updates the analysis of ensemble mean and perturbations separately based on the following equations as:

$$\bar{\mathbf{x}}_t^a = \bar{\mathbf{x}}_t^b + \mathbf{K}(\mathbf{y}^o - \mathbf{H}(\bar{\mathbf{x}}_t^b)), \quad (2)$$

$$5 \quad \mathbf{x}'_i^a = \mathbf{x}'_i^b - \tilde{\mathbf{k}}\mathbf{H}(\mathbf{x}'_i^b), \quad (3)$$

where \mathbf{x}^a and \mathbf{x}^b describe the analysis and background value of the state vector (\mathbf{x}); $\bar{\mathbf{x}}$ and \mathbf{x}' are the ensemble mean and perturbation of the state vector; \mathbf{y}^o is the observation vector; and \mathbf{H} describes the observation operator that transforms the state vector from the model space to the observation space. TM5
 10 acts as the observation operator in CT2013B (Krol et al., 2005; Peters et al., 2005; Kim et al., 2016, 2018a). \mathbf{K} and $\tilde{\mathbf{k}}$ denote the Kalman gain matrix and the reduced Kalman gain calculated as:

$$\mathbf{K} = (\mathbf{P}_\xi^b \mathbf{P}^b \mathbf{H}^T) (\mathbf{H} \mathbf{P}^b \mathbf{H}^T + \mathbf{R})^{-1}, \quad (4)$$

$$15 \quad \tilde{\mathbf{k}} = \mathbf{K} \cdot \alpha, \quad (5)$$

Where \mathbf{P}_ξ^b , \mathbf{P}^b is is the background error covariance; \mathbf{R} is the observation error covariance for each observation; and α is a scalar value that is multiplied to Kalman gain matrix at every calculation of the analysis, defined as:

20

$$\alpha = \left(1 + \sqrt{\frac{\mathbf{R}}{\mathbf{H} \mathbf{P}_\xi^b \mathbf{H}^T \mathbf{P}^b \mathbf{H}^T + \mathbf{R}}}\right)^{-1}. \quad (6)$$

By calculating the ensemble mean and perturbation independently, the underestimation of the analysis
 25 error covariance could be prevented (Whitaker and Hamill, 2002; Kim et al., 2012). $\mathbf{P}^b \mathbf{H}^T$, $\mathbf{P}_\xi^b \mathbf{H}^T$ and $\mathbf{H} \mathbf{P}_\xi^b \mathbf{H}^T \mathbf{P}^b \mathbf{H}^T$ can be calculated as:

$$\mathbf{PH}^T \approx \frac{1}{m-1} (\mathbf{x}'_1, \mathbf{x}'_2, \dots, \mathbf{x}'_m) \cdot (\mathbf{Hx}'_1, \mathbf{Hx}'_2, \dots, \mathbf{Hx}'_m)^T, \quad (7)$$

$$\mathbf{HP}^b \mathbf{H}^T \approx \frac{1}{m-1} (\mathbf{Hx}'_1, \mathbf{Hx}'_2, \dots, \mathbf{Hx}'_m) \cdot (\mathbf{Hx}'_1, \mathbf{Hx}'_2, \dots, \mathbf{Hx}'_m)^T, \quad (8)$$

5 where m is the number of ensemble members.

Unlike the approach of NWP, the time for CO₂ dispersing around the atmosphere needs to be considered for ~~CO₂ carbon~~ data assimilation. Accordingly, a time lag is introduced in updating the scaling factor during the data assimilation process to consider the information for analysis time as well as for pre-analysis time. A time lag of five weeks is employed in this study, consistent with previous studies (Peters et al., 2007, 2010, Kim et al., 2012, 2014a, 2014b, 2017).

In the EnSRF, the covariance localization method is necessary to reduce the impact of the sampling error due to the limited size of the ensemble and to avoid filter divergence due to the underestimation of the background error covariance (Houtekamer and Mitchell, 2001). Because calculating the physical distance between scaling factors is not feasible, instead of the covariance localization method, a
 15 statistical method is applied in this study ~~because calculating the physical distance between scaling factors is not feasible~~. In this method, a Student's t test is applied on the correlations between the ensemble of the model CO₂ concentrations and the ensemble of the scaling factors, and the Kalman gain matrix is then made to be zero for the cases where it has an insignificant statistical t value (i.e. 95 % significance level), to exclude those insignificant impacts (Peters et al., 2007).

20 The optimized mean scaling factor after one analysis cycle is used as one of the prior mean scaling factors for the next analysis step as:

$$\lambda_t^b = \left(\frac{\lambda_{t-2}^a + \lambda_{t-1}^a + 1}{3} \right), \quad (9)$$

25 where, λ_t^b is a prior mean scaling factor for the current analysis step; and λ_{t-2}^a and λ_{t-1}^a denote posterior mean scaling factors of previous analysis cycles. The information of current analysis propagates to the next step using Eq. (9) (Peters et al., 2007).

2.2 Influence matrix

The influence matrix of the EnKF system can be calculated as described in Liu et al. (2009) and Kim et al. (2014a). The analysis of the state vector and the influence matrix (\mathbf{S}^o) that shows the contribution of the observation vector (\mathbf{y}^o) to the analysis at the observation space (\mathbf{y}^a) (i.e., the projection of analysis state vector \mathbf{x}^a on the observation space or model analysis equivalent to observations at observation locations) can be defined as:

$$\mathbf{x}^a = \mathbf{K}\mathbf{y}^o + (\mathbf{I}_n - \mathbf{K}\mathbf{H})\mathbf{x}^b, \quad (10)$$

$$10 \quad \mathbf{S}^o = \frac{\partial \mathbf{y}^a}{\partial \mathbf{y}^o} = \mathbf{K}^T \mathbf{H}^T = \mathbf{R}^{-1} \mathbf{H} \mathbf{P}^a \mathbf{H}^T, \quad (11)$$

where, \mathbf{I}_n is the identity matrix with corresponding to the size of n -dimensional analysis state vector ~~observation~~. The influence matrix is proportional to the analysis error covariance and inversely proportional to the observation error covariance. Using Eq. (8), \mathbf{S}^o is expressed as:

$$15 \quad \mathbf{S}^o = \mathbf{R}^{-1} \mathbf{H} \mathbf{P}^a \mathbf{H}^T = \frac{1}{m-1} \mathbf{R}^{-1} (\mathbf{H} \mathbf{X}^a) (\mathbf{H} \mathbf{X}^a)^T, \quad (12)$$

where $\mathbf{H} \mathbf{X}^a$ is the analysis of the ensemble perturbation at the observation space. The i th component of $\mathbf{H} \mathbf{X}^a$ is defined as:

$$20 \quad \mathbf{H} \mathbf{X}_i^a \cong h(\mathbf{x}_i^a) - \frac{1}{m} \sum_{i=1}^m h(\mathbf{x}_i^a), \quad (13)$$

where \mathbf{x}_i^a is the i th member of the analysis ensemble; and $h(\cdot)$ denotes the linearized or non-linearized observation operators. If there are no correlations between observation errors, the diagonal element of this influence matrix (i.e. self-sensitivity) is calculated as:

$$\mathbf{S}_{jj}^o = \frac{\partial y_j^a}{\partial y_j^o} = \left(\frac{1}{m-1} \right) \frac{1}{\sigma_j^2} \sum_{i=1}^m (\mathbf{HX}_i^a)_j \cdot (\mathbf{HX}_i^a)_j, \quad (14)$$

where σ_j^2 is the observation error variance for the j th observation.

According to Liu et al. (2009) and Kim et al. (2014a), \mathbf{S}^o represents the sensitivity of the analysis state vector \mathbf{y}^a to the observation state vector \mathbf{y}^o in the observation space (i.e., location). \mathbf{S}^o has a value between 0 and 1, which shows the contribution of an CO_2 observation to the analyzed CO_2 at the observation sites. If \mathbf{S}^o is close to 0, the analysis is mainly derived from the background. In contrast, the influence of observation data to the analysis increases as \mathbf{S}^o goes to 1. The self-sensitivity was used as a criterion for selecting the observation locations in designing the observation network.

10

2.3 Simulated hypothetical observation and experimental setup

In this paper, simulated hypothetical observations were created and used to design the observation network. Simulated hypothetical observations with similar values and seasonal variations compared to real CO_2 observations were generated by averaging combining two model CO_2 mole fractions from the experiment conducted with real NOAA observation data (EXTASI) and model CO_2 mole fractions from the experiment with a fixed scaling factor of 1 (SF1). In EXTASI experiment, the real CO_2 mole fraction data were used to update the scaling factors in Eq. (1) to estimate the surface CO_2 fluxes. In contrast, in SF1 experiment, the scaling factors were fixed as 1.

15

Figure 2 shows the station-averaged time series of CO_2 mole fractions from real observations (OBS), EXTASI, SF1, and an average (i.e., simulated hypothetical observations: TRUE, hereafter) of EXTASI and SF1 (i.e., simulated hypothetical observations: TRUE, hereafter). The time series of EXTASI is the closest to that of OBS, whereas that of SF1 with a static scaling factor (i.e., 1) differs from OBS, particularly in summer. Kim et al. (2017, 2018) have shown that the largest difference in surface CO_2 flux estimation between experiments with different settings appears in summer, which is associated with more sensitive response of inversion results to the inversion model configurations for the active season of the terrestrial ecosystem. The time series of TRUE is located between that of EXTASI and SF1, which implies that the difference between TRUE and OBS is smaller compared with that between SF1 and OBS. TRUE

25

is the simulated hypothetical observation that is similar to the EXTASI assimilating real NOAA observation data, but is not the same as the EXTASI. This setup prevents EXTASI from having an advantage in the observation network experiments. If TRUE is the same as EXTASI, then assimilating TRUE data at the observation locations used in EXTASI would render the observation network used in
5 EXTASI the optimal network in terms of several verification measures used in this study.

Each hypothetical observation site has one CO₂ observation per day and exists within the limited Asia domain shown in Fig. 1. ~~On the basis of the nautical time zone, t~~The simulated values around afternoon
(i.e., 13 ~~local standard time (LST)~~LST) in the mid-latitudes in the northern hemisphere are averaged and
utilized as TRUE data. The observation height of TRUE data at each site is set to 5 meters greater than
10 the model elevation of the grid-point in order to use the observation operator for flask observation
developed in NOAA. Moreover, each observation site is more than 1,000 km apart from other sites,
located lower than 2,000 meters above sea level, and located on the land regions in the Transcom Region
from Gurney et al. (2002). This configuration was made to consider real-world constraints to optimize
the surface ~~CO₂carbon~~ fluxes in Asia. Model-data-mismatch (MDM) (i.e., observation error) for CO₂
15 observation was set to 3 ppm, consistent with the previous setting of 3 ppm for continuous observation
site types (Peters et al., 2007; Kim et al., 2014b, 2017).

All simulation results were produced under identical conditions except for the observation locations
and data. 150 ensemble members were used for data assimilation, and experiments were carried out from
27 September 2007 to 4 January 2009. The first three months of the experiments were considered as the
20 spin-up period, thus the analysis was conducted from 27 December 2007 to 4 January 2009.

As the experimental results depend on the distribution of observation sites, appropriate choices of the
observation network are important. Experiments are therefore configured to investigate the impact of
redistributing observation sites of CT2013B (hereafter, existing observation sites or network) and that of
adding extra observation sites to the existing observation network based on random, self-sensitivity, and
25 ecoregion information. Figure 3 shows the hypothetical observation networks used in this study. Figure
3a presents the distribution of seven observation sites in Asia from the observation network of CT2013B,
which are mostly located between 30 °N and 45 °N. The experiment and simulation results using this
observation network were denoted as CNTL. Since the CNTL could have disadvantages due to the use of

real observation information (i.e. the observation height of simulated sites are always above 5 meters from model topography, but this is not the case for CNTL), an additional experiment identical to CNTL, except that the observation heights were assigned above 5 meters from the model topography in the same way as for hypothetical observations, was also conducted and denoted as CNTL_MOD. Figures 3b, c, and d show the distribution of three observation networks, in which the seven observation sites in Asia are randomly redistributed. To obtain general results without sampling error, each random redistribution experiment was performed three times with different sets of randomly distributed observation sites, as denoted in previous observation network studies (e.g., Yang et al. 2014). The average of three random redistribution experiments was denoted as REDIST, to check the impact of the reallocation of the existing observation network.

Figures 3e-m suggest the distributions of the observation networks to examine the impact of adding additional observation sites to the existing observation network. The 10 extra observation sites were added as this number seems realistically viable for the future, considering the cost of operating and maintaining CO₂ observation sites. Specifically, Figures 3e-h show the distribution of three observation networks with additional 10 observation sites added randomly to the existing observation network. The average of these three experiments was denoted as ADD. The experiment adding 10 observation sites to the existing observation network based on self-sensitivity is denoted as the SS experiment (Fig. 3h). The experiment adding 10 observation sites to the existing observation network based on both self-sensitivity and ecoregion information is denoted as the ECOSS experiment (Fig. 3i). The ECOSS experiment was conducted as the scaling factor in CT2013B is updated based on ecoregion, thus only considering self-sensitivity makes the added observation sites cluster in a specific ecoregion and causes disadvantages in optimizing the scaling factor. As the self-sensitivity is generally inversely proportional to the number of assimilated observations (Kim et al., 2014a; 2017), the self-sensitivity normalized by the number of assimilated observations is also considered and utilized. Figures 3j-l show the distributions of the observation network for three experiments that used the normalized self-sensitivity as the selection criterion for added observation sites. The NSS experiment (Fig. 3j) used only the normalized self-sensitivity as the selection strategy. The observation sites of the NECOSS1 (Fig. 3k) and NECOSS2 (Fig. 3l) experiments were added based on the normalized self-sensitivity and ecoregion information. The

NECOSS1 experiment allocated one or two observation sites per ecoregion, whereas NECOSS2 allocated one observation site per ecoregion. In addition, the observation networks that have observation sites at every 2° intervals on the land (Fig. 3m, ALL experiment) are suggested as the reference to examine the maximum possible impact of additional observation sites. In ALL experiment, the observation locations that are located 2000 m above the mean sea level over the Tibetan Plateau are not included due to difficult accessibility and maintenance as practical observing sites.

The normalized self-sensitivity for j th observation is defined as:

$$NS_{jj}^0 = \frac{N_j}{N_{ALL}} \times S_{jj}^0, \quad (15)$$

where N_{ALL} denotes the total count of observation sites of the ALL experiment; and N_j is the number of observation sites that have the same ecoregion as the j th observation site in the ALL experiment. Thus, normalized self-sensitivities were calculated by multiplying self-sensitivities by the ratio of the number of observation sites in a specific ecoregion to that in the ALL experiment.

The effect of the redistribution of the existing observation network and adding additional observation sites on the existing observation network can be diagnosed through the experiments detailed above. The method of adding observation sites in the experiments using self-sensitivity and ecoregion information is described in more detail in Sect. 3. Table 2 describes the list of observation network experiments and their relevant information.

2.4. Verification method

The nested model domain over Asia and the verification area (-9.5°S – -66.5°N, 60.5°E – 149.5°E) are shown in Fig. 1. The optimized surface CO₂ flux in each experiment was verified against the hypothetical surface CO₂ fluxes corresponding to TRUE. Weekly surface CO₂ fluxes were analyzed to evaluate the performance of observation network experiments because the scaling factor has a weekly resolution. The Pearson product-moment correlation coefficient (Pattern Correlation; PC), the bias (BIAS), and the root mean square difference (RMSD) were compared and calculated as:

$$PC = \frac{\sum_{i=1}^n (EXP_i - \overline{EXP})(TRUE_i - \overline{TRUE})}{[(\sum_{i=1}^n (EXP_i - \overline{EXP})(\sum_{i=1}^n (TRUE_i - \overline{TRUE})))]}, \quad (16)$$

$$BIAS = \frac{1}{n} \sum_{i=1}^n (EXP_i - TRUE_i), \quad (17)$$

$$RMSD = \sqrt{\frac{1}{n} \sum_{i=1}^n (EXP_i - TRUE_i)^2}, \quad (18)$$

5

where EXP_i and $TRUE_i$ are the surface CO₂ fluxes at the i th model grid-point of an experiment and TRUE, respectively, and n is the total number of model grid-point in the verification domain shown in Fig. 1.

To investigate the reduction of uncertainties for each experiment after data assimilation, uncertainty reduction (UR; Peters et al., 2005; Meirink et al., 2008; Chevallier et al., 2009b, Feng et al., 2009; Kim et al., 2014a, 2017, Kim et al., 2018b) was calculated as:

$$UR = \left(1 - \frac{\sigma_{EXP}}{\sigma_{CNTL}}\right) \times 100, \quad (19)$$

15 where σ_{CNTL} and σ_{EXP} denote 1σ standard deviations of the optimized scaling factor for the CNTL and an experiment. The UR was used to check the improvement of observation network experiments by comparing the posterior uncertainties of experiments with those of CNTL (i.e., the reference experiment).

3. Results

3.1. Effect of an observation network with observation sites redistributed randomly

20 Figure 4 shows the time series of the three-week moving average of PC, BIAS, and RMSD for surface CO₂ fluxes from the CNTL, CNTL_MOD, and REDIST experiments. Overall, REDIST is closer to TRUE compared to CNTL and CNTL_MOD. The PC of CNTL with the NOAA observation network decreases in mid-April and mid-July, as well as in late August compared to other months. In particular, the PC of CNTL fell to 0.919 in late August (Fig. 4a). This implies that, occasionally, the CNTL experiment may

not be effective in optimizing surface CO₂ fluxes in Asia. The PC of CNTL_MOD is quite similar to that of CNTL, except for the much lesser drop in late July compared to CNTL. In contrast, REDIST maintains a higher PC at almost every time compared to CNTL and CNTL_MOD. Particularly in late August, the PC of REDIST is comparatively higher (i.e., 0.955) than those of CNTL and CNTL_MOD (approximately 5 0.93). This implies that surface CO₂ fluxes in Asia could be optimized more effectively when using the observation sites of the REDIST experiment.

Regarding the BIAS, the three experiments have common variations that increase and decrease around zero, and have high amplitudes in summer compared to other seasons (Fig. 4b), which is associated with large uncertainties in the CO₂ mole fraction observations in summer shown in Fig. 2. In particular, 10 CNTL_MOD (CNTL) shows the maximum positive BIAS of 23.74 (16.43) in early June. In contrast, the BIAS of REDIST is approximately 10.28 at the same time and maintains its value closest to zero among the three experiments. Considering the impact of BIAS on steady simulations of the model, the time series of BIAS also supports that the observation network of REDIST can perform more reliably in optimizing surface CO₂ fluxes in Asia compared to that of CNTL.

15 The RMSDs of all three experiments increase much in summer (Fig. 4c), which may be caused by large uncertainties in the CO₂ mole fraction observations in summer shown in Fig. 2. The time series of RMSDs of CNTL and CNTL_MOD have similar variations except for a slight phase shift, whereas that of REDIST shows a comparatively smaller increase in the RMSD in the summer. Specifically, the maximum RMSD of CNTL is 200.61 in mid-July and that of CNTL_MOD is 192.19 early in July, but 20 that of REDIST is 127.32 at the beginning of June. Thus, REDIST is better than CNTL in simulating surface CO₂ fluxes in Asia in summer.

REDIST clearly outperforms CNTL and CNTL_MOD in summer, and an overall improvement is also observed from the comparison of the three experiments. The PC increases and the magnitudes of BIAS and RMSD decrease in REDIST compared to CNTL and CNTL_MOD. This implies that merely 25 redistributing current observation sites in Asia could have more benefits in optimizing surface CO₂ fluxes. This result seems to be somewhat attributable to the fact that most observation sites in Asia in the NOAA observation network of CT2013B are located in mid-latitudes (~35–45 ° N).

Furthermore, CNTL and CNTL_MOD are not much different in simulating surface CO₂ fluxes, which implies that the selection strategy of observation height in making hypothetical observations does not greatly affect the evaluation of the various observation networks. The real height information of the NOAA observation network in CNTL is therefore used for existing observation sites in Asia, and the observation height of additional hypothetical sites is set to 5 meters above the model topography in the experiments.

3.2. Effect of an observation network with extra observation sites added randomly

Figure 5 presents the time series of the three-week moving average of PC, BIAS, and RMSD for surface CO₂ fluxes from the CNTL, ADD, and ALL experiments, which clearly show the effect of randomly added observation sites. The decreases in the PC in the middle of April and in late July and August in CNTL do not appear in ADD and ALL (Fig. 5a). In particular, ALL maintains PC close to 1 during the experimental period. Although keeping the observation network as ALL is difficult in reality, this result demonstrates the impact of holding many observation sites in Asia. The minimum of the PC of ADD is 0.962, which is higher than that of CNTL (0.919), implying that adding extra observation sites in Asia could increase the stability in simulating surface CO₂ fluxes.

Compared to the BIAS of CNTL with high variability, the BIAS of ADD decreased by approximately 50% compared to that of CNTL and the absolute value of the maximum BIAS in ADD is 7.45 (Fig. 5b). Although ADD shows slightly higher BIAS than CNTL during the first two months, the time series of BIAS in ADD remains close to zero during the simulation period. The BIAS of ALL is the closest to 0 compared to those of CNTL and ADD throughout the experimental period.

In terms of the RMSD, the three experiments show larger values ~~increasing trends~~ in the summer compared to other seasons (Fig. 5c), which is similar to the previous random redistribution experiments in Sect. 3.1. However, the RMSDs of ADD and ALL with more observation sites generally remain low during the simulation period. Specifically, compared to other seasons, the RMSD of CNTL in the summer increases by approximately three times and shows a four-fold increase in late July, rising to 200.61. Except in summer, the time series of RMSD of ADD is similar to or slightly lower than that of CNTL. In

summer, the maximum RMSD of ADD is reduced to 109.18, maintaining lower values during the summer and not showing any sudden increase. ALL has the minimum RMSD among the three experiments throughout the simulation period, and reaches a maximum of only 34.37 in early July. Since this number does not exceed the minimums of CNTL and ADD, the ALL experiment can be regarded as the best
5 observation network. This suggests that an accurate and stable optimization of surface CO₂ fluxes in Asia is possible if CO₂ observation sites are sufficient.

The result of the observation network experiments with randomly added extra observation sites (i.e., ADD) also implies that the seven observation sites in Asia described in CT2013B do not seem to be sufficient to fully optimize the surface CO₂ fluxes in the region. Although the ADD experiment with 10
10 randomly added extra observation sites shows an improvement in optimization, more observation sites are necessary for optimizing surface CO₂ fluxes in Asia, considering the result of the ALL experiment. Moreover, the simulation result of the ADD experiment does not much outperform that of the REDIST experiment, although more observations were used. This implies that further consideration is required when adding observation sites to the existing observation network. Thus, rather than just adding
15 observation sites randomly, selecting and adding more influential observation sites for Asia is crucial to construct an efficient surface CO₂ observation network.

3.3. Effect of an observation network with extra observation sites added using self-sensitivity and ecoregion information

20 Considering the simulation results of Sect. 3.2, the addition of extra observation sites to the existing observation sites could improve the performance in simulating surface CO₂ fluxes in Asia. In particular, the ALL experiment, which added many observation sites ~~under the given modeling enabled in the~~
~~CT2013B_~~framework, shows a high level of reproducibility of TRUE. However, adding more than 900
25 observation sites in Asia does not seem to be possible in real situations. Moreover, the expected effect from the extra observation sites may not be effective if the additional observations are not influential. Thus, the efficient selection and supplementation of observation sites is inevitable considering these constraints under realistic conditions.

In this study, self-sensitivity information obtained from the ALL experiment and ecoregion information used in CT2013B were used as additional strategies for the purpose of adding possible efficient observation sites in Asia. Since the self-sensitivity is the metric showing the impact of observations at each observation site for the model simulation results, as stated in Sect. 2.2, it can be used as a strategy for selecting potential observation sites. In addition, the proportion of each ecoregion in the Asia domain can also be utilized as a strategy in choosing observation sites, as the calculation of surface CO₂carbon fluxes is based on the scaling factor for each ecoregion in CT2013B, and the scaling factor updated in the data assimilation process has the possibility to be more affected by the observation sites located in the same ecoregion (CarbonTracker Documentation CT2013B Release, 2015).

Figure 6 shows the spatial distribution of self-sensitivity from the ALL experiment. Although the self-sensitivity of each observation site varies from the others, four influential regions with high sensitivities are located in western Siberia, the southern part of the Tibetan Plateau, and southeastern and northeastern Asia. The highest (lowest) self-sensitivity of the hypothetical observation sites is 4.02% (0.04%). Thus, the likelihood of using observations located in the aforementioned four regions increases when considering the self-sensitivity as the selection strategy. In contrast, the observation sites located in southwestern Asia and eastern Siberia are rarely chosen for the optimization due to the low value of self-sensitivity.

The self-sensitivity used for the SS and ECOSS experiments is the pure self-sensitivity without considering the number of assimilated observations. The 10 observation sites of the SS experiment were selected by employing self-sensitivity from the numerical order (highest first) and following the addition criteria (i.e., 1000 km distance between sites and observation height 5 meters above the model topography) used in Sect. 2.3. For the ECOSS experiment, the proportions of ecoregions in the Asia verification domain were calculated from the model grid-points. Following this, the observation sites were selected from the order of principal ecoregions with self-sensitivity information. Specifically, the land ecoregion information, omitting that of the oceans, was utilized for the selection criteria as the land in the northern hemisphere is crucial for the global carbon exchange. Table 3 displays the proportions of ecoregions in the Asia verification domain and the distribution of observation sites in SS and ECOSS. As the ecoregions with 115 (Conifer Forest, Eurasia Boreal) and 137 (Grass/Shrub, Eurasia Temperate) (~~Transeom~~

~~Region 도 같이 표시하는 게 좋지 않을까 생각됩니다. 특히 Grass/Shrub 의 경우 EB, ET, SA 모두 존재하는 생태계입니다. 115 (Conifer Forest, Eurasia Boreal) and 137 (Grass/Shrub, Eurasia Temperate)~~

indices constitute relatively large proportions of the ecoregions in Asia (Table 3), two observation sites were assigned for each of these two ecoregions. The other ecoregions have one observation site per ecoregion. When selecting the aforementioned two and one observation sites in the ecoregions, the observation sites with the highest self-sensitivities were selected. The observation sites of SS are mostly located in ecoregions that constitute lower proportions compared to those of ECOSS because the self-sensitivity is generally inversely proportional to the number of assimilated observations, as shown in Kim et al. (2014a, 2017).

The time series of the three-week moving average of PC, BIAS, and RMSD of the simulated surface CO₂ fluxes for the ADD, SS, and ECOSS experiments are shown in Fig. 7, which shows the impact of additional observation sites considering self-sensitivity information. The SS and ECOSS experiments show higher PC compared with ADD, except that the PC of SS is lower than that of ADD in late April and mid-August. In particular, the PC of ECOSS is superior to that of ADD throughout the experimental period and is more stable than that of SS. This result implies that the impact of extra observation sites added from self-sensitivity and ecoregion information is greater in optimizing surface CO₂ fluxes in Asia than that of randomly added observation sites.

However, the BIAS of SS shows a sudden increase in early ~~June~~^{July}, with a maximum positive BIAS of 21.79 (Fig. 7b), ~~which is associated with concentrated sites by large SS values in certain ecoregions that cause not enough DA in other ecoregions.~~ Although the BIAS of ECOSS is generally closer to 0 than that of ADD, except in July, ECOSS shows the maximum negative BIAS of -15.78 in late July. These tendencies suggest that the DA method that optimizes parameters such as the scaling factor used in CT2013B may occasionally have trouble in optimizing surface CO₂ fluxes when using limited observation sites for a larger area.

Nevertheless, the ECOSS experiment that considered both self-sensitivity and ecoregion information maintains lower RMSD than the ADD experiment over the experimental period. Additionally, ~~except in the period from April to late-August,~~ the RMSD of SS is lower than that of ADD, ~~except in the period from April to late-August which differs from. This is in contrast to the ADD experiment, that~~ which is

mainly better than CNTL in summer, as shown in Fig. 5. Thus, ~~compared in contrast~~ to ADD ~~and CNTL~~, the ~~SS (ECOSSSS and ECOSS)~~ experiments demonstrates improvement in the other seasons except summer ~~(over the experimental period)~~.

The increased RMSD of SS during the spring-summer period compared to that of ADD seems to be related to the DA method used in CT2013B. As most observation sites added in SS are located in the ecoregions with relatively small proportions of the Asia domain (Table 3), they may have disadvantages in optimizing the scaling factor of major ecoregions. This is somewhat relevant to the distribution of observation sites in the ALL experiment, which has observation sites at 2° intervals, consequently leading to the uneven distribution of observation sites (i.e., major ecoregions with more observation sites and minor ecoregions with fewer observation sites) in Asia. As the self-sensitivity generally has an inverse relationship with the number of assimilated observations, the self-sensitivities of major ecoregions are typically lower than those of minor ecoregions, as shown in Table 4.

The simulation results of SS and ECOSS confirm that influential observation sites for optimizing surface CO₂ fluxes in Asia certainly exist, and the self-sensitivity information could be used for designing the observation network. The ECOSS experiment especially, which considers both ecoregion information and self-sensitivity, shows a better performance compared to the SS experiment, which suggests that considering characteristics of the specific model and data assimilation configurations can also contribute to the improvement in optimization. This further implies that an observation network based on the self-sensitivity and ecoregion information could be better for optimizing surface CO₂ fluxes in Asia than that based on randomly added observation sites, though the same number of observations are used.

3.4. Effect of an observation network with extra observation sites added using normalized self-sensitivity and ecoregion information

As stated in Sect. 3.3, using the pure self-sensitivities acquired from the ALL experiment for observation network studies could be inappropriate in certain occasions because they were derived from an uneven ~~number of sites for each ecoregion~~ ~~distribution of observation sites~~. Thus, self-sensitivity could be normalized (Eq. (15)) and used for the selection of observation sites. Table 5 shows the information for observation sites in the NSS, NECOSS1, and NECOSS2 experiments that used the normalized self-

sensitivities as the selection strategy. The observation sites of the NSS experiment are located only in the 115 (Conifer Forest) and 137 (Grass/Shrub)~~and 137~~ ecoregions. This is because they have higher normalized sensitivities than other regions as they constitute large proportions of the ecoregions of Asia, as shown in Table 3. Additionally, the NECOSS1 and NECOSS2 experiments were conducted to examine the impact of additional observation sites depending on the choice of ecoregion. For the NECOSS1 experiment, two observation sites were added to the 115 (Conifer Forest) and 137 (Grass/Shrub)~~and 137~~ ecoregions and one observation site each was allocated to the other six ecoregions. In contrast, the NECOSS2 experiment allotted one observation site to each ecoregion. The observation sites in NECOSS1 and NECOSS2 in the ecoregions were selected by the order of highest normalized sensitivities in each ecoregion.

Figure 8 shows the time series of the three-week moving average of PC, BIAS, and RMSD of the simulated surface CO₂ fluxes for the ADD, NSS, NECOSS1, and NECOSS2 experiments, which shows the impact of using normalized self-sensitivities for the selection of additional observation sites. For the PC, all the experiments using normalized self-sensitivities (i.e., NSS, NECOSS1, and NECOSS2) show higher PC than the ADD experiment for most of the time (Fig. 8a). In particular, the PC of NSS is always higher than the PC of SS that showed temporarily lower PC compared to ADD from late April to mid-August. Furthermore, the NECOSS1 and NECOSS2 experiments that also considered ecoregion information perform better than the NSS experiment without ecoregion information.

Regarding BIAS, the experiments using the normalized self-sensitivities show a strong negative BIAS in mid- and late July (Fig. 8b). Although such tendencies are similar to that of ECOSS shown in Fig. 7b, the maximum negative BIAS of NSS, NECOSS1, and NECOSS2 are -14.40, -12.23, and -11.45, respectively, which is comparatively smaller than that of ECOSS. Such an abrupt increase in BIAS could be associated with the sudden transition of surface CO₂carbon sources and sinks during summer.

The NSS, NECOSS1, and NECOSS2 experiments show lower RMSDs compared to the ADD experiment (Fig. 8c). The RMSD of NSS is lower than that of ADDSS for most of the time, which is different and this is in contrast to from -SS that showed a degradation in summer and little improvement in other seasons compared to ADD in Fig. 7c. Moreover, the NECOSS1 and NECOSS2 experiments that additionally considered the ecoregion information demonstrate a further reduction in RMSD, especially

in summer. The NECOSS1 and NECOSS2 experiments have a slightly lower RMSD than ECOSS that considered pure self-sensitivities and ecoregion information. The NECOSS1 and NECOSS2 experiments do not show significant differences due to minor differences in the choice of observation sites.

The simulation results using the normalized self-sensitivities reconfirm that the self-sensitivity information could be used in designing the observation network. By considering the DA method of CT2013B that optimizes scaling factors assigned in ecoregions, the experiments using normalized self-sensitivities could make simulations better than those using pure self-sensitivity. In addition, the additional consideration of ecoregion in the experiments using normalized self-sensitivities also contributes to improvements, which implies that the model's characteristics, such as ecoregion information, could also be one of the factors to be used in designing the surface CO₂ observation network.

3.5. Horizontal distributions of RMSD and uncertainty reduction

Figure 9 shows the spatial distribution of the average of weekly RMSD calculated from the surface CO₂ fluxes in Asia. The CNTL shows the highest RMSD among the experiments, with peaks mainly located in the Siberian area (Fig. 9a). The REDIST experiment shows a decrease in the high RMSD of the Siberian area shown in CNTL, but the RMSDs of eastern China and the southeastern part of the Tibetan Plateau (the Indochina Peninsula) slightly increase, and the RMSDs of northern India and the northeastern part of Asia remain nearly unchanged compared to CNTL (Fig. 9b). The distribution of RMSD in the ADD experiment is fairly similar to that of REDIST, except for the decrease of RMSD near the Tibetan Plateau and in southeastern Asia (Fig. 9c). Such a spatial distribution of RMSD in the ADD experiment implies the need for supplementing observation sites efficiently. Figure 9d clearly shows the reduction in RMSD of northern India and the southeastern region of the Tibetan Plateau in the SS experiment compared to the REDIST and ADD experiments. This proves the impact of considering self-sensitivity information for observation network studies. However, the performance of the SS experiment on some Siberian inland areas is poorer than those of the REDIST and ADD experiments, due to the relative absence of observation sites for that region. The ECOSS experiment using the ecoregion information shows comparatively lower RMSD in the Asia domain, except for the southeastern part of

the Tibetan Plateau and northeastern Asia (Fig. 9e). The RMSD distribution of the NSS experiment confirms that the RMSD of the Siberian area is much reduced compared to that of the SS experiment, though its overall pattern is similar (Fig. 9f). The RMSDs of the NECOSS1 and NECOSS2 experiments are analogous to that of the ECOSS experiment (Fig. 9g). This can be attributed to the fact that most observation sites in those three experiments are identical (Tables 4 and 5). The simulated RMSD of the ALL experiment is the lowest in most of the domain among all sensitivity experiments (Fig. 9i). Such simulation results reconfirm that the observation network in Asia needs to be organized in a more efficient way to gain better optimization results of surface CO₂ fluxes. The spatial RMSD distribution during the summer from June to August (not shown) is also similar to that for whole year shown in Fig. 9.

10

Figure 10 shows the UR derived from the experiments, which corresponds with the previous results. Compared to the CNTL experiment, the uncertainty of the REDIST experiment is much reduced in the Siberian area, but the impact of REDIST is low south of below-50° N (Fig. 10a). Such a result seems to be related with the high UR values in that region in CNTL, because most observation sites in CNTL are located from 30° to 45° N. The ADD experiment with randomly added sites demonstrates slightly more increases in UR for the inland Siberian area and the nearby areas of the Tibetan Plateau, including China and India, than REDIST (Fig. 10b). However, the UR in the Asian mid-latitudes is still lower than that in other Asian regions. Although the SS and ECOSS experiments have the same number of observation sites compared with the ADD experiment, the overall UR in the Asia domain in SS and ECOSS is higher than that of ADD (Figs. 10b, c, and d). The uncertainty in the SS experiment, which has comparatively more observation sites in India and southeastern Asia, is clearly reduced for that area. In contrast, the ECOSS experiment retaining comparatively more observation sites in the inland areas of Asia shows higher UR in the land areas, although UR in India and southeastern Asia is lower than that in the SS experiment. The experiments using normalized self-sensitivities generally show distinct uncertainty reductions in inland Asia, although the UR of India and southeastern Asia in NSS is slightly lower than that of SS (Fig. 10e). This is because the observation sites of NSS are located only in the 115 (Conifer Forest) and 137 (Grass/Shrub) and 137 ecoregions. Although the UR distributions of the NECOSS1 and NECOSS2 experiments are generally similar to those of the ECOSS experiment, the uncertainties in India and

20

25

southeastern Asia decrease further in NECOSS1 and NECOSS2 (Figs. 10f and g). The UR of the ALL experiment increases compared to those of other experiments as a number of observation sites in ALL sufficiently cover the Asian domain (Fig. 10h).

Table 6 summarizes the overall scores of the simulations conducted in this study. The CNTL (ALL) experiment shows the lowest (highest) skill score among the simulations. The skill scores of other experiments range between these. The statistics shown in Table 6 reconfirm the impacts of redistributing current observation sites and adding extra observation sites discussed in this study. Firstly, the height specification for hypothetical observations does not seem to be very influential for the results of OSSEs results—as only small differences were observed between the results of CNTL and CNTL_MOD. The impact of redistribution is noticeable because the performance of the REDIST experiment was generally better than that of the CNTL experiment. Moreover, the comparison between ADD, SS, and ECOSS reaffirms that adding more observation sites to the existing sites is effective in optimizing surface CO₂ fluxes, and the addition strategy needs to be more effective to have better optimization results for surface CO₂ fluxes. Moreover, the NSS, NECOSS1, and NECOSS2 experiments that used both normalized self-sensitivities and ecoregion information show that the normalized self-sensitivity and configuration of the data assimilation and model can be utilized as appropriate strategies in designing an observation network that enhances simulation results. The simulation result of the ALL experiment seems to suggest a possible limit of the improvement when using the DA method in CT2013B.

20 3.6. Additional experiments with more surface observation sites

Until now, the seven observation sites in Asia from the observation network of CT2013B was used to evaluate several strategies to determine an effective observation network for optimizing surface CO₂ fluxes in Asia. Currently, surface CO₂ mole fraction observations from 18 observation sites are used for CT2017 (Fig. 11). In this section, the experimental results based on 18 observation sites similar to those based on seven observation sites above are shown to reaffirm the validity of the normalized self-sensitivity and ecoregion information as selection strategies for potential observation sites. Descriptions of additional

experiments are shown in Table 2. Instead of CNTL, ADD, NSS, and NECOSS1 based on seven sites, CNTL 18, ADD 18, NSS 18, and NECOSS1 18 are configured.

5 Figure 12 shows the time series of the three-week moving average of PC, BIAS, and RMSD of the simulated surface CO₂ fluxes for the ALL, CNTL_18, ADD_18, NSS_18, and NECOSS1_18 experiments, which shows the impact of using normalized self-sensitivities for the selection of additional observation sites. CNTL_18 with 11 more sites shows a better performance when compared to CNTL shown in Fig. 4, and other experiments with 10 more observation sites compared to CNTL_18 show more improved results. For the PC, the ALL shows a best score and the ADD_18, NSS_18, and NECOSS1_18 experiments show similar PC values (Fig. 12a). Although no discernible big difference exists, the more
10 stable and higher one is the NECOSS1_18. The CNTL_18 and NSS_18 show slightly higher positive BIAS in July and NECOSS1_18 shows higher negative BIAS in June and August, but the BIAS seems to be held close to zero for all experiments (Fig. 12b). For the RMSD, the experiments with 10 more observation sites are located between the ALL and CNTL_18, and the NECOSS1_18 shows the lowest RMSD among three of them though the differences are slightly small (Fig. 12c).

15 The impact of using normalized self-sensitivities and ecoregions in determining observation sites is still shown in the additional experiments based on 18 observation sites, although the improvement is slightly reduced compared to the experiments based on 7 observation sites. The less improvement in the experiments based on 18 observation sites compared to those based on 7 observation sites seems to be associated with the locations of 11 additional observation sites mostly in Siberian regions where lack
20 observation data in CNTL and show high sensitivities in Fig. 6. Most of additional observation sites based on CT2017 are mainly located in highly sensitive regions in Siberia in Fig. 6. Thus, they can cover the regions that lack observation data in the experiments based on 7 observation sites.

4. Conclusions

25 In this study, observation system simulation experiments using hypothetical observations were conducted to investigate the potential for an effective observation network for optimizing surface CO₂ fluxes in Asia. Several experiments, including redistributing existing stations and adding observation

stations to the existing observation network, were conducted to assess the performance of the current observation network and the impact of additional observation sites. For the addition experiment, random addition and addition strategies based on self-sensitivities, normalized self-sensitivities, and ecoregion information were tested and compared. The performance of each observation network was evaluated from statistics calculated from simulated surface CO₂ fluxes and the uncertainty reduction.

The results indicate that further optimization of the surface CO₂ fluxes in Asia could be made by redistributing existing observation sites, given that the RMSD of the redistributed experiment was reduced by 12.8% compared to the experiment using the existing observation network (i.e., CNTL). The RMSD of the random addition experiment was reduced by 21.9% compared to CNTL. Although the experiment based on only self-sensitivity information was not better than that based on randomly added observation sites, the experiment based on both self-sensitivity and ecoregion information reduced the RMSD by 35.2% compared to that of CNTL. Moreover, the experiment based on both normalized self-sensitivity and ecoregion information further reduced the RMSD by approximately 40% compared to that of CNTL. Thus, the normalized self-sensitivity and ecoregion information could be used as strategies to select observation sites to construct the surface CO₂ observation network. The additional experiments based on 18 observation sites used for CT2017 also show similar results compared to the experiments based on 7 observation sites used for CT2013B, which reaffirms the validity of the normalized self-sensitivity and ecoregion information as selection strategies for potential observation sites.

Although the simulation results showed an improvement in performance, the results also suggested that adding 10 extra observation sites in Asia may not be sufficient to fully optimize surface CO₂ fluxes, and more observation sites are required. Reliable observation data from some satellite sensors could supplement the model simulations on the basis of continuous surface observation sites. As the quality of satellite observation data increases, the observation network design for both surface and satellite observation data using the strategies (i.e., normalized self-sensitivity and ecoregion information) of this study will be investigated in the future.

This study suggests a method to design and evaluate the observation network to optimize surface CO₂ fluxes at the continental scale without a myriad of simulations (iterations) of the genetic algorithm or the incremental optimization used in previous studies. Thus, this approach could constitute a practical method

to conduct such simulations with relatively limited computer resources. The observation network design method in this study could also be used to design an observation network to optimize global surface CO₂ fluxes.

Data availability

- 5 CarbonTracker data are available at the NOAA CarbonTracker homepage: <http://carbontracker.noaa.gov/>. Observation data distributed by NOAA ESRL are available at the obspack homepage: [doi:10.3334/OBSPACK/1001](https://doi.org/10.3334/OBSPACK/1001). The experimental results are available upon request to the corresponding author.

Author contribution

- 10 Hyun Mee Kim proposed the main scientific ideas and Jun Park contributed the supplementary ideas during the process. Jun Park ran the observation system simulation experiments using CarbonTracker. Jun Park and Hyun Mee Kim analyzed the simulation results and completed the manuscript.

Acknowledgements

- 15 The authors appreciate two reviewers for their valuable comments. This study was supported by the Korea Meteorological Administration Research and Development Program under grant KMI2018-03712 and a National Research Foundation of Korea (NRF) grant funded by the South Korean government (Ministry of Science and ICT) (Grant 2017R1E1A1A03070968). The authors are grateful to Andrew R. Jacobson (ESRL, NOAA, USA) for providing resources to run CarbonTracker.

References

- Byrne, B., Jones, D. B. A., Strong, K., Zeng, Z. C., Deng, F. and Liu, J.: Sensitivity of CO₂ surface flux constraints to observational coverage, *J. Geophys. Res. Atmos.*, 122(12), 6672–6694, doi:10.1002/2016JD026164, 2017.
- 5 Boden, T., Marland, G., and Andres, R.: Global, regional, and national fossil-fuel CO₂ emissions, Carbon Dioxide Information Analysis Center, Oak Ridge National Laboratory, US Department of Energy, Oak Ridge, TN, USA, 10, doi:10.3334/CDIAC/00001_V2010, 2010.
- CarbonTracker Documentation CT2013B Release, CarbonTracker Team, available at: https://www.esrl.noaa.gov/gmd/ccgg/carbontracker/CT2013B/CT2013B_doc.php (last access: January 10 2019), 2015.
- Cardinali, C., Pezzulli, S. and Andersson, E.: Influence-matrix diagnostic of a data assimilation system, *Q. J. R. Meteorol. Soc.*, 130(603 PART B), 2767–2786, doi:10.1256/qj.03.205, 2004.
- Cheng, Y. L., Aa, X. Q., Yun, F. H., Zhou, L. X., Liu, L. X., Fang, S. X. and Xu, L.: Simulation of CO₂ variations at Chinese background atmospheric monitoring stations between 2000 and 2009: Applying a 15 CarbonTracker model, *Chinese Sci. Bull.*, 58(32), 3986–3993, doi:10.1007/s11434-013-5895-y, 2013.
- Cheng, S., Zhou, L., Tans, P. P., An, X. and Liu, Y.: Comparison of atmospheric CO₂ mole fractions and source–sink characteristics at four WMO/GAW stations in China, *Atmos. Environ.*, 180(March), 216–225, doi:10.1016/j.atmosenv.2018.03.010, 2018.
- Chevallier, F., Engelen, R. J., Carouge, C., Conway, T. J., Peylin, P., Pickett-Heaps, C., Ramonet, M., 20 Rayner, P. J. and Xueref-Remy, I.: AIRS-based versus flask-based estimation of carbon surface fluxes, *J. Geophys. Res. Atmos.*, 114(20), 1–9, doi:10.1029/2009JDO12311, 2009a.
- Chevallier, F., Maksyutov, S., Bousquet, P., Bréon, F. M., Saito, R., Yoshida, Y. and Yokota, T.: On the accuracy of the CO₂ surface fluxes to be estimated from the GOSAT observations, *Geophys. Res. Lett.*, 36(19), 1–5, doi:10.1029/2009GL040108, 2009b.
- 25 Chevallier, F., Ciais, P., Conway, T. J., Aalto, T., Anderson, B. E., Bousquet, P., Brunke, E. G., Ciattaglia, L., Esaki, Y., Fröhlich, M., Gomez, A., Gomez-Pelaez, A. J., Haszpra, L., Krummel, P. B., Langenfelds, R. L., Leuenberger, M., MacHida, T., Maignan, F., Matsueda, H., Morguá, J. A., Mukai, H., Nakazawa, T., Peylin, P., Ramonet, M., Rivier, L., Sawa, Y., Schmidt, M., Steele, L. P., Vay, S. A., Vermeulen, A.

- T., Wofsy, S. and Worthy, D.: CO₂ surface fluxes at grid point scale estimated from a global 21 year reanalysis of atmospheric measurements, *J. Geophys. Res. Atmos.*, 115(21), 1–17, doi:10.1029/2010JD013887, 2010.
- Enting, I. G.: Inverse problems in atmospheric constituent transport, Cambridge University Press., 2002.
- 5 European Commission: Joint Research Centre (JRC)/Netherlands Environmental Assessment Agency (PBL): Emission Database for Global Atmospheric Research (EDGAR), release version 4.0, 2009.
- Evensen, G.: Sequential data assimilation with a nonlinear quasi-geostrophic model using Monte Carlo methods to forecast error statistics, *J. Geophys. Res. Oceans*, 99(C5), 10143, doi:10.1029/94JC00572, 1994.
- 10 Feng, L., Palmer, P. I., Bösch, H. and Dance, S.: Estimating surface CO₂ fluxes from space-borne CO₂ dry air mole fraction observations using an ensemble Kalman Filter, *Atmos. Chem. Phys.*, 9, 2619–2633, doi:10.5194/acp-9-2619-2009, 2009.
- Feng, L., Palmer, P. I., Parker, R. J., Deutscher, N. M., Feist, D. G., Kivi, R., Morino, I. and Sussmann, R.: Estimates of European uptake of CO₂ inferred from GOSAT XCO₂ retrievals: Sensitivity to
15 measurement bias inside and outside Europe, *Atmos. Chem. Phys.*, 16(3), 1289–1302, doi:10.5194/acp-16-1289-2016, 2016.
- Fischer, M. L., Parazoo, N., Brophy, K., Cui, X., Jeong, S., Liu, J., Keeling, R., Taylor, T. E., Gurney, K., Oda, T. and Graven, H.: Simulating estimation of California fossil fuel and biosphere carbon dioxide exchanges combining in situ tower and satellite column observations, *J. Geophys. Res. Atmos.*, 122(6),
20 3653–3671, doi:10.1002/2016JD025617, 2017.
- Gurney, K. R., Law, R. M., Denning, A. S., Rayner, P. J., Baker, D., Bousquet, P., Bruhwiler, L., Chen, Y.-H., Ciais, P., Fan, S., Fung, I. Y., Gloor, M., Heimann, M., Higuchi, K., John, J., Maki, T., Maksyutov, S., Masarie, K., Peylin, P., Prather, M., Pak, B. C., Randerson, J., Sarmiento, J., Taguchi, S., Takahashi, T. and Yuen, C.-W.: Towards robust regional estimates of CO₂ sources and sinks using atmospheric
25 transport models, *Nature*, 415(6872), 626–630, doi:10.1038/415626a, 2002.
- Hayes, D. J., McGuire, A. D., Kicklighter, D. W., Gurney, K. R., Burnside, T. J. and Melillo, J. M.: Is the northern high-latitude land-based CO₂ sink weakening?, *Global Biogeochem. Cycles*, 25(3), 1–14, doi:10.1029/2010GB003813, 2011.

- Houghton, R. A., Butman, D., Bunn, A. G., Krankina, O. N., Schlesinger, P. and Stone, T. A.: Mapping Russian forest biomass with data from satellites and forest inventories, *Environ. Res. Lett.*, 2(4), doi:10.1088/1748-9326/2/4/045032, 2007.
- Houtekamer, P. L. and Mitchell, H. L.: A Sequential Ensemble Kalman Filter for Atmospheric Data Assimilation, *Mon. Weather Rev.*, 129(1), 123–137, doi:10.1175/1520-0493(2001)129<0123:ASEKFF>2.0.CO;2, 2001.
- Jacobson, A. R., Fletcher, S. E. M., Gruber, N., Sarmiento, J. L. and Gloor, M.: A joint atmosphere-ocean inversion for surface fluxes of carbon dioxide: 1. Methods and global-scale fluxes, *Global Biogeochem. Cycles*, 21(1), doi:10.1029/2005GB002556, 2007.
- 10 Kang, J.-S., Kalnay, E., Liu, J., Fung, I., Miyoshi, T. and Ide, K.: “Variable localization” in an ensemble Kalman filter: Application to the carbon cycle data assimilation, *J. Geophys. Res. Atmos.*, 116(D9), D09110, doi:10.1029/2010JD014673, 2011.
- Kang, J.-S., Kalnay, E., Miyoshi, T., Liu, J. and Fung, I.: Estimation of surface carbon fluxes with an advanced data assimilation methodology, *J. Geophys. Res. Atmos.*, 117(D24),
15 doi:10.1029/2012JD018259, 2012.
- Kim, H., Kim, H. M., Kim, J. and Cho, C.-H.: A Comparison of the Atmospheric CO₂ Concentrations Obtained by an Inverse Modeling System and Passenger Aircraft Based Measurement, *Atmos.*, 26(3), 387-400, doi:10.14191/Atmos.2016.26.3.387, 2016. (in Korean with English abstract)
- Kim, H., Kim, H. M., Cho, M., Park, J., and Kim, D.-H.: Development of the Aircraft CO₂ Measurement
20 Data Assimilation System to Improve the Estimation of Surface CO₂ Fluxes Using an Inverse Modeling System, *Atmos.*, 28(2), 113-121, doi:10.14191/Atmos.2018.28.2.113, 2018a. (in Korean with English abstract)
- Kim, H., Kim, H. M., Kim, J. and Cho, C.-H.: Effect of data assimilation parameters on the optimized surface CO₂ flux in Asia, *Asia-Pacific J. Atmos. Sci.*, 54(1), 1–17, doi:10.1007/s13143-017-0049-9,
25 2018b.
- Kim, J., Kim, H. M. and Cho, C. H.: Influence of CO₂ observations on the optimized CO₂ flux in an ensemble Kalman filter, *Atmos. Chem. Phys.*, 14(24), 13515–13530, doi:10.5194/acp-14-13515-2014, 2014a.

- Kim, J., Kim, H. M. and Cho, C. H.: The effect of optimization and the nesting domain on carbon flux analyses in Asia using a carbon tracking system based on the ensemble Kalman filter, *Asia-Pacific J. Atmos. Sci.*, 50(3), 327–344, doi:10.1007/s13143-014-0020-y, 2014b.
- Kim, J., Kim, H. M., Cho, C. H., Boo, K. O., Jacobson, A. R., Sasakawa, M., Machida, T., Arshinov, M.
5 and Fedoseev, N.: Impact of Siberian observations on the optimization of surface CO₂ flux, *Atmos. Chem. Phys.*, 17(4), 2881–2899, doi:10.5194/acp-17-2881-2017, 2017.
- Kim, J., Kim, H. M. and Cho, C.: Application of Carbon Tracking System based on Ensemble Kalman Filter on the Diagnosis of Carbon Cycle in Asia, *Atmos.*, 22(4), 415–427, 2012. (in Korean with English abstract)
- 10 Kou, X., Tian, X., Zhang, M., Peng, Z. and Zhang, X.: Accounting for CO₂ Variability over East Asia with a Regional Joint Inversion System, *J. Meteorol. Res.*, 31(5), 834-851, doi:10.1007/s13351-017-6149-8. 2017.
- Krol, M., Houweling, S., Bregman, B., van den Broek, M., Segers, A., van Velthoven, P., Peters, W., Dentener, F. and Bergamaschi, P.: The two-way nested global chemistry-transport zoom model TM5:
15 algorithm and applications. *Atmos. Chem. Phys.*, 5, 417-432. 2005.
- Kurganova, I. N., Kudeyarov, V. N. and Lopes De Gerenyu, V. O.: Updated estimate of carbon balance on Russian territory, *Tellus, Ser. B Chem. Phys. Meteorol.*, 62(5), 497–505, doi:10.1111/j.1600-0889.2010.00467.x, 2010.
- Lacis, A. A., Schmidt, G. A., Rind, D. and Ruedy, R. A.: Atmospheric CO₂: Principal control knob
20 governing earth's temperature, *Science*, 330(6002), 356–359, doi:10.1126/science.1190653, 2010.
- Le Quéré, C., Andrew, R. M., Friedlingstein, P., Sitch, S., Pongratz, J., Manning, A. C., Korsbakken, J. I., Peters, G. P., Canadell, J. G., Jackson, R. B., Boden, T. A., Tans, P. P., Andrews, O. D., Arora, V. K., Bakker, D. C. E., Barbero, L., Becker, M., Betts, R. A., Bopp, L., Chevallier, F., Chini, L. P., Ciais, P., Cosca, C. E., Cross, J., Currie, K., Gasser, T., Harris, I., Hauck, J., Haverd, V., Houghton, R. A., Hunt,
25 C. W., Hurtt, G., Ilyina, T., Jain, A. K., Kato, E., Kautz, M., Keeling, R. F., Klein Goldewijk, K., Körtzinger, A., Landschützer, P., Lefèvre, N., Lenton, A., Lienert, S., Lima, I., Lombardozi, D., Metz, N., Millero, F., Monteiro, P. M. S., Munro, D. R., Nabel, J. E. M. S., Nakaoka, S.-I., Nojiri, Y., Padin, X. A., Peregon, A., Pfeil, B., Pierrot, D., Poulter, B., Rehder, G., Reimer, J., Rödenbeck, C., Schwinger, J.,

- Séférian, R., Skjelvan, I., Stocker, B. D., Tian, H., Tilbrook, B., Tubiello, F. N., Van Der Laan-Luijkx, I. T., Van Der Werf, G. R., Van Heuven, S., Viovy, N., Vuichard, N., Walker, A. P., Watson, A. J., Wiltshire, A. J., Zaehle, S. and Zhu, D.: Global Carbon Budget 2017, *Earth Syst. Sci. Data*, 10, 405–448, doi:10.5194/essd-10-405-2018, 2018.
- 5 Liu, J., Kalnay, E., Miyoshi, T., and Cardinali, C.: Analysis sensitivity calculation in an ensemble Kalman filter, *Q. J. R. Meteorol. Soc.*, 135, 1842–1851, doi:10.1002/qj.511, 2009.
- Lucas, D. D., Yver Kwok, C., Cameron-Smith, P., Graven, H., Bergmann, D., Guilderson, T. P., Weiss, R. and Keeling, R.: Designing optimal greenhouse gas observing networks that consider performance and cost, *Geosci. Instrumentation, Methods Data Syst.*, 4(1), 121–137, doi:10.5194/gi-4-121-2015, 2015.
- 10 Maksyutov, S., Takagi, H., Valsala, V. K., Saito, M., Oda, T., Saeki, T., Belikov, D. A., Saito, R., Ito, A., Yoshida, Y., Morino, I., Uchino, O., Andres, R. J. and Yokota, T.: Regional CO₂ flux estimates for 2009–2010 based on GOSAT and ground-based CO₂ observations, *Atmos. Chem. Phys.*, 13(18), 9351–9373, doi:10.5194/acp-13-9351-2013, 2013.
- Meirink, J. F., Bergamaschi, P. and Krol, M. C.: Four-dimensional variational data assimilation for
15 inverse modelling of atmospheric methane emissions: Method and comparison with synthesis inversion, *Atmos. Chem. Phys.*, 8(21), 6341–6353, doi:10.5194/acp-8-6341-2008, 2008.
- Nickless, A., Ziehn, T., Rayner, P. J., Scholes, R. J. and Engelbrecht, F.: Greenhouse gas network design using backward Lagrangian particle dispersion modelling - Part 2: Sensitivity analyses and South African test case, *Atmos. Chem. Phys.*, 15(4), 2051–2069, doi:10.5194/acp-15-2051-2015, 2015.
- 20 Olson, J., Watts, J., and Allsion, L.: Major World Ecosystem Complexes Ranked by Carbon in Live Vegetation: a Database, Tech. rep., Carbon Dioxide Information Analysis Center, U.S. Department of Energy, Oak Ridge National Laboratory, Oak Ridge, TN, USA, doi:10.3334/CDIAC/lue.ndp017, 1992.
- [Patra, P. K., Maksyutov, S. and TransCom-3 modelers: Sensitivity of optimal extension of observation networks to the model transport, *Tellus B*, 55, 498– 511, 2003.](#)
- 25 Peters, W., Krol, M. C., Dlugokencky, E. J., Dentener, F. J., Bergamaschi, P., Dutton, G., Velthoven, P. v., Miller, J. B., Bruhwiler, L. and Tans, P. P.: Toward regional-scale modeling using the two-way nested global model TM5: Characterization of transport using SF₆, *J. Geophys. Res. Atmos.*, 109(19), doi:10.1029/2004JD005020, 2004.

- Peters, W., Miller, J. B., Whitaker, J., Denning, A. S., Hirsch, A., Krol, M. C., Zupanski, D., Bruhwiler, L. and Tans, P. P.: An ensemble data assimilation system to estimate CO₂ surface fluxes from atmospheric trace gas observations, *J. Geophys. Res. Atmos.*, 110(D24), D24304, doi:10.1029/2005JD006157, 2005.
- 5 Peters, W., Jacobson, A. R., Sweeney, C., Andrews, A. E., Conway, T. J., Masarie, K., Miller, J. B., Bruhwiler, L. M. P., Petron, G., Hirsch, A. I., Worthy, D. E. J., van der Werf, G. R., Randerson, J. T., Wennberg, P. O., Krol, M. C. and Tans, P. P.: An atmospheric perspective on North American carbon dioxide exchange: CarbonTracker, *Proc. Natl. Acad. Sci.*, 104(48), 18925–18930, doi:10.1073/pnas.0708986104, 2007.
- 10 Peters, W., Krol, M. C., van der Werf, G. R., Houweling, S., Jones, C. D., Hughes, J., Schaefer, K., Masarie, K. A., Jacobson, A. R., Miller, J. B., Cho, C. H., Ramonet, M., Schmidt, M., Ciattaglia, L., Apadula, F., Heltai, D., Meinhardt, F., di Sarra, A. G., Piacentino, S., Sferlazzo, D., Aalto, T., Hatakka, J., Ström, J., Haszpra, L., Meijer, H. A. J., van Der Laan, S., Neubert, R. E. M., Jordan, A., Rodó, X., Morguá, J. A., Vermeulen, A. T., Popa, E., Rozanski, K., Zimnoch, M., Manning, A. C., Leuenberger, M., Uglietti, C., Dolman, A. J., Ciais, P., Heimann, M. and Tans, P.: Seven years of recent European net
- 15 terrestrial carbon dioxide exchange constrained by atmospheric observations, *Glob. Chang. Biol.*, 16(4), 1317–1337, doi:10.1111/j.1365-2486.2009.02078.x, 2010.
- Peylin, P., Law, R. M., Gurney, K. R., Chevallier, F., Jacobson, A. R., Maki, T., Niwa, Y., Patra, P. K., Peters, W., Rayner, P. J., Rödenbeck, C., Van Der Laan-Luijkx, I. T. and Zhang, X.: Global atmospheric carbon budget: Results from an ensemble of atmospheric CO₂ inversions, *Biogeosciences*, 10(10), 6699–
- 20 6720, doi:10.5194/bg-10-6699-2013, 2013.
- Reuter, M., Buchwitz, M., Hilker, M., Heymann, J., Schneising, O., Pillai, D., Bovensmann, H., Burrows, J. P., Bösch, H., Parker, R., Butz, A., Hasekamp, O., O'Dell, C. W., Yoshida, Y., Gerbig, C., Nehrkorn, T., Deutscher, N. M., Warneke, T., Notholt, J., Hase, F., Kivi, R., Sussmann, R., Machida, T., Matsueda, H. and Sawa, Y.: Satellite-inferred European carbon sink larger than expected, *Atmos. Chem. Phys.*,
- 25 14(24), 13739–13753, doi:10.5194/acp-14-13739-2014, 2014.
- Saeki, T., Maksyutov, S., Sasakawa, M., Machida, T., Arshinov, M., Tans, P., Conway, T. J., Saito, M., Valsala, V., Oda, T., Andres, R. J. and Belikov, D.: Carbon flux estimation for siberia by inverse modeling

- constrained by aircraft and tower CO₂ measurements, *J. Geophys. Res. Atmos.*, 118(2), 1100–1122, doi:10.1002/jgrd.50127, 2013.
- Sasakawa, M., Shimoyama, K., Machida, T., Tsuda, N., Suto, H., Arshinov, M., Davydov, D., Fofonov, A., Krasnov, O., Saeki, T., Koyama, Y. and Maksyutov, S.: Continuous measurements of methane from a tower network over Siberia, *Tellus, Ser. B Chem. Phys. Meteorol.*, 62(5), 403–416, doi:10.1111/j.1600-0889.2010.00494.x, 2010.
- Sasakawa, M., Machida, T., Tsuda, N., Arshinov, M., Davydov, D., Fofonov, A. and Krasnov, O.: Aircraft and tower measurements of CO₂ concentration in the planetary boundary layer and the lower free troposphere over southern taiga in West Siberia: Long-term records from 2002 to 2011, *J. Geophys. Res. Atmos.*, 118(16), 9489–9498, doi:10.1002/jgrd.50755, 2013.
- Schepaschenko, D., McCallum, I., Shvidenko, A., Fritz, S., Kraxner, F. and Obersteiner, M.: A new hybrid land cover dataset for Russia: A methodology for integrating statistics, remote sensing and in situ information, *J. Land Use Sci.*, 6(4), 245–259, doi:10.1080/1747423X.2010.511681, 2011.
- Schulze, E. D., Lloyd, J., Kelliher, F. M., Wirth, C., Rebmann, C., Luhker, B., Mund, M., Knohl, A., Milyukova, I. M., Schulze, W., Ziegler, W., Varlagin, A. B., Sogachev, A. F., Valentini, R., Dore, S., Grigoriev, S., Kolle, O., Panfyorov, M. I., Tchebakova, N. and Vygodskaya, N. N.: Productivity of forests in the eurosiberian boreal region and their potential to act as a carbon sink - a synthesis, *Glob. Chang. Biol.*, 5(6), 703–722, doi:10.1046/j.1365-2486.1999.00266.x, 1999.
- Siewert M. B., Hanisch J., Weiss N., Kuhry P., Maximov T. C., and H. G.: Comparing carbon storage of Siberian tundra and taiga permafrost ecosystems at very high spatial resolution, *J. Geophys. Res. Biogeosciences*, 120, 1973–1994, doi:10.1002/2015JG002999, 2015.
- Tamocai, C., Canadell, J. G., Schuur, E. A. G., Kuhry, P., Mazhitova, G. and Zimov, S.: Soil organic carbon pools in the northern circumpolar permafrost region, *Global Biogeochem. Cycles*, 23(2), 1–11, doi:10.1029/2008GB003327, 2009.
- van der Werf, G. R., Randerson, J. T., Giglio, L., Collatz, G. J., Kasibhatla, P. S. and Arellano, Avelino F., J.: Interannual variability in global biomass burning emissions from 1997 to 2004, *Atmos. Chem. Phys.*, 6(11), 3423–3441, doi:10.5194/acpd-6-3175-2006, 2006.

- van der Werf, G. R., Randerson, J. T., Giglio, L., Collatz, G. J., Mu, M., Kasibhatla, P. S., Morton, D. C., Defries, R. S., Jin, Y. and Van Leeuwen, T. T.: Global fire emissions and the contribution of deforestation, savanna, forest, agricultural, and peat fires (1997-2009), *Atmos. Chem. Phys.*, 10(23), 11707–11735, doi:10.5194/acp-10-11707-2010, 2010.
- 5 Wang, Y., Broquet, G., Ciais, P., Chevallier, F., Vogel, F., Wu, L., Yin, Y., Wang, R. and Tao, S.: Potential of European ¹⁴CO₂ observation network to estimate the fossil fuel CO₂ emissions via atmospheric inversions, *Atmos. Chem. Phys.*, 18(7), 4229–4250, doi:10.5194/acp-18-4229-2018, 2018.
- Whitaker, J. S. and Hamill, T. M.: Ensemble Data Assimilation without Perturbed Observations, *Mon.*
10 *Weather Rev.*, 130(7), 1913–1924, doi:10.1175/1520-0493(2002)130<1913:EDAWPO>2.0.CO;2, 2002.
- Wu, K., Lauvaux, T., Davis, K. J., Deng, A., Lopez Coto, I., Gurney, K. R. and Patarasuk, R.: Joint inverse estimation of fossil fuel and biogenic CO₂ fluxes in an urban environment: An observing system simulation experiment to assess the impact of multiple uncertainties, *Elem. Sci. Anthropocene*, 6(1), 17, doi:10.1525/elementa.138, 2018.
- 15 Yang, E.-G., H. M. Kim, J. Kim, and Kay J. K.: Effect of observation network design on meteorological forecasts of Asian dust events, *Monthly Weather Review*, 142, 4679-4695, doi:10.1175/MWR-D-14-00080.1, 2014.
- Ziehn, T., Nickless, A., Rayner, P. J., Law, R. M., Roff, G. and Fraser, P.: Greenhouse gas network design using backward Lagrangian particle dispersion modelling - Part 1: Methodology and Australian test case,
20 *Atmos. Chem. Phys.*, 14(17), 9363–9378, doi:10.5194/acp-14-9363-2014, 2014.
- Ziehn, T., Law, R. M., Rayner, P. J. and Roff, G.: Designing optimal greenhouse gas monitoring networks for Australia, *Geosci. Instrumentation, Methods Data Syst.*, 5(1), 1–15, doi:10.5194/gi-5-1-2016, 2016.

Table 1. The model configuration and a priori fluxes used in this study.

Prior Flux	Biosphere	Carnegie-Ames-Stanford Approach Global Fire Emission Database (CASA-GFED) v3.1 (van der Werf et al., 2006, 2010)
	Ocean	Jacobson et al. (2007)
	Fossil Fuel	CASA-GFED v3.1 (van der Werf et al., 2006, 2010)
	Fires	Carbon Dioxide Information and Analysis Center (CDIAC; Boden et al., 2010) and Emission Database for Global Atmospheric Research (EDGAR, European Commission, 2009) databases
Model	Transport Model 5 (TM5) using ERA-interim reanalysis	
Model Resolution	Domain 1(3°×2°)	Globe
	Domain 2(1°×1°)	Asia (12°S-70°N, 30°-168°E)

Table 2. Brief description of the experiments conducted in this study.

Exp. name	No. of stations	Description
CNTL	7	The control experiment that uses the observation site information in Asia of the existing 7 NOAA observation network.
CNTL_MOD	7	The same as the CNTL except for modifying observation station height information for hypothetical observations.
REDIST	7	The experiment that redistributes 7 observations sites at random in Asia.
ADD	17	The experiment that added 10 observation sites at random to the existing 7 NOAA observation network.
SS	17	The experiment that added 10 observation sites to the existing 7 NOAA observation network with the self-sensitivity information.
ECOSS	17	The experiment that added 10 observation sites to the existing 7 NOAA observation network with the self-sensitivity and ecoregion information (1-2 stations for each ecoregion)
NSS	17	The experiment that added 10 observation sites to the existing 7 NOAA observation network with the normalized self-sensitivity information.
NECOSS1	17	The experiment that added 10 observation sites to the existing 7 NOAA observation network with the normalized self-sensitivity and ecoregion information (1-2 stations for each ecoregion).
NECOSS2	17	The experiment that added 10 observation sites to the existing 7 NOAA observation network with the normalized self-sensitivity and ecoregion information (1 station per ecoregion).
ALL	905	The experiment that added observation sites at horizontal 2° intervals on land to the existing 7 NOAA observation network.
<u>CNTL_18</u>	<u>18</u>	<u>The control experiment that uses the observation site information in Asia of the existing 18 NOAA observation network.</u>
<u>ADD_18</u>	<u>28</u>	<u>The experiment that added 10 observation sites at random to the existing 18 NOAA observation network.</u>
<u>NSS_18</u>	<u>28</u>	<u>The experiment that added 10 observation sites to the existing 18 NOAA observation network with the normalized self-sensitivity information.</u>
<u>NECOSS1_18</u>	<u>28</u>	<u>The experiment that added 10 observation sites to the existing 18 NOAA observation network with the normalized self-sensitivity and ecoregion information (1-2 stations for each ecoregion).</u>

Table 3. The ~~information proportion~~ of the ecoregions in the ~~Asia~~-verification domain and the distribution of observation sites for the SS and ECOSS experiments.

<u>Ecoregion Index</u>	<u>Transcom Region</u>	<u>Land Ecosystem Type</u>	<u>Count</u>	<u>Proportion (%)</u>	<u>SS</u>	<u>ECOSS</u>
<u>137</u>	<u>Eurasia Temperate</u>	<u>Grass/Shrub</u>	<u>744</u>	<u>19.36</u>		<u>2</u>
<u>115</u>	<u>Eurasia Boreal</u>	<u>Conifer Forest</u>	<u>657</u>	<u>17.1</u>		<u>2</u>
<u>140</u>	<u>Eurasia Temperate</u>	<u>Semitundra</u>	<u>262</u>	<u>6.82</u>		<u>1</u>
<u>147</u>	<u>Eurasia Temperate</u>	<u>Crops</u>	<u>248</u>	<u>6.45</u>		<u>1</u>
<u>123</u>	<u>Eurasia Boreal</u>	<u>Northern Taiga</u>	<u>228</u>	<u>5.93</u>		<u>1</u>
<u>157</u>	<u>Tropical Asia</u>	<u>Tropical Forest</u>	<u>222</u>	<u>5.78</u>		<u>1</u>
<u>145</u>	<u>Eurasia Temperate</u>	<u>Deserts</u>	<u>200</u>	<u>5.2</u>		
<u>117</u>	<u>Eurasia Boreal</u>	<u>Mixed Forest</u>	<u>150</u>	<u>3.9</u>		<u>1</u>
<u>118</u>	<u>Eurasia Boreal</u>	<u>Grass/Shrub</u>	<u>122</u>	<u>3.17</u>		<u>1</u>
<u>136</u>	<u>Eurasia Temperate</u>	<u>Mixed Forest</u>	<u>122</u>	<u>3.17</u>		
<u>121</u>	<u>Eurasia Boreal</u>	<u>Semitundra</u>	<u>95</u>	<u>2.47</u>		
<u>166</u>	<u>Tropical Asia</u>	<u>Crops</u>	<u>80</u>	<u>2.08</u>		
<u>135</u>	<u>Eurasia Temperate</u>	<u>Broadleaf Forest</u>	<u>62</u>	<u>1.61</u>		
<u>141</u>	<u>Eurasia Temperate</u>	<u>Fields/Woods/Savanna</u>	<u>59</u>	<u>1.54</u>		
<u>143</u>	<u>Eurasia Temperate</u>	<u>Forest/Field</u>	<u>58</u>	<u>1.51</u>	<u>1</u>	
<u>171</u>	<u>Tropical Asia</u>	<u>Water</u>	<u>54</u>	<u>1.41</u>		
<u>125</u>	<u>Eurasia Boreal</u>	<u>Wetland</u>	<u>45</u>	<u>1.17</u>	<u>1</u>	
<u>162</u>	<u>Tropical Asia</u>	<u>Forest/Field</u>	<u>44</u>	<u>1.14</u>		
<u>122</u>	<u>Eurasia Boreal</u>	<u>Fields/Woods/Savanna</u>	<u>42</u>	<u>1.09</u>		
<u>154</u>	<u>Tropical Asia</u>	<u>Broadleaf Forest</u>	<u>39</u>	<u>1.01</u>	<u>1</u>	
<u>155</u>	<u>Tropical Asia</u>	<u>Mixed Forest</u>	<u>37</u>	<u>0.96</u>		
<u>156</u>	<u>Tropical Asia</u>	<u>Grass/Shrub</u>	<u>36</u>	<u>0.94</u>		
<u>124</u>	<u>Eurasia Boreal</u>	<u>Forest/Field</u>	<u>35</u>	<u>0.91</u>		
<u>134</u>	<u>Eurasia Temperate</u>	<u>Conifer Forest</u>	<u>34</u>	<u>0.88</u>		
<u>116</u>	<u>Eurasia Boreal</u>	<u>Broadleaf Forest</u>	<u>33</u>	<u>0.86</u>		
<u>128</u>	<u>Eurasia Boreal</u>	<u>Crops</u>	<u>24</u>	<u>0.62</u>	<u>1</u>	
<u>138</u>	<u>Eurasia Temperate</u>	<u>Tropical Forest</u>	<u>19</u>	<u>0.49</u>	<u>1</u>	
<u>160</u>	<u>Tropical Asia</u>	<u>Fields/Woods/Savanna</u>	<u>15</u>	<u>0.39</u>		
<u>146</u>	<u>Eurasia Temperate</u>	<u>Shrub/Tree/Suc</u>	<u>12</u>	<u>0.31</u>		
<u>144</u>	<u>Eurasia Temperate</u>	<u>Wetland</u>	<u>11</u>	<u>0.29</u>	<u>1</u>	

<u>139</u>	<u>Eurasia Temperate</u>	<u>Scrub/Woods</u>	<u>10</u>	<u>0.26</u>	<u>1</u>
<u>163</u>	<u>Tropical Asia</u>	<u>Wetland</u>	<u>9</u>	<u>0.23</u>	<u>2</u>
<u>152</u>	<u>Eurasia Temperate</u>	<u>Water</u>	<u>8</u>	<u>0.21</u>	
<u>130</u>	<u>Eurasia Boreal</u>	<u>Wooded Tundra</u>	<u>5</u>	<u>0.13</u>	<u>1</u>
<u>133</u>	<u>Eurasia Boreal</u>	<u>Water</u>	<u>5</u>	<u>0.13</u>	
<u>191</u>	<u>Europe</u>	<u>Conifer Forest</u>	<u>5</u>	<u>0.13</u>	
<u>193</u>	<u>Europe</u>	<u>Mixed Forest</u>	<u>4</u>	<u>0.1</u>	
<u>194</u>	<u>Europe</u>	<u>Grass/Shrub</u>	<u>4</u>	<u>0.1</u>	
<u>197</u>	<u>Europe</u>	<u>Semitundra</u>	<u>3</u>	<u>0.08</u>	
<u>201</u>	<u>Europe</u>	<u>Wetland</u>	<u>1</u>	<u>0.03</u>	

Ecoregion Index	Count	Proportion (%)	SS	ECOSS
137	744	19.36		2
115	657	17.10		2
140	262	6.82		1
147	248	6.45		1
123	228	5.93		1
157	222	5.78		1
145	200	5.20		
117	150	3.90		1
118	122	3.17		
136	122	3.17		
121	95	2.47		
166	80	2.08		
135	62	1.61		
141	59	1.54		
143	58	1.51	1	
171	54	1.41		
125	45	1.17	1	
162	44	1.14		
122	42	1.09		
154	39	1.01	1	
155	37	0.96		
156	36	0.94		
124	35	0.91		
134	34	0.88		
116	33	0.86		
128	24	0.62	1	
138	19	0.49	1	
160	15	0.39		
146	12	0.31		
144	11	0.29	1	

139	10	0.26	1
163	9	0.23	2
152	8	0.21	
130	5	0.13	1
133	5	0.13	
191	5	0.13	
193	4	0.10	
194	4	0.10	
197	3	0.08	
201	1	0.03	

Table 4. The locations and self-sensitivities for the observation sites in the SS and ECOSS experiments.

SS				ECOSS			
Ecoregion Index	Lat	Lon	SS (%)	Ecoregion Index	Lat	Lon	SS (%)
138	26.5	96.5	4.02	137	26.5	92.5	0.87
163	4.5	114.5	3.83	137	28.5	118.5	0.65
163	-5.5	138.5	3.29	115	58.5	62.5	1.35
143	6.5	80.5	3.17	115	46.5	142.5	1.28
139	24.5	74.5	2.48	140	44.5	54.5	0.29
130	66.5	78.5	2.32	147	10.5	76.5	0.96
128	56.5	84.5	1.99	123	66.5	80.5	1.12
125	60.5	62.5	1.91	157	8.5	126.5	1.17
144	46.5	124.5	1.87	117	52.5	118.5	0.68
154	18.5	104.5	1.75	118	56.5	86.5	0.87

SS					ECOSS				
Transcom Region	Land Ecosystem Type	Lat	Lon	SS (%)	Transcom Region	Land Ecosystem Type	Lat	Lon	SS (%)
<u>Eurasia Temperate</u>	<u>Tropical Forest</u>	<u>26.5</u>	<u>96.5</u>	<u>4.02</u>	<u>Eurasia Temperate</u>	<u>Grass/Shrub</u>	<u>26.5</u>	<u>92.5</u>	<u>0.87</u>
<u>Tropical Asia</u>	<u>Wetland</u>	<u>4.5</u>	<u>114.5</u>	<u>3.83</u>	<u>Eurasia Temperate</u>	<u>Grass/Shrub</u>	<u>28.5</u>	<u>118.5</u>	<u>0.65</u>
<u>Tropical Asia</u>	<u>Wetland</u>	<u>-5.5</u>	<u>138.5</u>	<u>3.29</u>	<u>Eurasia Boreal</u>	<u>Conifer Forest</u>	<u>58.5</u>	<u>62.5</u>	<u>1.35</u>
<u>Eurasia Temperate</u>	<u>Forest/Field</u>	<u>6.5</u>	<u>80.5</u>	<u>3.17</u>	<u>Eurasia Boreal</u>	<u>Conifer Forest</u>	<u>46.5</u>	<u>142.5</u>	<u>1.28</u>
<u>Eurasia Temperate</u>	<u>Scrub/Woods</u>	<u>24.5</u>	<u>74.5</u>	<u>2.48</u>	<u>Eurasia Temperate</u>	<u>Semitemundra</u>	<u>44.5</u>	<u>54.5</u>	<u>0.29</u>
<u>Eurasia Boreal</u>	<u>Wooded Tundra</u>	<u>66.5</u>	<u>78.5</u>	<u>2.32</u>	<u>Eurasia Temperate</u>	<u>Crops</u>	<u>10.5</u>	<u>76.5</u>	<u>0.96</u>
<u>Eurasia Boreal</u>	<u>Crops</u>	<u>56.5</u>	<u>84.5</u>	<u>1.99</u>	<u>Eurasia Boreal</u>	<u>Northern Taiga</u>	<u>66.5</u>	<u>80.5</u>	<u>1.12</u>
<u>Eurasia Boreal</u>	<u>Wetland</u>	<u>60.5</u>	<u>62.5</u>	<u>1.91</u>	<u>Tropical Asia</u>	<u>Tropical Forest</u>	<u>8.5</u>	<u>126.5</u>	<u>1.17</u>
<u>Eurasia Temperate</u>	<u>Wetland</u>	<u>46.5</u>	<u>124.5</u>	<u>1.87</u>	<u>Eurasia Boreal</u>	<u>Mixed Forest</u>	<u>52.5</u>	<u>118.5</u>	<u>0.68</u>

Tropical Asia

Broadleaf Forest

18.5

104.5

1.75

Eurasia Boreal

Grass/Shrub

56.5

86.5

0.87

Table 5. The locations and ecoregion indices for the observation sites in the NSS, NECOSS1, and NECOSS2 experiments.

<u>NSS</u>				<u>NECOSS1</u>				<u>NECOSS2</u>			
<u>Transcom Region</u>	<u>Land Ecosystem Type</u>	<u>Lat</u>	<u>Lon</u>	<u>Transcom Region</u>	<u>Land Ecosystem Type</u>	<u>Lat</u>	<u>Lon</u>	<u>Transcom Region</u>	<u>Land Ecosystem Type</u>	<u>Lat</u>	<u>Lon</u>
<u>Eurasia Boreal</u>	<u>Conifer Forest</u>	<u>58.5</u>	<u>62.5</u>	<u>Eurasia Boreal</u>	<u>Conifer Forest</u>	<u>58.5</u>	<u>62.5</u>	<u>Eurasia Boreal</u>	<u>Conifer Forest</u>	<u>58.5</u>	<u>62.5</u>
<u>Eurasia Boreal</u>	<u>Conifer Forest</u>	<u>46.5</u>	<u>142.5</u>	<u>Eurasia Boreal</u>	<u>Conifer Forest</u>	<u>46.5</u>	<u>142.5</u>	<u>Eurasia Temperate</u>	<u>Grass/Shrub</u>	<u>26.5</u>	<u>92.5</u>
<u>Eurasia Temperate</u>	<u>Grass/Shrub</u>	<u>26.5</u>	<u>92.5</u>	<u>Eurasia Temperate</u>	<u>Grass/Shrub</u>	<u>26.5</u>	<u>92.5</u>	<u>Tropical Asia</u>	<u>Tropical Forest</u>	<u>8.5</u>	<u>126.5</u>
<u>Eurasia Boreal</u>	<u>Conifer Forest</u>	<u>54.5</u>	<u>84.5</u>	<u>Eurasia Temperate</u>	<u>Grass/Shrub</u>	<u>28.5</u>	<u>118.5</u>	<u>Eurasia Boreal</u>	<u>Northern Taiga</u>	<u>66.5</u>	<u>80.5</u>
<u>Eurasia Boreal</u>	<u>Conifer Forest</u>	<u>52.5</u>	<u>120.5</u>	<u>Tropical Asia</u>	<u>Tropical Forest</u>	<u>8.5</u>	<u>126.5</u>	<u>Eurasia Temperate</u>	<u>Crops</u>	<u>10.5</u>	<u>76.5</u>
<u>Eurasia Temperate</u>	<u>Grass/Shrub</u>	<u>28.5</u>	<u>118.5</u>	<u>Eurasia Boreal</u>	<u>Northern Taiga</u>	<u>66.5</u>	<u>80.5</u>	<u>Eurasia Boreal</u>	<u>Mixed Forest</u>	<u>48.5</u>	<u>132.5</u>
<u>Eurasia Temperate</u>	<u>Grass/Shrub</u>	<u>26.5</u>	<u>104.5</u>	<u>Eurasia Temperate</u>	<u>Crops</u>	<u>10.5</u>	<u>76.5</u>	<u>Eurasia Boreal</u>	<u>Semitundra</u>	<u>60.5</u>	<u>148.5</u>
<u>Eurasia Temperate</u>	<u>Grass/Shrub</u>	<u>46.5</u>	<u>54.5</u>	<u>Eurasia Boreal</u>	<u>Semitundra</u>	<u>60.5</u>	<u>148.5</u>	<u>Tropical Asia</u>	<u>Crops</u>	<u>0.5</u>	<u>110.5</u>
<u>Eurasia Boreal</u>	<u>Conifer Forest</u>	<u>62.5</u>	<u>132.5</u>	<u>Tropical Asia</u>	<u>Crops</u>	<u>0.5</u>	<u>110.5</u>	<u>Eurasia Boreal</u>	<u>Grass/Shrub</u>	<u>56.5</u>	<u>86.5</u>
<u>Eurasia Temperate</u>	<u>Grass/Shrub</u>	<u>34.5</u>	<u>72.5</u>	<u>Eurasia Boreal</u>	<u>Mixed Forest</u>	<u>52.5</u>	<u>118.5</u>	<u>Tropical Asia</u>	<u>Mixed Forest</u>	<u>-7.5</u>	<u>146.5</u>

NSS			NECOSS1			NECOSS2		
Ecoregion Index	Lat	Lon	Ecoregion Index	Lat	Lon	Ecoregion Index)	Lat	Lon
115	58.5	62.5	115	58.5	62.5	115	58.5	62.5
115	46.5	142.5	115	46.5	142.5	137	26.5	92.5
137	26.5	92.5	137	26.5	92.5	157	8.5	126.5
115	54.5	84.5	137	28.5	118.5	123	66.5	80.5
115	52.5	120.5	157	8.5	126.5	147	10.5	76.5
137	28.5	118.5	123	66.5	80.5	117	48.5	132.5
137	26.5	104.5	147	10.5	76.5	121	60.5	148.5
137	46.5	54.5	121	60.5	148.5	166	0.5	110.5
115	62.5	132.5	166	0.5	110.5	118	56.5	86.5
137	34.5	72.5	117	52.5	118.5	155	-7.5	146.5

Table 6. The averaged statistics of surface CO₂ fluxes (gC m⁻² yr⁻¹) for the experiments conducted in this study.

Exp. name	CNTL	CNTL_MOD	REDIST	ADD	SS	ECOSS	NSS	NECOSS1	NECOSS2	ALL
PC	0.965	0.966	0.973	0.977	0.98	0.984	0.983	0.987	0.986	0.998
BIAS	1.169	1.245	1.055	1.679	1.627	-0.211	-0.168	0.232	-0.28	-0.17
RMSD	70.06	70.528	60.547	54.708	53.572	45.388	47.034	41.9	42.218	15.947

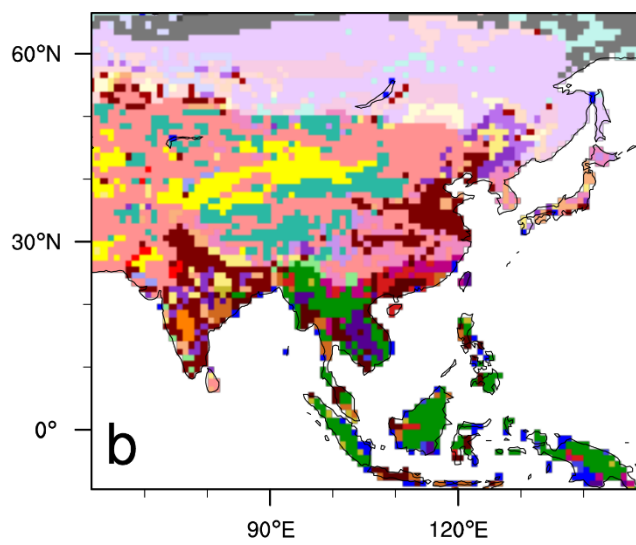
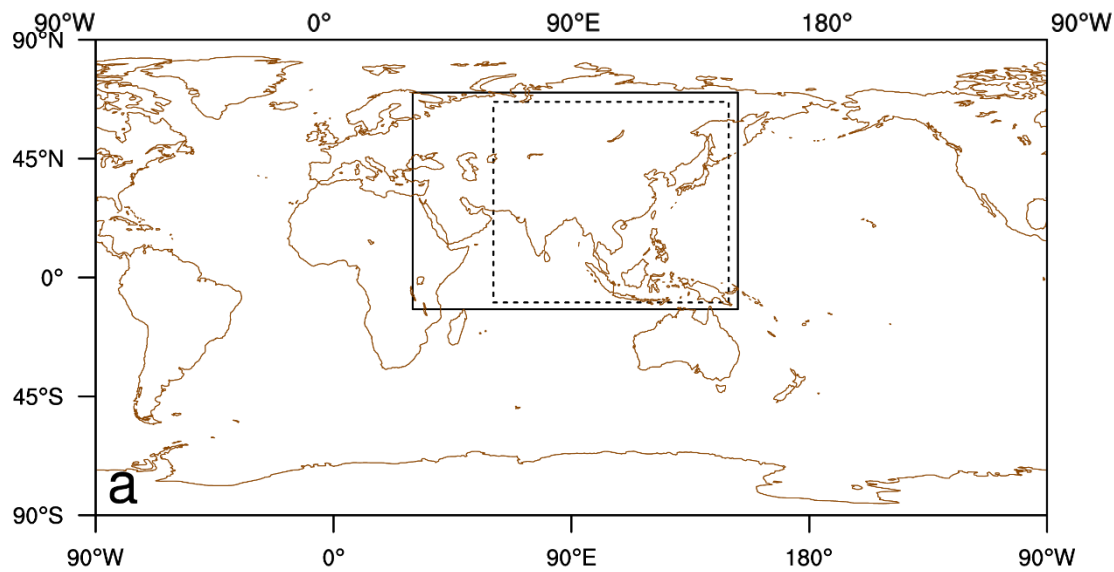
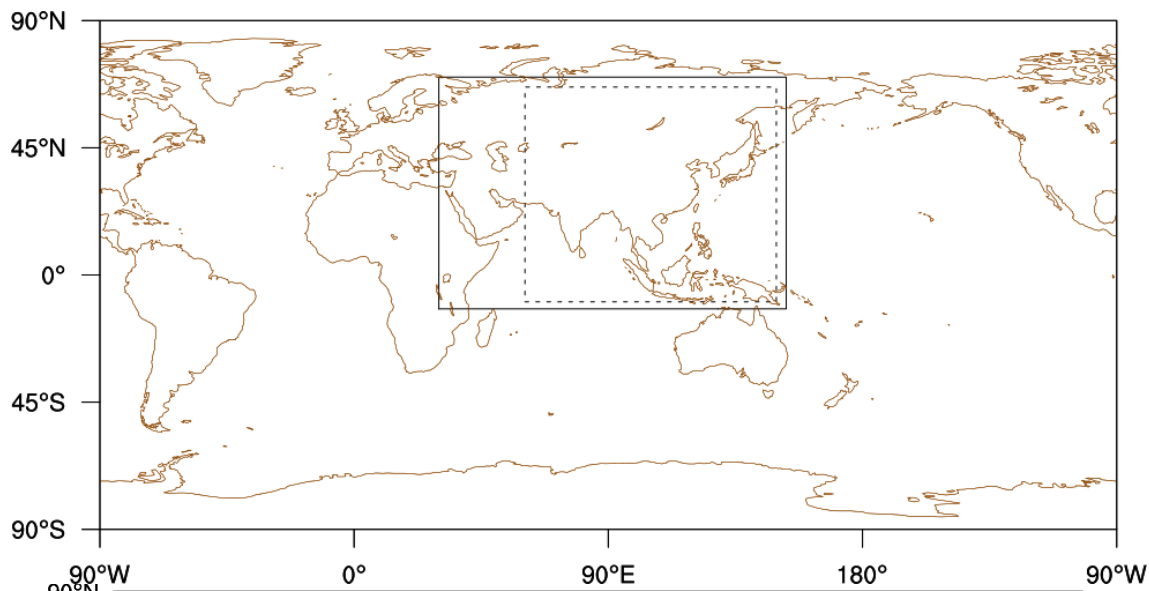


Figure 1. ~~The distribution of the nested TM5 model domain over Asia (black solid rectangle) and verification domain (black dashed rectangle) used in this study.~~ The distribution of a) the nested TM5 model domain over Asia (black solid rectangle) and verification domain (black dashed rectangle) and b) ecoregions in Asia used in this study.

5

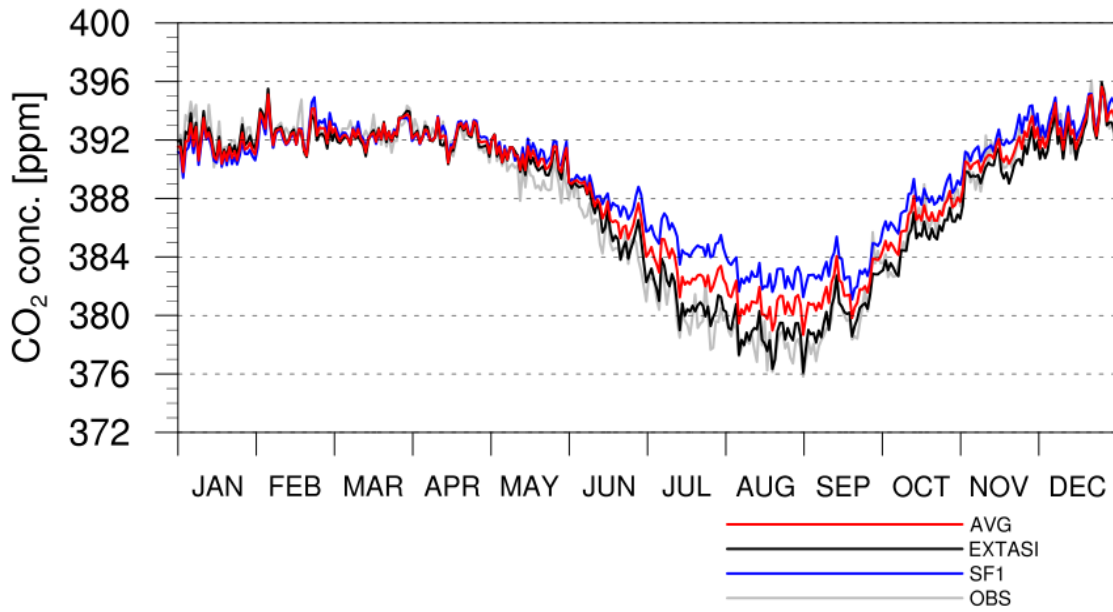


Figure 2. Time series of CO₂ concentration from hypothetical observations, model simulations, and real observations. The gray solid line (OBS) denotes the value of real observation data, the black solid line indicates the value from the EXTASI experiment, the blue solid line denotes the value of the SF1 experiment, and the red solid line (AVG) denotes the average of the EXTASI and SF1, which regarded as True observation data in this study.

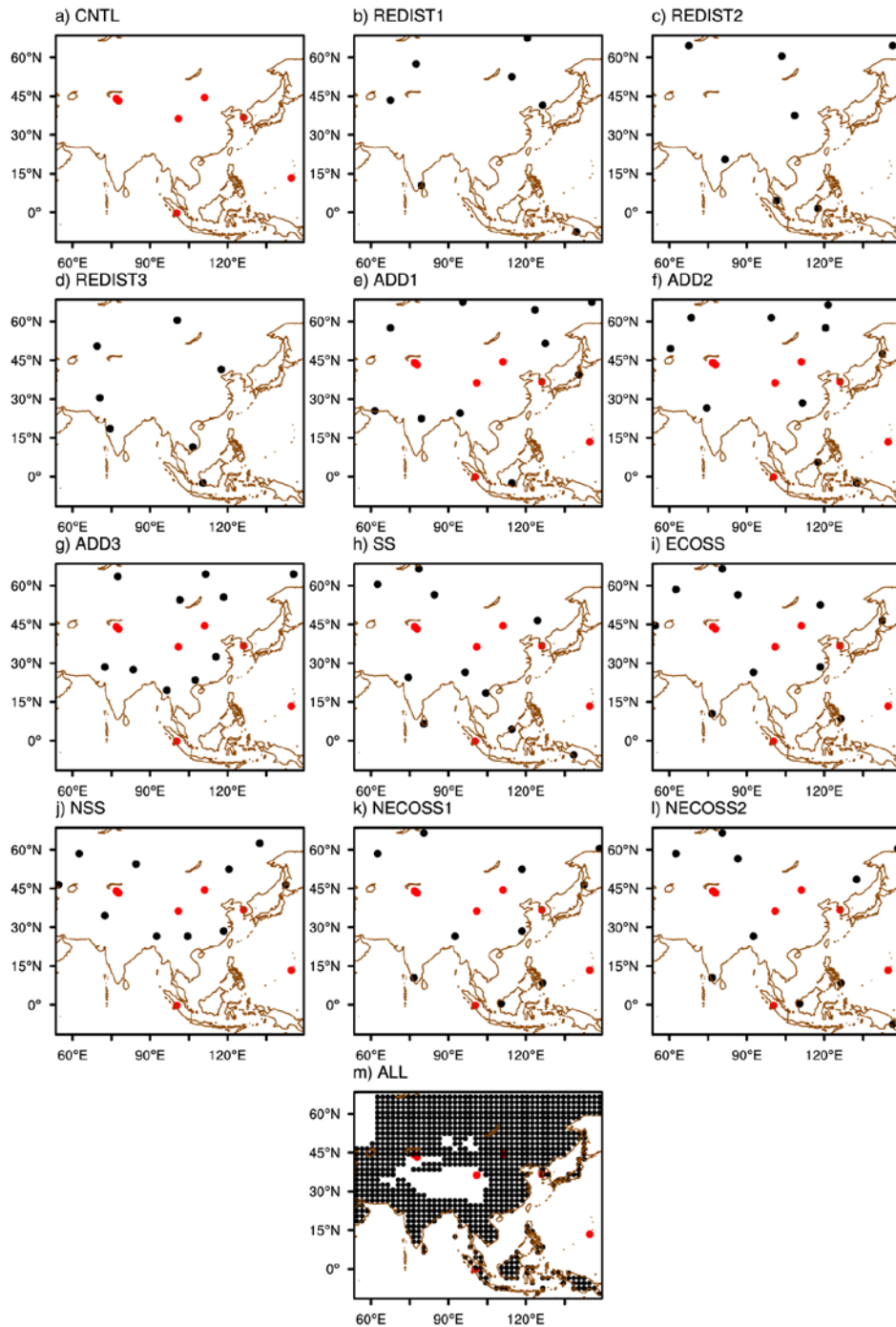


Figure 3. The distribution of observation sites in each observation network: a) the CNTL and CNTL_MOD, b–d) the REDIST, e–g) the ADD, h) the SS, i) the ECOSS, j) the NSS, k) the NECOSS1, l) the NECOSS2, and m) the ALL experiment. Red dots denote the observation sites of the NOAA observation network and black dots denote the hypothetical observation sites.

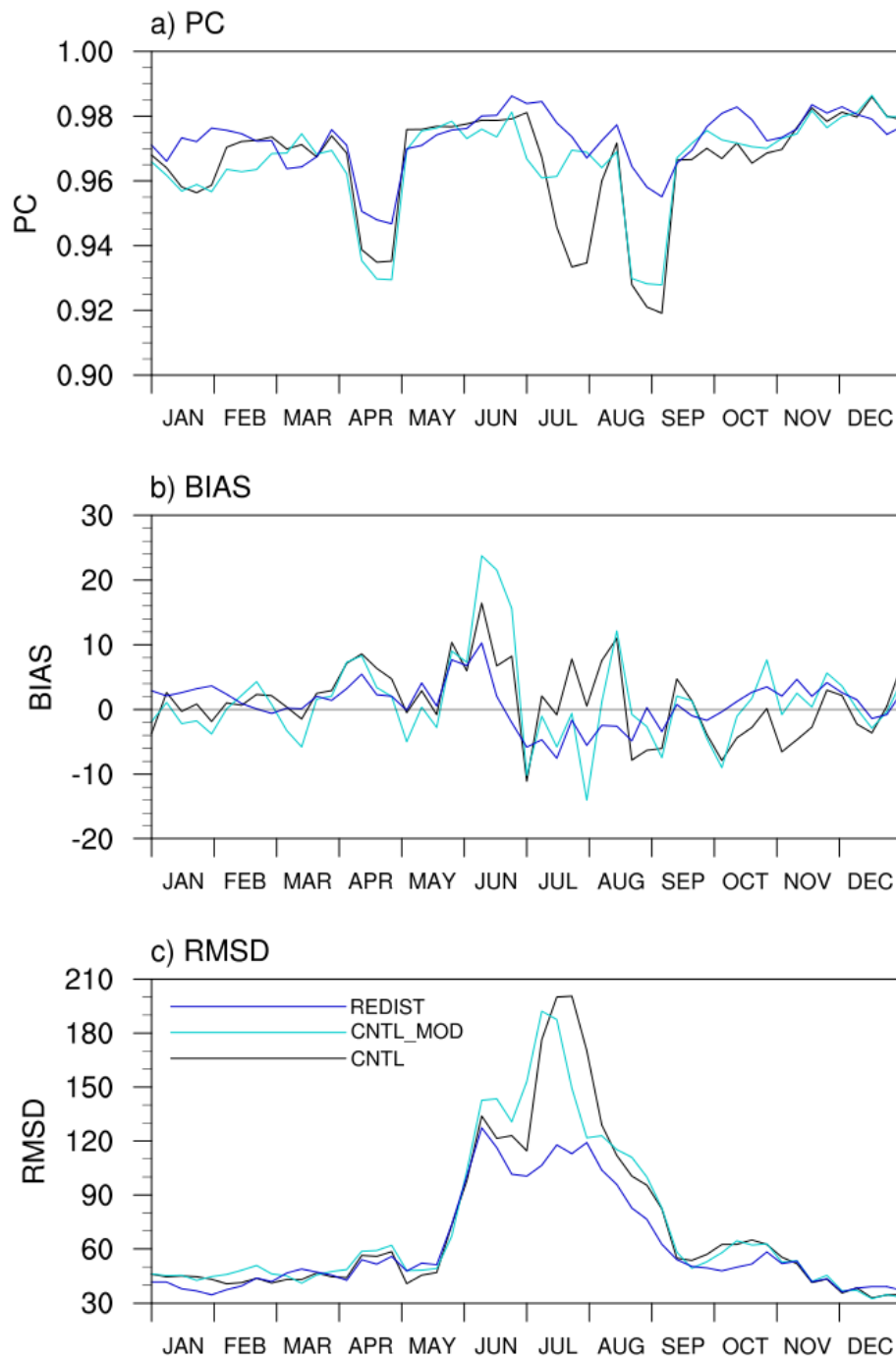


Figure 4. Time series of the three-week moving average of a) PC, b) BIAS, and c) RMSD of surface CO₂ flux (gC m⁻² yr⁻¹) for the CNTL (black solid line), CNTL_MOD (cyan solid line), and REDIST (blue solid line) experiments.

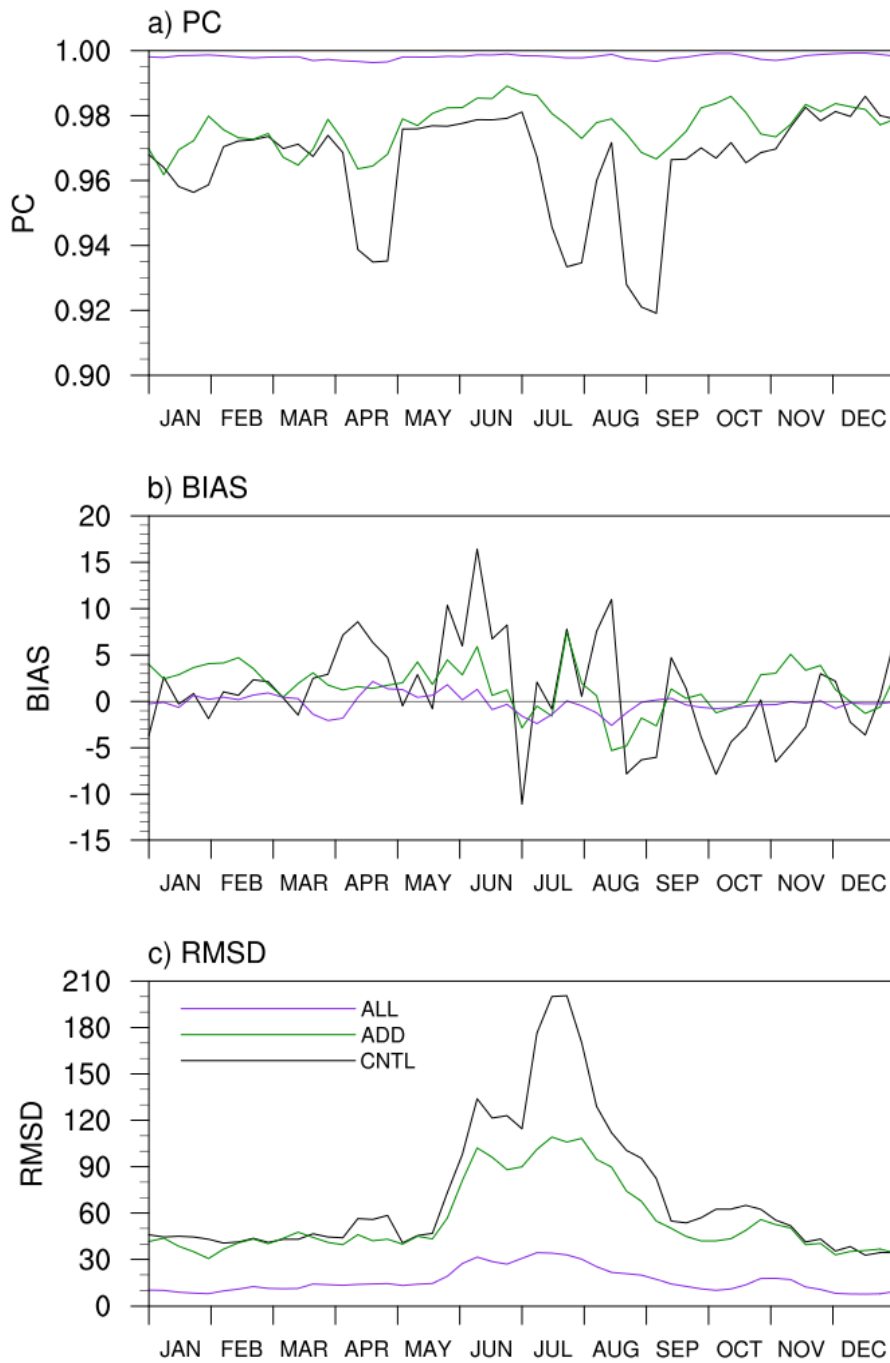


Figure 5. The same as Fig. 4 except for the CNTL (black solid line), ADD (dark green solid line), and ALL (purple solid line) experiments.

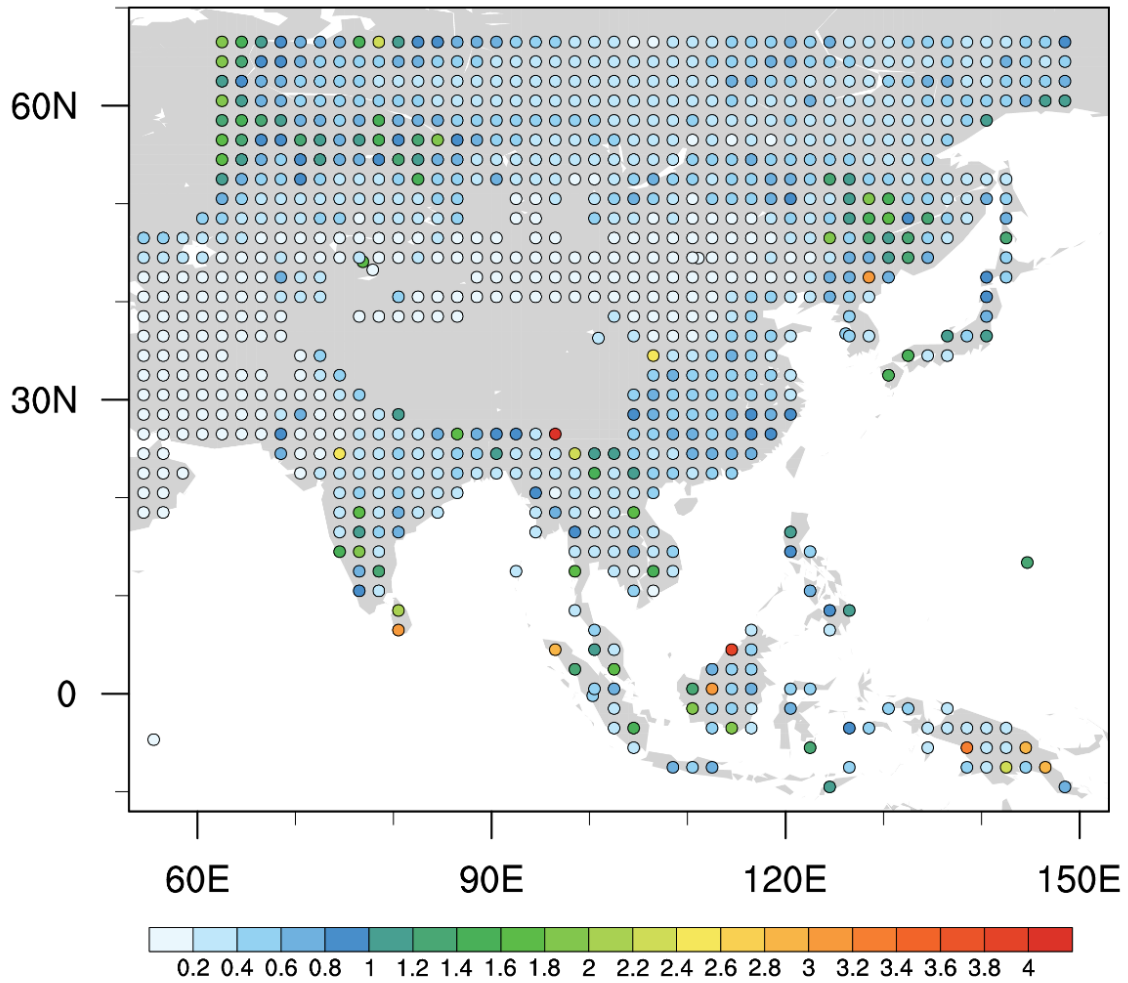


Figure 6. The spatial distribution of self-sensitivities (%) during the experimental period obtained from the ALL experiment.

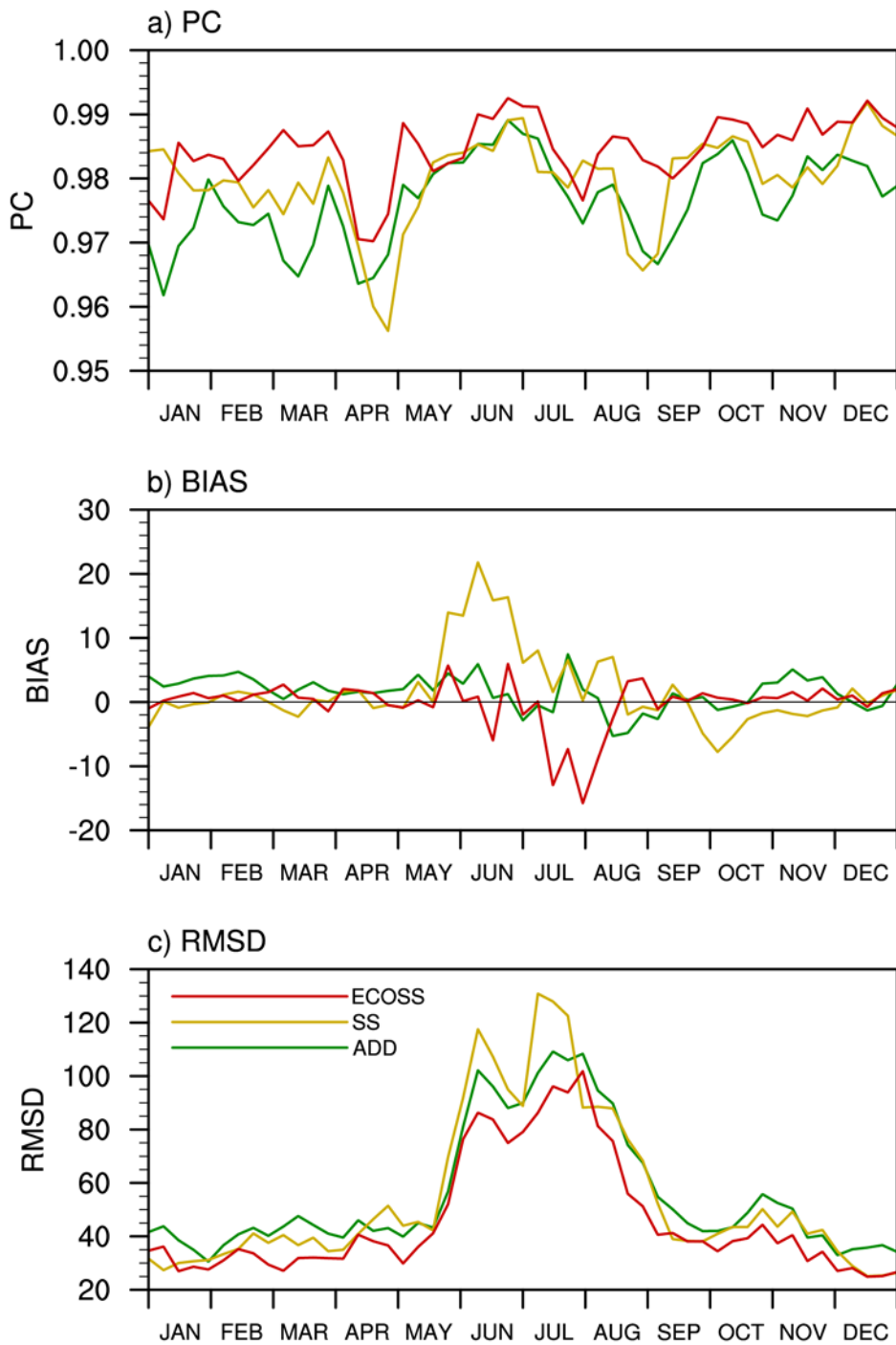


Figure 7. The same as Fig. 4 except for the ADD (dark green solid line), SS (yellow solid line), and ECOSS (red solid line) experiments.

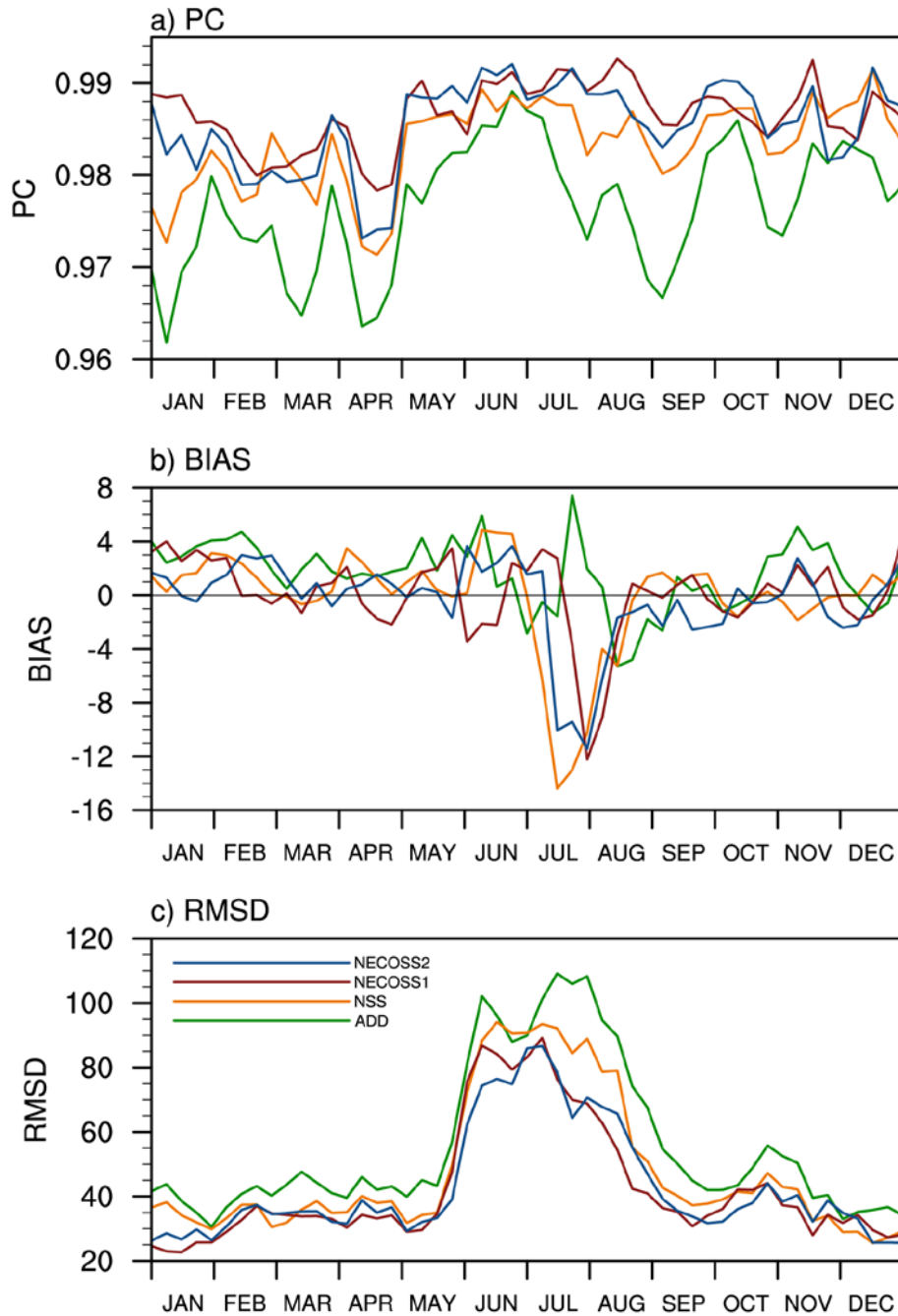


Figure 8. The same as Fig. 4 except for the ADD (dark green solid line), NSS (dark orange solid line), NECOSS1 (dark red solid line), and NECOSS2 (navy blue solid line) experiments.

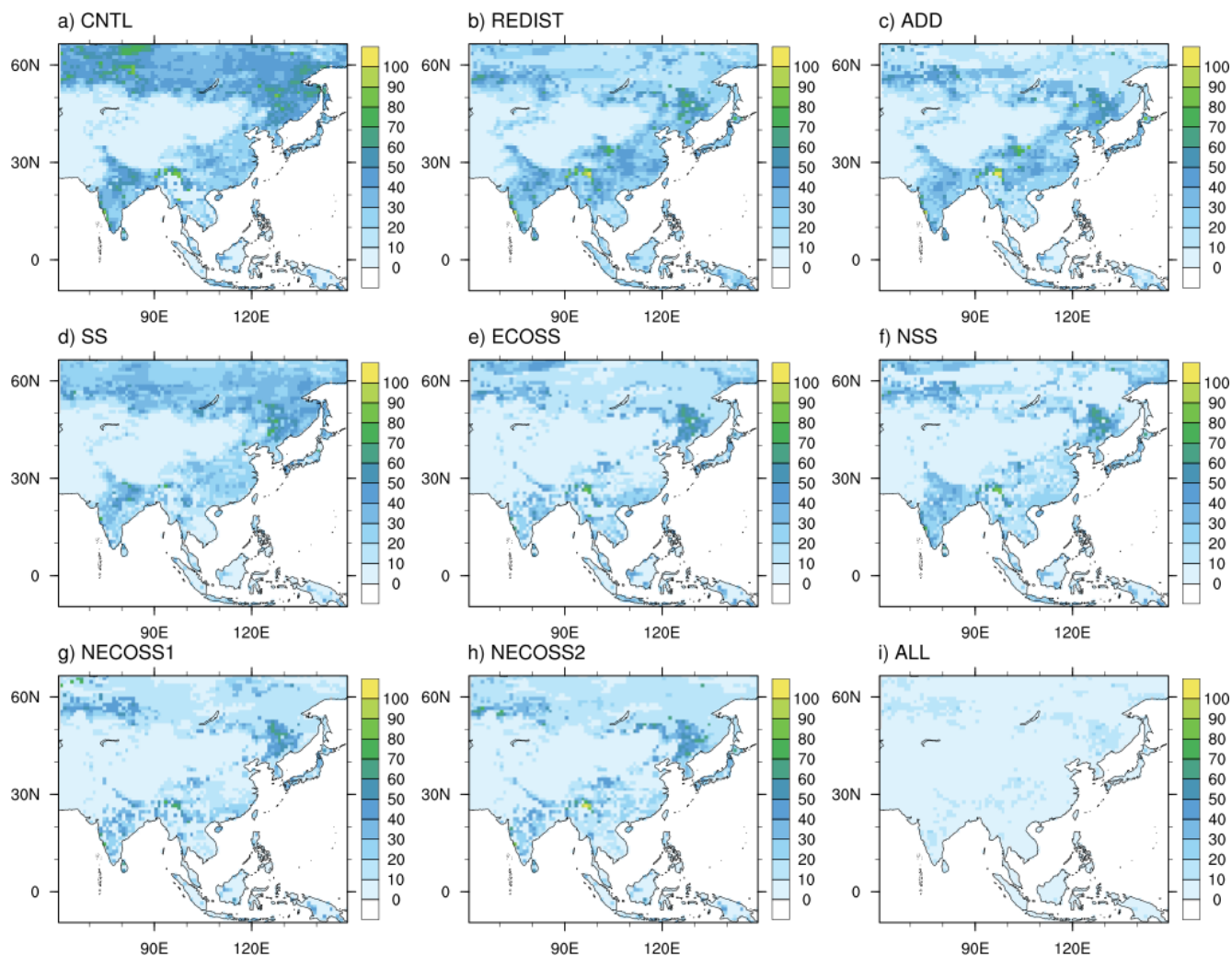


Figure 9. The spatial distribution of the average of weekly RMSD of surface CO₂ fluxes ($\text{gC m}^{-2} \text{yr}^{-1}$) for a) the CNTL, b) the REDIST, c) the ADD, d) the SS, e) the ECOSS, f) the NSS, g) the NECOSS1, h) the NECOSS2, and i) the ALL experiments.

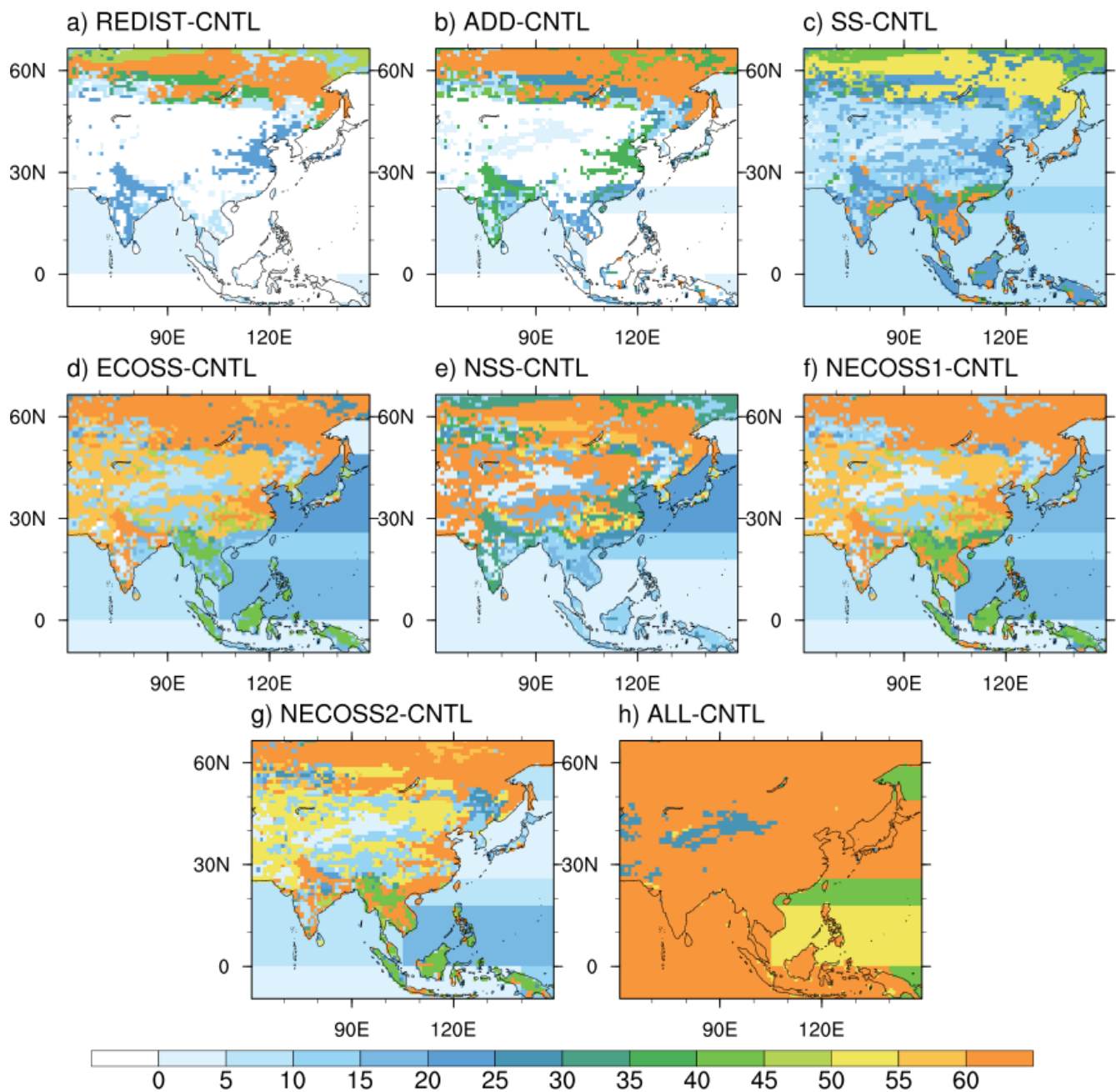


Figure 109. The spatial distribution of uncertainty reduction (%) for a) the REDIST, b) the ADD, c) the SS, d) the ECOSS, e) the NSS, f) the NECOSS1, g) the NECOSS2, and h) the ALL experiment, against the CNTL experiment.

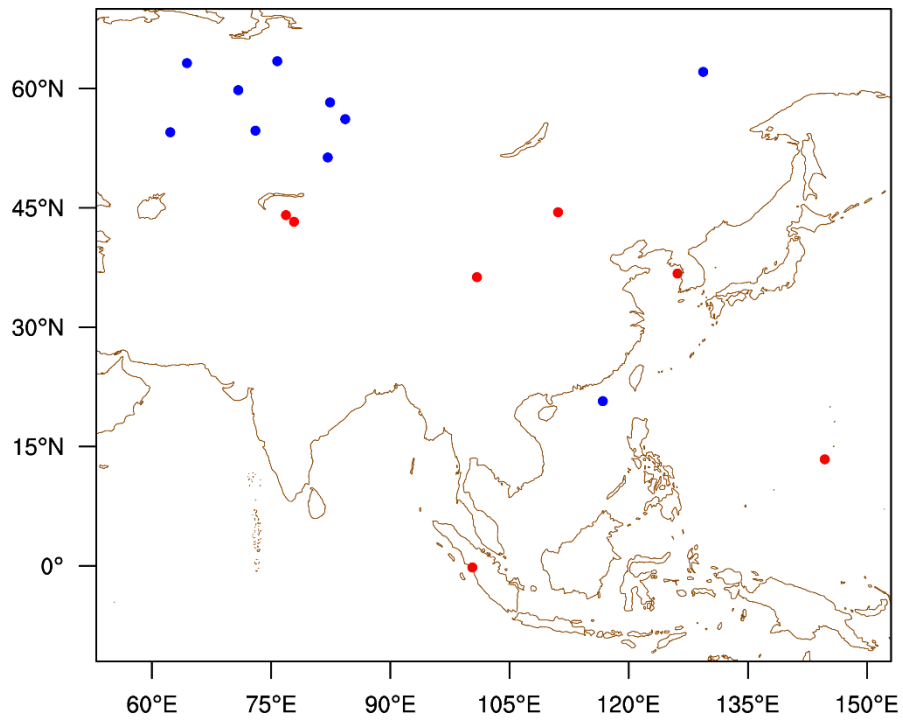


Figure 11. The distribution of observation sites of CNTL_18 in Asia domain: Red dots denote 7 observation sites of CT2013B and blue dots denote additional 11 observation sites of CT2017.

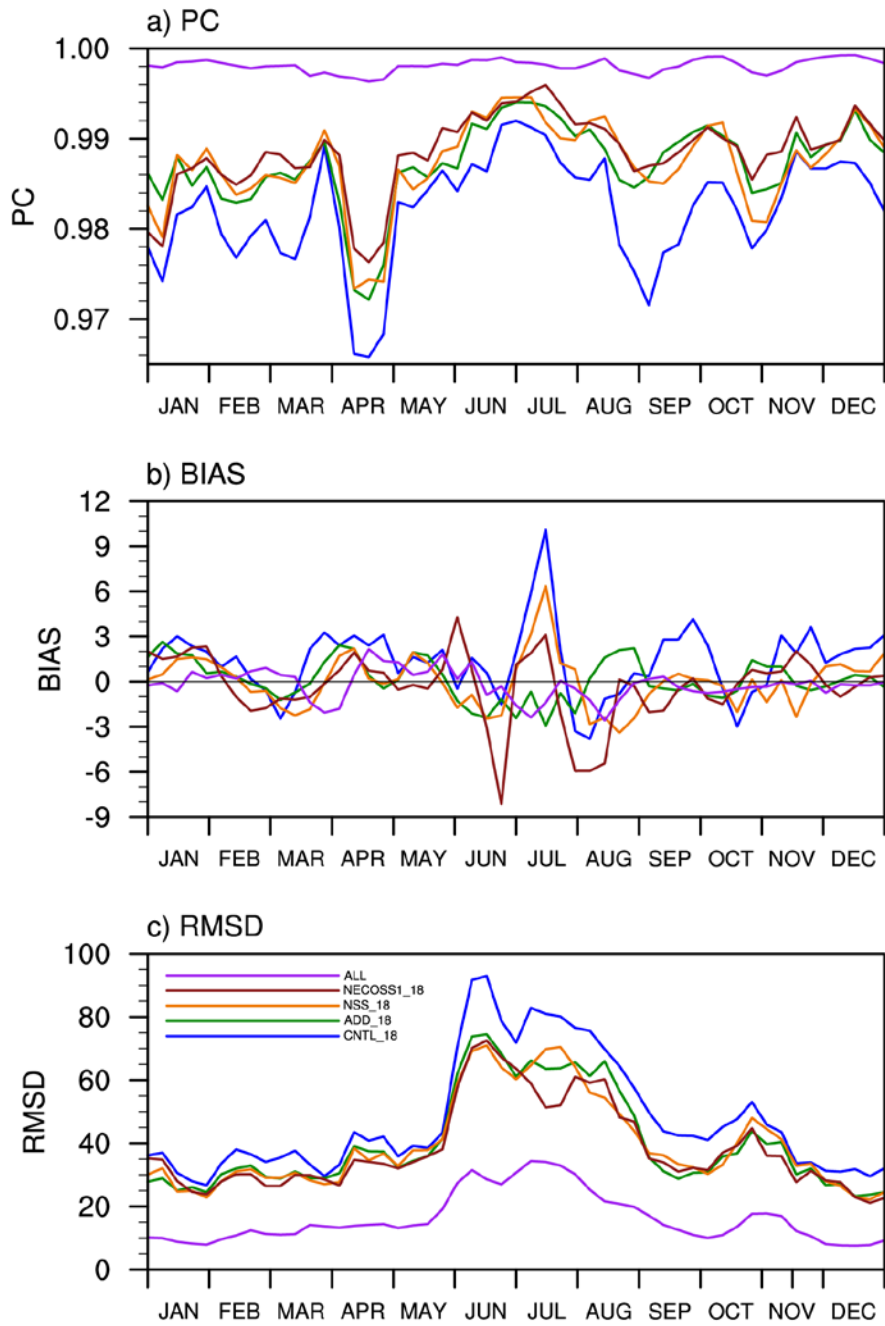


Figure 12. The same as Fig. 4 except for the CNTL_18 (blue solid line), ADD_18 (dark green solid line), NSS_18 (dark orange solid line), NECOSS1_18 (dark red solid line), and ALL (purple solid line) experiments.